7-22-2019 2:15 PM

Resting State Network Dynamics Across Wakefulness and Sleep

Evan Houldin, *The University of Western Ontario*

Supervisor: Owen, Adrian M., *The University of Western Ontario*

A thesis submitted in partial fulfillment of the requirements for the Doctor of Philosophy degree in Neuroscience

Abstract

The function of sleep is a longstanding mystery of the brain. By contrast, the function of resting state networks (RSNs) is one of its most recent mysteries. The relationship between RSNs and neuronal activity has been unclear since RSNs were discovered during the advent of functional magnetic resonance imaging (fMRI). Somewhat paradoxically, investigating these enigmatic phenomena in parallel can help to illuminate the function of both. The three studies described as part of this thesis all involve an evaluation of RSN dynamics across wakefulness and sleep. They are all based on the same dataset, derived from an experimental paradigm in which healthy, non sleep-deprived participants (N=36, 21 female) slept in an MRI scanner, as their brain activity was recorded using simultaneous electroencephalography (EEG)-fMRI. An independent component analysis (ICA) was performed in the first study. Spatial boundaries of components in each sleep stage were compared with those of wakefulness, in the first attempt to catalogue RSNs across all healthy alternate functional modes of the brain. Against expectations, all non-wake-RSN components were positively identified as noise. This indicated that sleep is supported by much the same RSN architecture as wakefulness, despite the unique operations performed during sleep. In the second study, between-RSN functional connectivity (FC) dynamics were evaluated across wakefulness and sleep, in order to determine whether they reflect known cortical neurophysiological dynamics. This was confirmed, highlighting the connection between RSNs and neuronal activity. Moreover, the dynamic pattern suggested that one of the functions of sleep may be to homeostatically counterbalance wakefulness RSN FC. A further pattern, indicating increased FC of "higher-order" RSNs (*e.g.,* default mode network), suggested that slow wave sleep might manifest an altered, rather than a reduced state of awareness, in contrast to historical depictions. Finally, the third study correlated frequency-banded oscillatory activity, as measured by EEG, with RSN activity, as measured with fMRI. This was done in order to track changes in representations of frequency-banded neuronal activity in each RSN across stages. It was discovered that the pattern of frequency band representation dynamics reflects the aforementioned cortical neurophysiological dynamics, further strengthening the connection between RSNs and neuronal activity.

Keywords

Sleep, Resting state networks, EEG-fMRI, Functional connectivity, Independent component analysis, Default mode network, REM, Slow wave sleep, Consciousness.

Lay Abstract

We spend a third of our lives disconnected from reality in a strange state called sleep. However it is presently unclear why it should be necessary for the sleeping brain to isolate itself in this way. One means of understanding why is to examine changes in brain network activity during sleep. A special set of "resting state" networks are particularly useful to understanding sleep because they have already been associated with known functions during wakefulness, for example, the processing of visual information. By observing communication changes amongst these networks, we can make use of these known associations to infer what the brain might be doing during sleep. This thesis makes use of data from a single experiment in which brain activity was recorded from sleeping participants. The first study found that the resting state networks that are consistently identifiable in wake are also consistently present during sleep, with no new networks appearing, despite the unique functions of sleep. This finding was foundational for the studies that followed however, because communication amongst these networks could be examined during sleep without having to consider changes to the networks themselves. The second study further discovered that this communication largely changes in a predictable manner, consistent with what is known about changes to brain chemistry during sleep. Moreover, the changes seem to reverse the patterns found in wakefulness, during deep sleep. This suggests that the function of deep sleep may be to "reset" brain activity closer towards a baseline pattern, so that the brain might be better prepared for the need to adapt and to create new patterns the following day. It is possible that this resetting process requires the brain to be isolated during sleep. Unexpectedly, deep sleep was also found to involve increased activity in networks associated with complex information processing, possibly suggesting that the brain might be more consciously aware during this stage than previously suspected. Finally, the third study found that, beyond the activity of the networks themselves, representing the collective activity of billions of neurons, subset neuronal populations appear to largely change their activity according to the aforementioned predictions.

Co-Authorship Statement

Chapters 2 – 4 includes content that was previously published (Chapter 2), is presently under review for publication (Chapter 3) or is intended for publication (Chapter 4). The co-authors on these papers are as follows:

Evan Houldin, Zhuo Fang, Laura Ray, Bobby Stojanoski, Adrian M. Owen, and Stuart M. Fogel

As author of this thesis and first author of all published and intended-for-publication papers associated with Chapters 2 – 4, Evan Houldin was the primary contributor to the following elements of these papers: conception of hypotheses and design of analyses, execution of analyses, interpretation of results, and writing of manuscripts. Drs. Fogel and Owen together conceived of the experimental design for the large sleep study, which produced the data that was utilized in the individual studies described by these Chapters. Data collection was conducted by Dr. Fang and Evan Houldin. Drs. Fogel and Fang performed EEG processing, and Laura Ray scored the sleep stages. Dr. Fang also ran first-level GLMs, and derived the EEG frequency-power timeseries, for the study described in Chapter 4. Dr. Fogel also provided expert advice, review, and assistance in generating hypotheses and interpretation of results. Dr. Owen provided supervision and expert review and feedback, particularly in the writing of the papers and during the journal submission process. Dr. Stojanoski provided expert advice on statistical methods used in the study described in Chapter 3.

Acknowledgments

I would like to thank my supervisor, Dr. Adrian Owen, for his exacting yet highly insightful feedback on my writing, in turn giving me an understanding of how to present a clear, but succinct scientific narrative, and for helping me to identify and build a story around the key messages buried in the results of a study. Thank you also for teaching me how to become a more efficient scientist, particularly how to run multiple projects in parallel (and for modeling how to do so with a healthy sense of curiosity and humor intact!). I will carry this guidance with me into my future career.

I would also like to thank my unofficial supervisor, Dr. Stuart Fogel, for his patient, detailed and illuminating feedback on my writing, and also for helping me to distinguish lines of analysis that will result in publishable results from investigative routes that will result in the opposite. I am grateful for all of your guidance and for your insight into the scientific process, and for instructing me in better grounding my conclusions by not drifting too far from my results. Also, thank you for first introducing me to the exciting idea that consciousness might be present in all stages of sleep!

A big thank-you to all the other members of the Owen lab, past and present, whose stimulating conversations, friendship and humor helped me to enjoy my doctoral experience. In particular, I would like to acknowledge Dr. Lydia Fang, for her patient explanations of fMRI analysis methodologies and for modeling a hard-working attitude without complaint. I also appreciated Dr. Bobby Stojanoski's valuable advice on statistical methods, and enlightening discussions. A special thank you to Dawn Pavich and Denise Soanes for their assistance with all things administrative and to Haitao Yang, for helping me to set up all the necessary hardware and software to complete my varied analyses. Thank you also to my thesis committee members, Dr. Penny MacDonald and Dr. Stefan Everling, for helping me to stay on track. I am also indebted to Dr. Andrea Soddu and Dr. Jörn Diedrichsen for their valuable advice and discussions.

Finally, I would like to thank my incredibly supportive and encouraging family; my two sisters, Julia and Adina, and my understanding parents, who remind me to focus on the forest when there seem to be too many trees, and to attend to the trees when the forest is a

distraction. Although it is impossible to repay you, I do have free tickets to visit Glenn the Goat (a local bovid wonder) - you will be getting these at the very first opportunity!

Table of Contents

List of Tables

List of Figures

List of Appendices

Chapter 1

1 General Introduction

The function of sleep is one of the most longstanding mysteries of the brain. By contrast, understanding the function of resting state networks (RSNs) is one of the most recent frontiers and mysteries of the brain. The relationship between RSNs and neuronal activity has been unclear since RSNs were discovered during the advent of functional magnetic resonance imaging (fMRI) technology (Biswal, Yetkin, Haughton, & Hyde, 1995). Somewhat paradoxically, investigating these enigmatic phenomena in parallel can help to illuminate the function of both. More specifically, by exploiting sleep stages (along with wakefulness) as a factor of interest, it becomes possible to explore RSN dynamics during radically different brain operational modes, and thereby generate inferences with respect to RSN functions. Reciprocally, sleep dynamics can be viewed through the lens of changing RSN functional connectivity (FC) configurations in order to generate inferences with respect to sleep function.

The three studies described as part of this thesis all involve an evaluation of RSN dynamics across wakefulness and sleep. In the first study, the spatial boundaries of RSNs were evaluated in each stage. Here, for the first time, in an effort to catalogue RSNs across all healthy alternate functional modes of the brain, we sought to determine whether sleep functions necessitate the manifestation of RSNs unique to those of wakefulness. In the second study, between-RSN FC dynamics were evaluated in order to determine whether they reflect known cortical neurophysiological dynamics, as a means of further highlighting the connection between RSNs and neuronal activity. Additionally, given known associations between RSN FC changes and varying states of conscious awareness, the second study had implications with respect to the dynamics of awareness during sleep. One limitation on the second study's potential for generating inferences with respect to the neuronal origins of RSNs is the nature of the fMRI blood oxygen level dependent (BOLD) signal, which only indirectly measures neuronal activity. Consequently, an additional brain phenomenon was taken into account; namely, frequency-banded oscillatory activity, as measured by electroencephalography (EEG).

This approach has the advantage of leveraging a brain-activity recording modality that more directly reflects neuronal activity, in order to inform the fMRI analyses. In the third study, correlations between RSNs and frequency-banded activity were assessed dynamically across wakefulness and sleep, in order to track the frequency representation of neuronal activity in each RSN during different brain states.

In sum, the purpose of the studies that make up this thesis was to make use of the conjunction of three ambiguous brain-related phenomena in order to help shed light on the nature and functions of all (with a particular focus on sleep and RSNs). This introductory chapter is structured to provide relevant background for each of these three phenomena in turn (*i.e.,* sleep, RSNs and frequency-banded oscillations), followed by open questions. The last subsection indicates how the aims of each of the three studies addresses these open questions. Chapters 2 - 4 report the motivations, methods, findings and implications for each study, in detail. Finally, a General Discussion (Chapter 5), describes the overall implications of all three studies.

1.1 Sleep

1.1.1 Sleep stages

Sleep stages are identified using a combination of EEG, electro-oculography (EOG) and electromyography (EMG), collectively called polysomnography, or PSG (Rechtschaffen & Kales, 1968). However, given that the focus of this thesis is on sleep-related brain activity, the following subsections will focus on the defining EEG characteristics of each sleep stage.

1.1.1.1 Stage W (wakefulness)

Wakefulness can appear as prolonged periods, or embedded as brief awakenings within any sleep stage (Shrivastava, Jung, Saadat, Sirohi, & Crewson, 2014). The criteria for scoring an EEG epoch as wakefulness is the presence of more than 50% alpha activity (Iber, Ancoli-Israel, Chesson, & Quan, 2007), or the absence of any sleep-specific features when eyes are either closed or open. Alpha appears most strongly in occipital cortex when a subject's eyes are closed during relaxed wakefulness, possibly marking the

active suppression of visual information represented in the occipital cortex (Toscani, Marzi, Righi, Viggiano, & Baldassi, 2010).

1.1.1.2 Non-REM stage 1

Non rapid eye movement stage 1 (NREM1), also called light sleep, marks the onset of sleep, however it is really a transitional stage between wakefulness and NREM2, during which true sleep features appear. It is marked by low amplitude mixed frequency EEG activity (mostly in the theta frequency band), and is also characterized by the loss of posterior alpha-band power (Iber et al., 2007).

1.1.1.3 Non-REM stage 2

Non-REM stage 2 (NREM2) is the first true sleep stage. It is characterized by the first appearance of sleep spindles, or K-complexes (Iber et al., 2007). The theta rhythm is predominant during this stage, however delta waves can begin to appear, reflecting increasing cortical synchronization during this stage.

Sleep spindles are phasic bursts of neuronal activity lasting >0.5 seconds and up to as much as 3 seconds. They are generated in the thalamus; however their appearance is very much the product of significant feedback between thalamus and cortex (Contreras, Destexhe, Sejnowski, & Steriade, 1996). They are first triggered by cortical oscillatory activity that recruits thalamocortical neurons (with inhibitory input from reticular neurons which act to modulate spindle oscillations), which finally entrain spindles in the cortex, where they can be recorded by EEG (Steriade, 2005). There are two distinct types of spindles that oscillate in different frequencies, depending on the scalp location in which they manifest; slow spindles (11-13.5 Hz) in frontal areas, fast spindles (13.5-16 Hz) in parietal areas.

K-complexes are one of the largest events recorded by EEG in the healthy human brain (Cash et al., 2009). They are identified as a high amplitude negative spike in the EEG, followed by positive deflection. They can be followed by a spindle event, or alpha arousal. K-complexes can be either triggered by external sounds (called *evoked* K complexes), or can occur spontaneously. The presence of K complexes indicate

processing of the external environment during sleep, however it is thought that their function in this respect is to serve as a mechanism for inhibiting arousal and thereby maintain sleep (Cote, De Lugt, Langley, & Campbell, 2002; Forget, Morin, & Bastien, 2011). It is worth noting that spindles have also been associated with this potential role (Cote, Epps, & Campbell, 2000a).

1.1.1.4 Slow wave sleep

Slow wave sleep (SWS, also called deep sleep, non-REM stage 3, or NREM3), as the name suggests, is marked by the increasing presence (*i.e.,* > 20% of a sleep-scoring epoch) of high-amplitude, low-frequency (*i.e.,* 0.5 - 3 Hz) slow oscillations (Iber, Ancoli-Israel, Chesson, & Quan, 2007). In the deepest epochs of SWS, the entire EEG tracing can be made up of continuous trains of large amplitude slow oscillations. SWS is the stage in which the trend of increasing cortical synchrony becomes fully expressed. According to a number of markers, this stage is most dissimilar to wakefulness; ascending reticular activating system (ARAS) activity is inhibited, acetylcholine (ACh) levels are at their lowest, and the arousal threshold is highest (Hobson & Pace-Schott, 2002). As detailed further below, the definitive feature of sleep in smaller networks of neurons, *i.e.,* a burst/pause firing pattern, is most widespread during this stage. Significantly, SWS is longest during the first 90-minute ultradian sleep cycle and takes up a smaller overall proportion during subsequent cycles (over which REM begins to increase). Further, fatigue due to sleep deprivation is marked by localized initiation of SWS, prior to whole brain sleep. There is a strong biological drive for SWS, as suggested by the strong homeostatic response in slow wave activity during prolonged wakefulness or sleep deprivation (Finelli, Borbély, & Achermann, 2001; Werth, Achermann, & Borbély, 1996).

1.1.1.5 Rapid eye movement sleep

REM is identified by the presence of theta and alpha waves, as well as EOG-recorded eye saccades. While the EEG is similar to that of wake, EMG is significantly lower and the eyes are closed (Iber, Ancoli-Israel, Chesson, & Quan, 2007). REM is also known as paradoxical sleep, on account of these similarities to wakefulness. The resemblance of the

EEG is backed up by perceptual accounts of REM dreaming. Dream reports from REM awakenings have been found to be the most vivid (Antrobus, 1983), comparable to the richness of wakefulness perception. However, dream content is notably bizarre, which may be a consequence of reduced executive processing in frontal cortical regions during this stage (Braun et al., 1998). REM is shortest during the first sleep cycle, and increases progressively with subsequent cycles.

REM neurophysiology is very different from that of NREM stages. The ARAS is brought back online, allowing for the upregulation of cortical ACh levels, which, in cats, have been found to increase by 116% of baseline SWS levels, which is comparable to quiet wakefulness (Marrosu et al., 1995). This dramatic increase facilitates cortical desynchronization, akin to wakefulness. This stage may also involve pontine-geniculo-occipital (PGO) waves; endogenously-generated, propagating neuronal activity. These are initiated in the pons and may be the reason behind the increased visual content (*i.e.,* the vivid quality) of REM dreams. PGO waves have been recorded in several species of non-human animals but have yet to be identified in humans, on account of the invasiveness of recording from the relevant brain areas. However it is presumed that humans have similar neural circuitry and mechanisms (Gott, Liley, & Hobson, 2017).

1.1.2 General sleep mechanisms

1.1.2.1 Bottom-up vs. top-down sleep mechanisms

Sleep is best understood as a collection of interacting bottom-up and top-down processes. Although the global *regulation* of sleep is dependent upon top-down coordination by specialized sleep circuitry, the spontaneous development of a generalized sleep/wakefulness rhythm, appears to be a bottom-up, emergent phenomenon of neuronal networks of any size[1]. That said, specific sleep features beyond general sleep/wake rhythms, such as sleep spindles, K-complexes and the rapid eye movement (REM) state,

[1] In this general case, sleep is simplified to synchronized activity (typically a bursting/pause firing pattern) and wakefulness is simplified to tonic, desynchronized neuronal activity capable of interacting with environmental stimuli.

manifest only as a consequence of the activity of more specialized circuitry. Specifically, circuitry capable of initiating unique interactions between cortical and non-cortical regions, particularly thalamocortical interactions (Hobson & Pace-Schott, 2002). Evidence for the bottom-up emergence of a sleep/wakefulness rhythm is as follows:

(1) Any population of neurons will spontaneously establish sleep/wakefulness rhythms. C. elegans, with only 302 neurons, enters a periodic, sleep-like state known as lethargus (Raizen et al., 2008). In the mammalian brain, individual cortical columns alternate between wake-like low-amplitude EEG activity and sleep-like high amplitude activity (Rector, Schei, Van Dongen, Belenky, & Krueger, 2009). Isolated neuronal networks from in-vitro cultures have also been shown to exhibit sleep-wake cycles (Hinard et al., 2012). Without stimulation, these cultures default to a low-frequency burst/pause firing pattern similar to that of cortical or thalamic neurons during non-REM (NREM) sleep. When stimulated with a mixture of excitatory neurotransmitters known to be upregulated during wakefulness, the cultures begin to exhibit a tonic firing pattern, similar to neurons in a wakefulness state, in vivo. Further, with the withdrawal of external stimulation, this firing pattern eventually reverts to a burst/fire pattern spontaneously.

(2) Significantly, no brain region is so crucial to sleep, that its loss or dysfunction is capable of preventing the eventual emergence of a sleep rhythm, disturbed or otherwise (Krueger, Huang, Rector, & Buysse, 2013). This is true even for damaged subcortical regions comprising circuits that have been discovered to specialize in the regulation of sleep cycles. Sleep in such cases will of course be disturbed, either in terms of behaviour, electrophysiology or timing, however it will still be present. Further, so long as brain-injured patients survive, even coma states are temporary states; with few exceptions, some form of sleep-wakefulness cycle will eventually emerge (although typical polysomnographic sleep-scoring criteria often cannot be applied to disorders of consciousness patients; Cologan et al., 2010).

By contrast, the evolution of specialized top-down sleep circuitry is largely concerned with carefully coordinating the global *timing* of whole-brain wakefulness/slow wave

sleep rhythms, rather than directly generating sleep itself. The following sections describe these global sleep-coordination mechanisms.

1.1.2.2 The two-process model

According to the two-process model (Borbély, 1982), sleep timing can be predicted from the interaction of a circadian (*i.e.,* 24 hour) process ("Process C") with an independent homeostatic process ("Process S") that moderates the distribution of sleep and wakefulness. Sleep is triggered by the coincidence of Process S reaching its upper bounds (as a consequence of sufficient sleep pressure, tracked by EEG slow wave activity, or SWA) and an increased probability of sleep onset caused by Process C (tracked via the release of melatonin and changes in core body temperature). A later elaboration (Achermann, Dijk, Brunner, & Borbély, 1993) includes the description of an ultradian cycle (lasting roughly 90 minutes), regulating the alternation of REM and NREM within sleep.

Importantly, Process S has been shown to have a local component, such that the amount of waking activity in a given cortical area influences the extent of SWA in that region during early sleep stages. For example, unilateral hand stimulation prior to sleep results in an increase in EEG-recorded delta frequency power (a marker of SWA, which comprises both delta frequencies and the slow oscillation) over the contralateral somatosensory cortex during the first NREM sleep cycle, relative to unilateral somatosensory cortex (Kattler, Dijk, & Borbély, 1994). Further, SWA follows an anterior to posterior power gradient, with higher power in frontal cortical regions, as compared with parietal and occipital cortex. This is particularly true during early sleep cycles and following sleep deprivation (Finelli, Borbély, & Achermann, 2001; Werth, Achermann, & Borbély, 1996). These latter findings could be a reflection of higher processing demands on frontal cortical regions, which are thought to implement higher-order cognitive operations during wakefulness.

Taken together, this evidence of a local component to Process S is consistent with the concept of sleep as both a top-down and a bottom-up process. Specifically, the timing of sleep is a consequence of global coordination, however local regions require different

levels of compensatory SWA, as a consequence of differing local sleep debt. In other words, local networks experience different sleep pressures depending on the demands of prior waking activity; however, top-down circuits coordinate sleep so that all regions enter sleep during similar timeframes regardless of this variability. Barring global coordination, local networks would otherwise enter sleep in accordance with their respective pressures. Indeed, there is evidence that sleep deprivation causes local cortical neuronal populations to express SWA, in advance of global signals for initiating sleep, and despite the remainder of the brain being in an awake state (Vyazovskiy et al., 2011). It has been suggested that the poor behavioural performance that accompanies sleep deprivation and fatigue may be a consequence of parts of the brain being in a sleep state. Sleep deprivation notwithstanding, these findings suggest that different cortical regions, as defined by RSNs or otherwise, necessarily experience different synchronization demands during sleep (possibly expressed as differential FC). Such synchronization demands would be commensurate with their activity, or function during wakefulness.

1.1.2.3 Sleep-specific circuitry

The circadian-timing of Process C is regulated by neurons in the suprachiasmatic nucleus (SCN), located in anterior hypothalamus. It is reciprocally connected to the ventrolateral preoptic nucleus (VLPO), an important trigger for NREM sleep that is also located in the hypothalamus. Process S is thought to be regulated by separate and mutually-inhibiting sleep- and wake-promoting nuclei located in the hypothalamus, the caudal midbrain and the rostral pons (Saper, Chou, & Scammell, 2001). NREM sleep is initiated when neurons in the VLPO release inhibitory neurotransmitters (gamma aminobutyric acid, or GABA, as well as galanin) that mitigate the activity of arousal-promoting nuclei located in the brainstem and in the posterior lateral hypothalamus. These nuclei are collectively known as the ARAS.

The principal function of the ARAS is to disrupt cortical synchronization (recorded as high-voltage, low-frequency slow wave oscillations in EEG) and thereby facilitate the low-voltage high-frequency desynchronized activity necessary for implementing wakefulness cognition (Moruzzi & Magoun, 1949). In a similar way, the ARAS is involved in the generation of REM sleep, which manifests rich, wake-like dream content

(Hobson, Pace-Schott, & Stickgold, 2000a). The ARAS does this primarily by upregulating the excitatory neurotransmitter acetylcholine (ACh) in the cortex, via nonspecific thalamocortical pathways (Jones, 2008). In cats, cortical ACh levels were found to be 130% higher during quiet wakefulness, as compared with baseline slow wave sleep (SWS) levels, and 180% higher during active waking (Marrosu et al., 1995). These mechanics have been replicated in isolated cell cultures, in which the introduction of ACh has been shown to reduce the synchronization of action potential firing (Pasquale, Massobrio, Bologna, Chiappalone, & Martinoia, 2008).

When the ARAS is inhibited during NREM, the activity of thalamocortical neurons is attenuated, resulting in the isolation of the cortex from exteroceptive input. Cortico-cortical communication is not attenuated however, and slow oscillations originate from the cortex, characterized by an extended hyperpolarization period followed by a comparably extended “bursting” fire period (Steriade, 2001). These slow oscillations serve to coordinate other NREM oscillations such as sleep spindles and slow waves (Steriade, 2006).

It is thought that the ultradian cycle is mediated by two opposing neuronal populations with reciprocal activity time-courses; a group of cholinergic "REM-on" neurons in the pontine reticular formation and aminergic "REM-off" neurons in the locus coeruleus and dorsal raphe nucleus (*i.e.,* the reciprocal interaction theory, McCarley & Hobson, 1975; updated as the limit cycle model, McCarley & Massaquoi, 1986).

1.1.3 Putative functions of sleep

The possible functions of sleep are perhaps best categorized into those that involve the brain and those that involve the body, *i.e.,* somatic theories. The first section will first briefly outline theories of somatic functions for sleep, namely; immune and metabolic functions. The apparent necessity of dramatically reduced conscious arousal during sleep, involving highly restricted processing of environmental stimuli that, in turn, radically compromises safety, strongly suggests that sleep largely exists to serve necessary brain-related functions. Brain-related functions are therefore outlined in greater detail.

1.1.3.1 Somatic functions of sleep

It has long been suggested by physicians that sleep serves an immune function. This has been tested experimentally; there is evidence suggesting that reduced sleep compromises immune function and further, that sleep facilitates recovery from disease (Toth, 1995). Sleep is also associated with reduced caloric consumption/metabolic activity, and lower body temperatures, and it has been suggested that at least one of its functions is to conserve energy for the following day (Jung et al., 2011). However, it is not clear why any of these functions cannot be accomplished during periods of wakeful rest (Frank, 2006; Watson & Buzsáki, 2015).

1.1.3.2 Brain-related functions of sleep

As discussed above, the heavily restricted processing of environmental stimuli during sleep strongly suggests that it serves a necessary brain-related function. It follows that studies of brain activity during sleep might therefore yield the greatest insight into the function of sleep. Brain-related functions can be further subdivided into neuro-metabolic and neuro-cognitive functions (Frank, 2006)

1.1.3.2.1 Neuro-metabolic functions of sleep

It has been suggested that sleep serves to conserve or to restore energy supply in the brain (Benington & Craig Heller, 1995). Notably, brain metabolism is lower in NREM sleep, with positron emission topography (PET) studies indicating reduced glucose consumption during these stages (Heiss, Pawlik, Herholz, Wagner, & Wienhard, 1985). However, glucose consumption returns to or exceeds waking levels during REM sleep. Further, sleep studies of adenosine triphosphate (ATP) levels, a marker of cellular energy usage, are inconclusive with respect to the restoration of energy in the brain across sleep (Krueger, Frank, Wisor, & Roy, 2016). Glymphatic theories have also been proposed, suggesting that sleep facilitates the removal of neurotoxins. Removal of amyloid-β, a marker of Alzheimer's disease, from the brain, has been found to improve during sleep (Xie et al., 2013). Overall however, evidence that sleep exists primarily to serve a neuro-metabolic function is weak. Further, it does not explain the necessity for prolonged

periods of lost consciousness, or the complexity of sleep features and architecture (Frank, 2006).

1.1.3.2.2 Neuro-cognitive functions of sleep

There is a growing body of evidence that strongly suggests that the primary function of sleep is related to cognition. Although long disputed, the connection between sleep and learning/memory now has significant experimental support; the present debate largely concerns which stages are relevant to memory consolidation, which kinds of memory are consolidated and by what mechanisms (Stickgold & Walker, 2005). Evidence of procedural memory improvements, particularly related to NREM2 spindles, has strong support (Fogel & Smith, 2011; Walker, Brakefield, Morgan, Hobson, & Stickgold, 2002). The theory of *active system consolidation* (Born & Wilhelm, 2012) suggests that memories that are weakly encoded by hippocampal circuits are actively replayed during SWS, in order to facilitate consolidation in the cortex. Further, there is evidence of a connection between sleep (spindles, in particular) and cognitive abilities, specifically reasoning (Fang, Ray, Owen, & Fogel, 2019a). This suggests that the normal and efficient generation of sleep spindles is necessary to support normal intellectual ability.

At the synaptic level, long term-potentiation (LTP) and –depression (LTD) respectively strengthen and weaken connectivity weightings between synapses, depending on usage (Bear & Malenka, 1994). These molecular mechanisms are thought to underlie learning and memory at the neuronal level (Cooke & Bliss, 2006). There is evidence that LTP can be induced during REM (Bramham, Maho, & Laroche, 1994), suggesting that memory is consolidated during this stage. Partially in contrast to the idea that sleep serves to strengthen connectivity via LTP, the synaptic homeostasis hypothesis (SHY; Tononi & Cirelli, 2003) proposes that the primary function of SWA during NREM is to globally downscale synaptic potentiation. This downscaling would act as a homeostatic mechanism, in order to return total synaptic weightings to a baseline level. Returning the brain to such a baseline would help maximize cognitive plasticity for the following day (“sleep is the price we have to pay for plasticity”).

However (as pointed out in Watson & Buzsáki, 2015), where SHY and other synaptic-homeostasis theories suggest that synaptic connections are weakened during sleep, memory-related theories seem to require the opposite. If sleep in fact serves both functions, how can these opposite processes be reconciled? Watson and Buzsaki draw attention to the sharp-wave ripple (SPW-R), a hippocampal rhythm that is coupled with many other rhythms (including slow waves and spindles), and which also seems to be involved in the neuronal replay of waking behaviour (Karlsson & Frank, 2009). They suggest that, during SWS, cortical slow waves prompt hippocampal SPW-Rs to replay waking memories to the cortex, where it can be encoded in long-term storage. They also point out, first, that neuronal firing rates steadily decrease across successive sleep cycles, but that the majority of this rate decrease is accounted for during REM, which only ever follows SWS. They suggest that LTP/memory consolidation is implemented first, during SWS, followed by global synaptic downscaling during REM. This allows for decreases in synaptic weighting, even in local circuits relevant to the encoding of a given memory, (consistent with a synaptic homeostasis function), without compromising the *relative* strengthening of these connections (consistent with a memory consolidation function). This contradicts the mechanisms proposed in SHY (which suggested that downscaling takes place during SWS), but at least explains how both functions can take place during sleep.

Finally, the REM "wakeup hypothesis" (Klemm, 2011) proposes that, irrespective of the specific function subserved by SWS, it is highly dysfunctional with respect to waking adaptive behaviour. The brain therefore needs a continual reminder of how to engage in waking cognition, lest it should get stuck in such a maladaptive brain state forever. This theory suggests that REM evolved as a means of implementing such a reminder. Hence the aforementioned similarities shared by REM and wakefulness (which are in direct contrast to both the neurophysiology of NREM and the mechanisms used to engage it).

1.1.4 Open questions: what can RSNs tell us about sleep?

If the primary function of sleep is truly neuro-cognitive, as the literature indicates, this would suggest an important role for RSNs. As will be elaborated upon in the following section, RSNs are an attractive way to parcellate brain activity due to their spatial

similarity to what is known about the neural substrates of various cognitive functions. Moreover, RSNs are inherently defined and distinguished from each other as regions of strongly correlated activity and, further, inter-RSN relationships are also defined by the extent of this correlated activity. Thus, their very nature is highly suggestive of a natural role in the implementation of synaptic strengthening and downscaling, which are recurrent themes in theories of sleep function. If RSNs do play a role in sleep function then the following questions remain:

(1) Do RSN dynamics during sleep provide evidence to support any of the aforementioned theories of neuro-cognitive sleep function?

(2) Do the aforementioned sleep functions necessitate the manifestation of new RSNs unique from those of wakefulness, such that RSNs might comprise an additional mechanism for implementing sleep functions? If not, is the reverse the case; *i.e.,* is one of the further functions of sleep to implement RSN FC changes?

1.2 Resting state networks

Much like sleep, RSNs are very much a phenomenon in search of a function. The first complication in this search is the nature of the BOLD signal used by fMRI to capture RSN activity. It is only due to a small quirk of the hemodynamic response that we are able to use BOLD to make inferences about neuronal activity. It turns out that neuronal activity causes a disproportionate local increase in arterial cerebral blood flow (CBF), and therefore in oxygenated hemoglobin, dwarfing the amount of oxygen that can be metabolized by local tissue. This, in turn, results in an increase in venous oxyhemoglobin and a proportionate decrease in venous deoxyhemoglobin (which has magnetic properties that cause it to interfere with the BOLD signal); the upshot is a BOLD signal increase. If, instead, oxygen supply always matched metabolic demand, there could never be a detectable BOLD signal difference in response to neuronal activity (Buxton, 2013). Nevertheless, fMRI only ever measures changes in venous deoxyhemoglobin

(technically, it does not even measure this directly[2]), not neuronal activity. This naturally begets uncertainty with respect to the neuronal activity dynamics that fMRI is purported to capture; an uncertainty that is exacerbated by the further inferential problems of the resting-state paradigms used to derive RSNs.

In a hypothesis-driven fMRI paradigm, the timing of the BOLD signal difference can be modeled in accordance with the timing of provided stimuli. A general linear model (GLM) can then be used to identify brain regions whose BOLD activity patterns match the expected model (Friston et al., 1994). By contrast, resting-state fMRI studies are inherently data-driven: there are no stimuli onsets that can be used to model expected signal responses. Without such a model, it is difficult to establish whether the resting-state signal represents a response to external stimuli, or even to endogenous cognitive processes. A lingering concern is that resting state activity might simply be a physiological artifact related to CBF only, and is not an account of neuronal activity at all (Tong, Hocke, Fan, Janes, & Frederick, 2015; van den Heuvel & Hulshoff Pol, 2010).

Fortunately, there are ways to infer a connection between RSNs and neuronal activity, without having to use *a priori* models. In a GLM paradigm, it is inferred that neuronal activity is taking place because the change in BOLD signal coincides with known changes in stimuli that would be expected to change neuronal activity. A similar inference can be made for RSNs; if BOLD RSN activity is in some way modulated by global brain state changes that are known to change global neuronal activity, then this could be used as evidence that RSNs have some relationship with neuronal activity. Fortunately, it appears that such modulation does occur (see section 1.2.3, below). This is partly why the concern of many contemporary RSN studies lies in establishing the precise nature of the relationship with neuronal activity (Chen et al., 2017), rather than determining whether there is a relationship at all. The second study (outlined in Chapter 3) serves this important role.

---

[2] The fMRI scanner actually records electromagnetic signals emitted from hydrogen protons that have previously absorbed radiofrequency pulses emitted by the scanner. The diamagnetic properties of deoxyhemoglobin cause it to interfere with this returned signal, thereby inferentially indicating its presence.

Beyond such inferential paradigms, it would also be helpful to clarify the nature and function of RSNs by relating them to neuronal activity in a more direct manner. Instead of correlating changes in RSN activity with contextual changes that are known to change neuronal activity, it would be more advantageous to correlate them with modulations of direct measures of neuronal activity. Studies interested in this more direct approach appear to have followed one of two general approaches. The first involves correlating BOLD RSN activity to concurrently collected data from a modality that is more closely tied to neuronal activity, such as electrocorticography (ECoG), or EEG (Chang, Liu, Chen, Liu, & Duyn, 2013; Hacker, Snyder, Pahwa, Corbetta, & Leuthardt, 2017; Mantini, Perrucci, Del Gratta, Romani, & Corbetta, 2007). The second approach involves generating inferences with respect to RSN activity based only on data collected from a non-fMRI modality, or relating such data to non-concurrently captured fMRI data (Florin & Baillet, 2015; He, Snyder, Zempel, Smyth, & Raichle, 2008). The drawback of the second approach is that it has the reverse problem that fMRI-only paradigms have: they are more directly related to neuronal activity at the cost of being only inferentially related to RSN activity, which is best captured via fMRI. The third study (Chapter 4) follows the first approach, by correlating RSN activity, as determined using fMRI, with frequency-band activity, as determined using concurrently-recorded EEG.

1.2.1 Identifying RSNs

There are two widely established means for identifying RSNs (van den Heuvel & Hulshoff Pol, 2010). The first uses independent component analysis (ICA) to derive RSNs from a data-driven approach. The second uses seed-based correlation analysis (SCA) to identify RSNs by making use of regions that have been determined *a priori* to localize RSNs.

ICA methodology

ICA is a methodology for separating signals recorded by multiple sensors into separate, independent “source” signals that are presumed to be (linearly) mixed within the recorded signals. ICA works by minimizing the Gaussianity of the recorded signals, in order to restore the original source signals (McKeown et al., 1998). In the context of resting state

fMRI, the recorded signals are the BOLD activity time-courses recorded for each voxel, and the source signals are independent components (ICs). If the voxel data is plotted on multidimensional axes (one axis per voxel), the distribution of BOLD amplitudes along a given axis should be Gaussian. By rotating and maximizing the entropy of such a multidimensional dataset along an *a priori*-defined number of axes (Bell & Sejnowski, 1995), the distributions of amplitudes along each axis become minimally Gaussian (this only works if the sources are themselves non-Gaussian). The source signals/ICs can then be derived from the axes of this transformed dataset. Notably, the number of *a priori*-defined axes selected (called *model order selection* or *dimensionality selection*) is arbitrary, although there are data-driven methods for making this decision somewhat less arbitrary (Beckmann & Smith, 2004). In practice, an ICA model order decomposition corresponding to approximately 20-30 ICs has been found to be optimal for deriving the "canonical" RSNs from fMRI data. As will be discussed further below, the rationale for this model order number is largely driven by the general interpretability of the canonical RSNs.

SCA methodology

SCA uses the average BOLD time-course activity of a given region (selected *a priori*) as a "seed" that is correlated with remaining areas of interest, in order to identify other regions that have similar activity profiles (van den Heuvel & Hulshoff Pol, 2010). In the case of RSNs, these seeds are generally RSN nodes derived from prior ICA analyses, so in this sense, SCA is a fundamentally hypothesis-driven methodology. One notable exception is the very first RSN study, which identified the bilateral somatomotor network from a unilateral motor cortex seed region (Biswal, Yetkin, Haughton, & Hyde, 1995). Importantly, given that the first study described in this thesis attempted to discover new RSNs during sleep, the data-driven ICA methodology was used, as the use of SCA would only bias findings towards previously established RSNs.

Based on the methodologies of these two techniques, one overriding property of RSNs becomes apparent; they are fundamentally defined as regions of correlated activity. However, as discussed, the boundaries of this activity are arbitrary in the sense that they

are wholly dependent on the arbitrary number of dimensions chosen for an ICA decomposition (or, in the case of SCA, boundaries are dependent, *a priori*, on nodes based on "arbitrary" ICA results). Using a model order of 1, for example, would yield the entire brain as a single RSN. Alternatively, at the other extreme, one could have one IC for nearly every individual voxel in the fMRI dataset. What can a decomposition of 20 or 30 provide that the extremes do not?

The most salient answer is improved interpretability (Tagliazucchi & van Someren, 2017). There are a host of different publicly available brain parcellations (Arslan et al., 2018). For example, the automated anatomic labeling (AAL) atlas (Tzourio-Mazoyer et al., 2002), with 90 regions of interest (ROIs) across both hemispheres, has been implemented in (Spoormaker et al., 2010) and (Tagliazucchi & Laufs, 2014) to generate resting state FC maps in NREM sleep. These studies facilitate general conclusions about the differences in FC between wakefulness and NREM sleep, indicating, for example, that NREM1 sleep involves an overall increase in FC, relative to wakefulness. However, it is difficult for such studies to generate claims about, say, sensory processing, or to distinguish between sensory and higher-order processing, without first clustering the parcels into larger ROIs that correspond to regions associated with sensory processing and higher-order processing. By contrast, an ICA model order of around 20 generally facilitates such interpretations, as this typically yields the highly reproducible, so called "canonical" RSNs, which have been discovered to spatially correspond to regions known to be associated with cognitive functions (Smith et al., 2009). For example, the bilateral "auditory" RSN maps onto Heschl's gyrus and bilateral superior temporal lobes, regions that are known to act as cortical substrates for auditory processing. Nevertheless, until the function of RSNs can be fully clarified, the spatial importance of even the canonical RSNs will remain an open question.

Of course, even within an RSN there is still variability of correlated activity. A useful illustration of the differences in within- vs. between-RSN variability is the robust finding that the DMN has reduced FC between anterior and posterior nodes during SWS. This finding is established by using the posterior cingulate cortex (PCC) as an SCA seed (Horovitz et al., 2009). This kind of approach can shed light onto the sub-functions of

smaller hubs that comprise the larger-scale networks. Nonetheless, the DMN can still be robustly established as a "whole" network using ICA with a 30 model-order IC decomposition (Houldin, Fang, Ray, Owen, & Fogel, 2019).

1.2.2 RSN properties

As discussed above, although RSN studies often use SCA, the *a-priori*-identified nodes used in SCA are largely based on the findings of ICA studies (with the first RSN study being the exception). It is therefore most appropriate to discuss RSN and non-RSN properties in terms of ICA-derived IC properties.

1.2.2.1 What isn't a resting state network? Spatial and temporal features of non-neuronal independent components

In any ICA decomposition, many of the IC sources will correspond to non-neuronal artifacts. Fortunately, the spatial and temporal profiles of these artifacts are well characterized; so much so that automated software for identifying and removing them has been developed (Griffanti et al., 2014; Salimi-Khorshidi et al., 2014). Spatial features include; indiscriminate overlap with non-grey matter regions, *e.g.,* white matter, or cerebrospinal (CSF)-containing spaces such as the ventricles and the sagittal sinus; large numbers of small clusters, and; motion artifacts, typified by ring or crescent shapes at the edges of the brain. Temporal features include; high power at fast frequencies, or power distributed randomly across all frequencies; sudden spikes in IC timecourses, and; high timeseries correlation with motion timeseries, or their derivatives (Griffanti et al., 2017; Kelly et al., 2010a). Importantly, artifacts can only be identified by a combination of spatial and temporal features. For example, artifacts can have high power at low frequency (*i.e.,* similar to RSNs), and can only be distinguished from RSNs, in such cases, by carefully examining their spatial features.

1.2.2.2 What is a resting state network? Spatial and temporal features of neuronal independent components. The canonical RSNs, and their putative functions

Spatial IC features thought to reflect neuronal activity include; low numbers of large clusters, also called "smoothness" (*e.g.,* four large clusters for the DMN), and; good

spatial mapping onto grey matter areas, with low mapping onto brain boundaries. Temporal features include; high power at low frequency (*i.e.,* < .1 Hz), with very little power at higher frequencies), and; rhythmic timeseries activity, devoid of sudden spikes or flat lines (De Luca, Beckmann, De Stefano, Matthews, & Smith, 2006; Griffanti et al., 2017).

RSNs are generally subcategorized into sensory RSNs and "higher-order", or executive RSNs (Heine et al., 2012a). The sensory RSNs are primarily involved in the processing of unimodal sensory information, although of course each RSN comprises some degree of multimodal and association circuitry. They typically include; a somatomotor network comprising supplementary motor area, sensorimotor cortex, and secondary somatosensory cortex; an auditory network comprising superior temporal gyrus, Heschl's gyrus, posterior insula, and primary and association auditory cortices, and finally; three visual networks: a primary visual network encompassing bilateral striate cortex, a bilateral extrastriate visual network and a ventral stream visual network, which extends across bilateral inferior temporal lobes (Smith et al., 2009). A cerebellar network is also robustly identifiable, and has been implicated in emotion processing, though the three studies described in this thesis primarily focus on cortical RSNs.

Higher-order RSNs include two fronto-parietal (F-P) networks, one for each hemisphere. They comprise lateral PFC, dmPFC, frontal eye fields (FEF), and posterior parietal cortex. F-P networks are also called cognitive control networks, and are thought to play an important role in mediating externally-directed attention and cognition (Mulders, van Eijndhoven, & Beckmann, 2016). F-P networks can also be dissociated into ventral and dorsal attention networks (Corbetta & Shulman, 2002; Vossel, Geng, & Fink, 2014). The dorsal attention network (DAN), comprising intraparietal and superior frontal cortex, facilitates top-down, goal-directed attention. By contrast, the ventral system, comprising the temporal-parietal junction (TPJ) and inferior frontal cortex, is capable of interrupting the dorsal system, in order to draw attention towards salient information in the environment. F-P networks are also called "task-positive" networks (Fox et al., 2005) to contrast them with their opposite complement, the so-called "default mode" network (DMN), or "task negative" network. The DMN includes bilateral ventral and dorsal

medial PFC (v/dmPFC), posterior cingulate cortex (PCC) and the precuneus, bilateral parietal cortex, as well as associations with bilateral entorhinal cortex.

The DMN was first discovered in a PET study in which brain processing of attention-demanding stimuli was contrasted with the brain at rest. DMN regions decreased their activity during attention tasks, yet increased their activity during rest, particularly when the eyes were closed (Raichle et al., 2001a). As a consequence of this connection to restful waking states, it was initially thought to act as a kind of baseline, or "default" processing network. However, it has since been associated with many other types of processing, including the regulation of moods, social behaviour, internally-directed thoughts/daydreaming/remembering, as well as self-awareness (Raichle, 2015). The DMN has also gained particular importance on account of its consistent prominence in studies involving manipulations of conscious arousal, such as deep sleep (Horovitz et al., 2009), sedation (Boveroux et al., 2010), and studies involving brain-injured patients (Boly et al., 2009). Consequently, it is thought to play an important role in the manifestation of consciousness.

1.2.3 RSN functional connectivity

As discussed above, one of the strongest arguments in favor of connecting RSNs to neuronal activity, despite the inferential limitations of the BOLD signal, is the fact that RSN FC is known to be modulated by state changes that are also known to modulate neuronal activity. Significantly, such state changes include sedation, pathology, brain injury, shifts of cognition, and most relevant to this thesis, sleep.

RSN FC modulation by cognitive operations

Taken by itself, the finding of significant spatial overlap between RSNs and what is known about the neural substrates of cognitive functions (Smith et al., 2009) is already strongly suggestive of an important relationship between the two. This impression is extended, however, by RSN FC studies, which indicate that between-RSN FC changes correlate with individual differences in cognitive/executive function (Reineberg, Andrews-Hanna, Depue, Friedman, & Banich, 2015; Reineberg, Gustavson, Benca,

Banich, & Friedman, 2018). In particular, it has been shown that improved performance on executive tasks is associated with stronger negative FC between F-P networks and the DMN. This suggests that higher cognitive ability, in general, may be dependent on the increased segregation of the task positive/negative networks. Another study found a positive correlation between verbal reasoning abilities (*e.g.,* language comprehension) and negative FC between the auditory network and DAN (Naci et al., 2018). It was suggested that enhanced functional separation of higher-order RSNs and sensory RSNs might be related to improved cognitive performance. These findings did not appear to extend to other higher-order RSNs, however.

By contrast, improved task-switching was associated with stronger positive FC between F-P and visual RSNs, and between the DMN and sensory RSNs, generally (Reineberg et al., 2015). Intriguingly, cognitive decline associated with benign senescent aging was found to parallel reduced FC involving higher-order RSNs, such as the F-P and DMN, but not involving "emotion"-related networks, which were identified as networks that included inferotemporal areas, mPFC, as well as the cerebellum (Nashiro, Sakaki, Braskie, & Mather, 2017). Taken together, the conflicting results of these studies suggest that a nuanced view of the relationship between cognition and RSN FC is warranted. Since "cognition" is an umbrella term covering a multitude of divergent functions (*e.g.,* task-switching versus language comprehension), the mediation of these functions by specific RSN FC relationships is likely highly idiosyncratic. Importantly, however, it does seem that RSN FC changes are sensitive to the facilitation of these individual functions, furthering the impression that they play an important role in their manifestation.

RSN FC modulation by pathology

It is important to stress that for pathological conditions, the brain is most likely attempting to achieve healthy waking function. Consequently, modulations of RSN FC configurations during these states are best understood as partially successful attempts to replicate healthy waking configurations, rather than attempts to achieve unique configurations in a teleological sense. Epilepsy is associated with several RSN FC

alterations; in particular, decreased within-DMN FC is associated with both focal epilepsy and idiopathic generalized epilepsy (Centeno & Carmichael, 2014). Alzheimers disease is associated with reduced within-RSN FC in both the DMN (in particular, FC between MTL regions and PCC) and in executive attention networks (Sorg et al., 2007; Vemuri, Jones, Jack, & Jr, 2012; Wang et al., 2006).

Schizophrenia is widely thought to be a disconnection syndrome; consequently RSN FC changes can be expected to play a particularly important role in this disorder (Yu et al., 2012). SCA-based studies largely indicate reduced FC associated with schizophrenia; when the PCC was used as a seed, FC with the remaining nodes of the DMN was found to be reduced (Bluhm et al., 2007). Intriguingly, schizophrenia patients with auditory hallucinations were found to have reduced interhemispheric FC between auditory networks, reinforcing the concept that disconnected information plays a role in schizophrenia (Gavrilescu et al., 2010). It is possible that this facilitates the misattribution of endogenous information to exteroceptive sources during hallucinations.

Finally, it is worth mentioning, here, two other conditions that, similar to pathology, could also be viewed from the perspective of (largely failed) attempts to replicate healthy waking RSN FC configurations and functions. These are sedation and traumatic brain injury (TBI). However, as these conditions are pertinent as context for a more speculative discussion in Chapter 5, it is more appropriate to review the relevant literature in that chapter (see Section 5.2.2).

RSN FC modulation by sleep

By contrast to the RSN FC configurations of pathology, sedation and TBI, the coordinated reconfiguration of RSN FC during sleep definitively does *not* reflect an attempt to facilitate healthy wakefulness functions or to replicate healthy wakefulness RSN FC configurations. Sleep comprises at least two healthy alternate functional modes of the brain (*i.e.,* NREM and REM), each with unique objectives distinct from those of wakefulness. As discussed above, although these objectives have not yet been fully ascertained, it is clear from sleep neurophysiology and behaviour (which can only be considered maladaptive to the imperatives of waking survival) that these functions are

necessarily different from wakefulness. Therefore, the coordinated modulation of RSN FC configurations during sleep is best understood as an attempt to *differentiate* RSN FC from that of wakefulness, in order to better support functions unique from those of wakefulness.

Likely as a consequence of the challenges of acquiring fMRI sleep data in a noisy and uncomfortable scanner environment, there is a paucity of sleep FC studies, in general. It is therefore useful to summarize results from both RSN FC studies and FC studies which used non-RSN based parcellations. Such studies consistently indicate an overall increase in FC during early NREM sleep (*i.e.,* NREM1 and NREM2), relative to wakefulness FC. They further indicate an overall decrease in FC during deeper NREM sleep *i.e.,* SWS, relative to both wakefulness and early NREM sleep FC (Spoormaker et al., 2010; Tagliazucchi & Laufs, 2014). Corticothalamic FC is also reduced during NREM1, indicating a possible mechanism for impeding environmental stimuli during this early sleep stage; however it is quickly restored in NREM2 (during which K-complexes partly subserve this function). Significantly, a complete accounting of sleep FC during REM is conspicuously absent from these studies. Since REM is more common in later sleep cycles, and arousal threshold is lower than NREM sleep, the scanner environment makes it particularly challenging to acquire these data.

Significantly, there are no RSN FC studies that comprehensively evaluate trends across the complete range of NREM and REM stages. An indication of the nature of such trends can be garnered from the studies that do exist, however. RSN FC sleep studies indicate the persistence of the canonical RSNs during NREM sleep, including SWS (Tagliazucchi et al., 2013). There is also evidence that the brain becomes more modular in general during NREM sleep, with one study indicating an increase in the ratio of within-RSN FC to between-RSN FC across NREM sleep (Boly et al., 2012). This trend is supported by findings that the anterior and posterior components of the DMN become less cohesive during SWS (Horovitz et al., 2009), with another study indicating evidence for this breakup beginning as early as NREM2 (Larson-Prior et al., 2011). Notably, studies of NREM1 indicate that DMN FC is little different from wakefulness, however (Horovitz et al., 2008; Larson-Prior et al., 2009). Finally, one study of DMN FC in REM sleep

indicated a return of anterior/posterior coupling during this stage, following SWS decoupling (Chow et al., 2013). This study also found that the negative FC between the DMN and DAN, characteristic of wakefulness, disappeared during REM, suggesting a possible substrate for the bizarre dreams typical of this stage.

Overall, these studies suggest that NREM is marked by a progressive breakdown of wakefulness-like FC, manifested as increasingly isolated RSNs and even isolated nodes within RSNs. This coincides nicely with what we know from NREM neurophysiology, discussed above (Section 1.1.1). Namely, the shutdown of the ARAS results in a progressive decrease in ACh levels in the cortex across NREM, allowing corticocortical FC to revert to highly synchronized activity, in contrast to the marked desynchronized activity characteristic of wakefulness. It is important to stress however that an increase in synchrony between neurons does not necessarily suggest a concomitant increase in between-RSN FC, across the board; it only suggests a breakdown of wakefulness FC patterns.

Despite these findings, two things are missing from the overall picture: (1) A complete understanding of FC dynamics across wakefulness, NREM and REM (*i.e.,* FC changes in REM are poorly understood), and (2) A complete picture of the interactions of all the canonical RSNs (*i.e.,* prior studies largely focused on the DMN, with insights into the activity of other RSNs primarily in early NREM stages only).

Clues indicating a potential pattern of RSN FC changes across *all* stages can be found in modulations of DMN FC, for which we have the most complete picture. Specifically, there is a progressive breakdown of the DMN during NREM; in NREM1 DMN FC is mostly indistinguishable from wakefulness; in NREM2 the anterior and posterior nodes begin to reduce their FC, culminating in their dissociation during SWS. Finally, within-DMN FC is restored during REM sleep. Applying this within-RSN FC pattern to between-RSN FC, one can imagine a progressive deviation away from wakefulness FC during NREM and a return during REM.

1.2.4 Open questions: what can sleep tell us about RSNs?

(1) As discussed above, there seems to be an arbitrary quality to RSN spatial boundaries, *i.e.,* there is variability in both within- and between-RSN FC, so it is not entirely clear that the boundaries used to distinguish these two kinds of variability are meaningful. Also, as discussed in section 1.1, sleep (NREM, in particular) facilitates dramatic cortical synchronization changes. Finally, unlike pathological, sedation, or TBI states (for which no new, spatially distinct RSNs have been discovered), sleep comprises at least two healthy, alternate modes of the brain, and therefore cannot be considered a compromised attempt to achieve healthy wakefulness functionality. As a consequence of these three considerations, is it possible that the boundaries of RSNs might shift during sleep, or that new, spatially distinct RSNs might manifest? This possibility remains to be explicitly tested and explored.

(2) If RSNs truly reflect neuronal activity, then they should be impacted by state changes that are known to affect neuronal activity. NREM sleep entails a progressive increase in synchronized neuronal activity, from NREM1 to SWS. REM entails a return to wakefulness-like desynchronized activity, however it is also distinguished from wakefulness in a number of ways (*e.g.,* cortical ACh levels are not quite as high and the content of REM dreams is marked by bizarre features not present in waking perception). Do these trends in neuronal synchrony across sleep impact RSN FC in a predictable way, as would be expected if RSNs represent neuronal activity?

1.3 Frequency banded oscillatory activity

As argued above, one of the more effective ways of clarifying the connection between RSNs and neuronal activity is to relate BOLD RSN activity to signals from brain activity recording modalities that more directly reflect neuronal activity. EEG is one of several technologies that capture fluctuating electromagnetic fields that are themselves directly generated by the summed oscillatory activity of large neuronal populations. By splitting such summed signals into different frequency bands and binning this banded activity according to the length of a volume used to record BOLD signals, an EEG frequency-band model can be created. This model can be directly correlated with BOLD RSN

activity timeseries, in order to derive a picture of the neuronal frequencies represented within each RSN. This was the purpose of the third study in this thesis (Chapter 4).

For clarification; the focus of the third study was to make use of EEG frequency-banded activity to probe neuronal representation in RSNs, in order to complement the second study, which generated inferences of neuronal RSN activity by using sleep to manipulate the neurophysiological context of the brain. The purpose of the third study was not to use RSN activity (or sleep) to elucidate the nature of frequency-banded activity. The present section therefore focuses on oscillatory activity only insofar as it is relevant to clarifying the nature of RSNs.

1.3.1 The mechanics of neuronal oscillatory recording. Correlating EEG and BOLD signals. Common frequency-band groupings

The summed activity of all ionic processes occurring in brain tissue (including, but not restricted to neuronal action potential firing[3]) generates an electrical potential, or voltage. Differences in voltage between separate cortical areas create an electromagnetic field. The changing activity of this field can be recorded extracellularly at the scalp (where it is called EEG), at the cortical surface (where it is called ECoG), or in electrodes implanted within the cortical tissue (where it is called the local field potential, or LFP). Alternatively, the magnetic field perpendicular to this electric field can be recorded as well (called magnetoencephalography, or MEG), however each of these recording modalities ultimately chronicles the same phenomenon (Buzsáki, Anastassiou, & Koch, 2012).

The more distant recording modalities, in particular EEG, have low spatial resolution however, since voltage scales with the inverse of distance, and greater distances also result in signal interference from nearby fields. In theory then, EEG and fMRI complement each other well (Huster, Debener, Eichele, & Herrmann, 2012), with fMRI

---

[3] Anything capable of facilitating a transmembrane current can generate an electrical potential; *e.g.,* ionic charge differences across membranes in the dendrites, soma, axons, as well as glia. The resulting electric field therefore represents more than just synchronized fire amongst neurons.

making up for deficiencies in EEG spatial resolution, and EEG making up for the poor inferential power of the BOLD signal, with respect to neuronal activity (not to mention the superior temporal resolution of EEG making up for the poor temporal resolution of fMRI recordings). Importantly, given that the captured EEG signal represents summed activity, it can be decomposed into multiple frequency bands representing the separate neural populations that express different oscillations. This process is called spectral analysis, or spectral decomposition. The amplitude/power of a given frequency band is proportional to the number of neurons involved in expressing that rhythm. This power can be summed across time bins corresponding to the length of an individual volume of concurrent fMRI data, thereby creating a model[4] of expected activity that can be correlated with the activity timeseries of each RSN. Models created in this way facilitate a hypothesis-driven methodology, similar to GLM studies. Consequently, another drawback of resting state studies can be overcome; namely the inferential challenges of data-driven approaches.

Neuronal activity is commonly grouped into a series of frequency bands, generally categorized as follows: slow oscillations (0.5-1 Hz), delta (1-4 Hz), theta (4-8 Hz), alpha (8-12 Hz), sigma (12-16 Hz), beta (16-30 Hz), and gamma (30-60 Hz). Frequencies slower than the slow oscillation are termed infraslow, frequencies above gamma are called high-gamma or ultra-fast. Notably, the specific bounds of a given frequency band are up for debate. Further, some believe that beta and gamma should be grouped into the same category ("fast"), due to the rapid ability for neurons to transition between the two frequencies and evidence that there is no precise cutoff between the two (Slotnick, Moo, Kraut, Lesser, & Hart, 2002; Steriade, 2006; Steriade, Amzica, & Contreras, 1996).

---

[4] This model can be improved by convolving the binned frequency power timeseries with a hemodynamic response function (HRF), which itself models the delayed (and overcompensating) blood flow response to neuronal activity.

1.3.2 Relationships between frequencies. Phase-amplitude coupling

A general principle of frequency bands is that small populations of neurons coordinate their firing quickly via fast oscillations, thereby expressing fast frequencies, in proportion to the reduced time needed for signals to cross small distances[5]. By contrast, large populations coordinate their timing slowly, expressing slow frequencies, for opposite reasons (Buzsaki & Draguhn, 2004). Any large neural population, for example an RSN, necessarily comprises a multiplicity of neurons involved in different networks, however; with some neurons facilitating communication over long distances, and others over shorter distances. An RSN therefore necessarily manifests multiple frequencies; this has also been established experimentally (Mantini, Perrucci, Del Gratta, Romani, & Corbetta, 2007).

Beyond this general principle, given that slow frequencies can synchronize larger neural populations, it has been suggested that slower oscillations coordinate the activity of faster rhythms, in a hierarchical manner. There are several indications that this is indeed the case; for example, theta phase is known to modulate gamma amplitude in the hippocampus (Bragin et al., 1995a). Similarly, a study of auditory cortex in monkeys indicated the modulation of theta amplitude by delta phase, and the further modulation of gamma amplitude by theta phase (Lakatos et al., 2005). This kind of coupling is known as phase-amplitude coupling (PAC).

Significantly, the slow oscillation is capable of grouping other brain rhythms during sleep (Steriade, 2006). For example, sleep spindles (in the sigma frequency band), as measured using intracellular recordings of the activity of thalamocortical neurons in cats, were found to occur only during the depolarization phase of the slow oscillation, which was measured using depth EEG recordings in the cortex (Steriade, 2006). Further, it was found that groups of delta waves occur at intervals that match the period of the slow oscillation.

---

[5] It is important to clarify that "distance" is largely a function of the number of synaptic connections, not necessarily the geometric distance.

1.3.3 Frequency-banded neuronal activity representations in RSNs

As discussed above, each RSN comprises different neuronal populations operating at different frequencies, presumably serving both local-, and between-network functions. The results of the first attempt to correlate frequency-banded activity (as recorded using EEG) with RSN activity (as recorded using fMRI) confirm that each RSN does indeed manifest neuronal activity at every frequency band of interest. However, they manifest in different proportions, thereby signifying a unique frequency band "fingerprint" for each RSN (Mantini, Perrucci, Del Gratta, Romani, & Corbetta, 2007). Similar studies indicate high within- and between-subject variability in these fingerprints however, strongly suggesting that the correlation between BOLD RSN activity and EEG frequency-band power is unstable, at least during wakefulness (Gonçalves et al., 2006; Goncalves et al., 2008; Meyer, Janssen, Van Oort, Beckmann, & Barth, 2013).

1.3.4 Open questions: what can frequency-banded oscillatory activity dynamics during sleep tell us about the nature of RSNs?

(1) Sleep is accompanied by very dramatic shifts in neuronal synchronization. It is possible that such coordinated synchrony changes might stabilize the aforementioned high variability in RSN-frequency band correlations noted in wakefulness studies. Does changing neuronal synchrony across sleep affect RSN frequency band fingerprints in a predictable manner, just as it might be expected to affect between-RSN FC in a predictable way? Are different RSNs affected in different ways?

(2) As discussed, it is known that slower frequencies are capable of modulating the power of faster frequencies, via PAC, and further, that the slow oscillation coordinates the activity of other oscillations during sleep. Further, RSNs are defined as regions of highly correlated activity. These three factors strongly suggest that frequency-banded activity changes within RSNs should be coordinated in some way across sleep stages. Is there evidence of such coordination? If so, what can this tell us about the nature of RSNs?

1.4 Thesis aims

1.4.1 RSN accounting: do sleep-specific RSNs exist?

Prior to speculating on RSN function, it is prudent to first ensure that we have a complete picture of them. As discussed above, putative sleep functions are very different from those of wakefulness. Further, unlike pathological states (let alone sedation, VS, or MCS), sleep stages have evolved as healthy alternate functional brain modes. Given the connection between RSNs and localizations of cognitive function during wakefulness, it is reasonable to posit that the radically different, healthy functions of sleep might necessitate the manifestation of entirely new RSNs. Prior investigations of RSNs during sleep only examined the canonical RSNs (for example, using SCA to identify DMN changes during NREM), without explicitly trying to search for new RSNs, and little is known of RSNs in REM. The aim of the first study, as detailed in Chapter 2, was to rectify this knowledge gap by using a data-driven methodology (*i.e.,* ICA) to explicitly search for spatially unique RSNs in all sleep stages, including REM. Moreover, since sleep stages constitute the *only* healthy alternate functional modes of the brain, sleep stages and wakefulness would together comprise the complete search field for new RSNs. Thus, a search across all stages would help to ensure that we have established a complete RSN taxonomy.

1.4.2 Do RSN FC dynamics vary in accordance with known physiological changes across wakefulness and sleep? If so, what can this tell us about changes to conscious awareness?

As discussed in section 1.2.3, one of the most important arguments in favor of connecting RSNs to neuronal activity is that RSN FC is modulated by changes that are known to also modulate neuronal activity, for example shifts in cognition. Changes in sleep state are known to impact neuronal activity in a far more dramatic fashion than shifts of cognition, however. This is largely due to significant modulations of ACh levels, which cause wakefulness desynchronized activity to become increasingly synchronized during deepening NREM, and which facilitate a return to wakefulness-like synchronized activity during REM. If RSN FC dynamics were not impacted by these changes in cortical

neuronal synchrony, in a predictable manner, then the connection between RSNs and neuronal activity would be cast into doubt. The primary aim of the second study, as detailed in Chapter 3, was to test whether the pattern of RSN FC changes across wakefulness and sleep corresponds with the pattern of neuronal synchronization changes across these stages. A further aim was to generate inferences with respect to conscious awareness during sleep, given known connections between changing RSN FC and alterations of conscious awareness, as determined by studies of sedation and TBI.

1.4.3 How do EEG frequency bands map onto RSNs?

Although the second study has significant value in terms of linking RSNs with neuronal activity, this link could only ever be indirect, given the nature of the BOLD signal. More specifically, it could only be concluded from this study that changing cortical neurophysiology across wakefulness and sleep affects *both* neuronal activity and RSNs, in parallel, without being able to directly infer that RSNs could in fact be the substrate for these neuronal activity changes. In order to strengthen the assertion of a more direct inference, it is necessary to exploit brain activity recording modalities that more directly reflect neuronal activity. The aim of the third study, as detailed in Chapter 4, is to help bridge the gap between RSNs and neuronal activity by directly correlating RSN activity with EEG-derived frequency band activity across wakefulness and sleep. Similar to the second study, it was expected that these correlations should change in a predictable manner, in accordance with known changes to cortical synchronization across wakefulness, NREM and REM. Further, known PAC between the slow oscillation and other rhythms during sleep suggests that such a study might provide evidence that changing frequency representations, within specific RSNs, might be coordinated in some manner across frequencies.

Chapter 2

2 Toward a complete taxonomy of resting state networks across wakefulness and sleep: an assessment of spatially distinct resting state networks using independent component analysis

A version of this chapter has been published elsewhere (citation below) and is reproduced here with permission from the publisher, Oxford University Press on behalf of the Sleep Research Society (Appendix A).

Houldin, E., Fang, Z., Ray, L. B., Owen, A. M., Fogel, S. M. (2019). Toward a complete taxonomy of resting state networks across wakefulness and sleep: an assessment of spatially distinct resting state networks using independent component analysis, *Sleep*, Volume 42, Issue 3.
https://doi.org/10.1093/sleep/zsy235

2.1 Introduction

Resting state network (RSN) functional connectivity (FC) has been investigated under a wealth of different conditions including healthy wakefulness (Biswal, Yetkin, Haughton, & Hyde, 1995; Smith et al., 2013), sleep states (Horovitz et al., 2009), as well as compromised conditions, or altered states of consciousness, such as sedation (Boveroux et al., 2010), vegetative state (Boly et al., 2009), epilepsy (Centeno & Carmichael, 2014), Alzheimer's disease (Sorg et al., 2007; Vemuri et al., 2012; Wang et al., 2006) and schizophrenia (Yu et al., 2012). Such investigations often include considerations of both within- and between-RSN FC. However, such considerations are themselves dependent upon the defined spatial boundaries of the RSNs being investigated.

For the most part, these boundaries are taken for granted, as RSNs have now been studied for over two decades, beginning with the identification of the first RSN more than two decades ago, when it was shown that spontaneous activity of bilateral motor networks were strongly correlated with each other (Biswal et al., 1995). Further studies recognized

the existence of other RSNs, including the default mode network, a set of regions which first came under scrutiny because they collectively reduced their activity during goal-directed tasks (Shulman et al., 1997) and were finally determined to be a unique RSN in their own right when it was acknowledged that they functioned as an interconnected network for supporting "baseline" and internally-focused brain activity (Raichle et al., 2001b). The catalogue of reproducible RSNs is now well established, and they are commonly grouped into about ten canonical networks (see Figure 1A), typically comprising primary sensory networks (*e.g.,* auditory, somatomotor, and up to three visual networks) as well as higher order networks (*e.g.,* DMN, executive control and two independent, lateralized frontoparietal networks). These RSNs noticeably resemble the spatial organization of networks that support discrete cognitive functions (Damoiseaux et al., 2006; Smith et al., 2009). For example, the so-called “auditory” RSN involves bilateral regions in the superior temporal gyrus.

It is the spatial bounds of these canonical RSNs that serve as the basis for between- and within-RSN FC analysis in the aforementioned compromised conditions, states of reduced arousal, reduced sensory processing, altered-consciousness and sleep states. Specifically, the regions of interest (ROIs) whose timecourses are used to define RSN FC are based on a priori knowledge of the nodes of RSNs, as they are defined in wakefulness. For example, the well-established finding (Horovitz et al., 2009) that FC between anterior and posterior nodes of the DMN is reduced in slow wave sleep makes use of seed-based correlation analysis (SCA) wherein the seed of interest is the posterior cingulate cortex (PCC), an important DMN node identified in wakefulness. However, the application of RSNs defined in wakefulness to non-healthy, or sleep-related RSN FC analyses is not fully justified and the existence of novel RSNs specific to other states has never been explicitly tested or explored. This is the major aim of the current study.

Indeed, given the established association between the canonical RSNs and networks that support cognitive function during healthy wakefulness, it could be expected that non-canonical RSNs would arise to support offline information processing. That said, additional, non-canonical RSNs have yet to be identified in any investigations of non-healthy conditions or healthy sleep states. However, it is possible that such negative

findings are at least partly a consequence of biased analysis approaches that make the implicit assumption that the set of RSNs typically found in wakefulness apply to all other conditions. For example, a number of sleep studies have restricted their analysis to RSNs taken from the canonical set (*e.g.,* the default mode network; Horovitz et al., 2009) or explicitly looked for RSNs that resemble the canonical set (Tagliazucchi et al., 2013), rather than explicitly investigate whether unique RSNs might exist. It therefore remains to be tested whether non-canonical RSNs exist in non-healthy conditions or across healthy sleep-wake states.

Sleep is a particularly salient target for such a test, as it is a healthy alternate mode of the brain, with known functions distinct from the cognitive functions sustained during wakefulness. It is therefore possible that an unbiased search for non-canonical RSNs might yield RSNs associated with these sleep-specific functions. By contrast, compromised conditions or altered states of consciousness are less likely to manifest non-canonical RSNs given that they do not express new functions; rather the same functions which are expressed in wakefulness become impaired. Unique sleep functions that could manifest unique non-canonical RSNs include; memory consolidation (via memory reactivation and replay), involving the striatum, hippocampus and medial temporal lobe (Fogel et al., 2017; Marshall & Born, 2007; Rattenborg, Martinez-Gonzalez, Roth, Pravosudov, & Pravosudov, 2011; Stickgold, 2005); sleep spindle related activation that supports reasoning abilities, involving thalamo-cortical regions and basal ganglia (Fang, Ray, Owen, & Fogel, 2017); rapid eye movement (REM) sleep maintenance, including dream production, involving thalamus and occipital regions (Hobson, Pace-Schott, & Stickgold, 2000a; Klemm, 2011; Nelson, McCarley, & Hobson, 1983). Not to mention other putative yet-to-be-discovered functions of sleep.

In addition, sleep can itself be subdivided into at least two further stages, each of which is characterized by unique EEG signatures; *e.g.,* REM (demarcated by the presence of eye movements, loss of muscle tone and desynchronized low-voltage electrophysiological oscillations) and non-REM (NREM) stages. NREM sleep can be further subdivided into NREM stage 1 (NREM1), defined by a loss of posterior alpha band power; stage 2 (NREM2), which sees the appearance of EEG waveforms called sleep spindles and K-

complexes; and stage 3 (NREM3) dominated by extensive slow wave delta oscillations (Iber et al., 2007). Any of these stages may be accompanied by the manifestation of non-canonical RSNs in relation to these unique forms of neuronal communication that are remarkably distinct from waking brain activity.

The purpose of this study was to explicitly test whether new RSNs exist in sleep by examining all sleep stages for RSNs that do not match the canonical set. It was hypothesized that new RSNs would be identified and that these could be related to sleep-specific neural activation, functions or mentation specific to sleep.

2.2 Methods

2.2.1 Participants

Forty-five subjects were recruited for this study. Of these, nine failed to meet the inclusion criteria by not complying with the pre-study sleep/wake schedule, and were thus not included in the study. The remaining 36 were healthy right-handed adults (21 female) 18-34 years of age (M = 23.7, SD = 3.6). An *a priori* statistical power analysis was not performed, which could be considered a limitation, however the number of subjects included is consistent with previous studies investigating RSNs in sleep (Horovitz et al., 2009; Larson-Prior et al., 2009; Tagliazucchi et al., 2013). All participants were non-shift workers and medication-free, with no history of head injury or seizures, had a normal body mass index (<25), and did not consume excessive caffeine, nicotine or alcohol. Further, all scored <10 on the Beck Depression (Beck, Steer, & Brown, 1993) and the Beck Anxiety (Beck, Epstein, Brown, & Steer, 1988) Inventories and had no history or signs of sleep disorders, as indicated by the Sleep Disorders Questionnaire (Douglass et al., 1994). All participants were required to keep a regular sleep-wake cycle (bed-time between 22h00-24h00, wake-time between 07h00-09h00) and to abstain from taking daytime naps at least 7 days prior to, and throughout participation in the study. Compliance with this schedule was monitored using both sleep diaries and wrist actigraphy (Actiwatch 2, Philips Respironics, Andover, MA, USA). All participants met the MRI safety screening criteria. In addition, participants were given a letter of information, provided informed written consent before participation, and were

financially compensated for their participation. This research was approved by the Western University Health Science Research Ethics Board.

Of the 36 participants who met the study inclusion criteria, data for 34 participants was included in the analysis (see Table 1). One participant withdrew from the study due to discomfort. Another did not sleep during the EEG-fMRI session, but did have wake resting state data. Of the remaining 34 participants (21 female, M = 23.7, SD = 3.7), all had wake resting state data, but only 28 had some stage of sleep data above the bare-minimum 3-minute threshold. In addition, not all of the wake resting state data was used, as initially 5 minute wake resting state scans were used, and this was later modified to be 8 minutes, in the interest of maximizing data availability. Thus 29 participants were used in the analysis of the wake data (18 females, M = 23.8, SD = 4.0), in order to capitalize on the longer resting state episodes. Of the 28 participants who slept, data from 25 participants was used in the analysis of sleep stage NREM2 (15 female, M = 24.2, SD = 4.0). Of these same 28, 11 participants (6 female, M = 22.5, SD = 3.8) had NREM3 data. Finally, of these same 28, 7 participants (3 female, M = 22.1, SD = 2.4) had REM data.

Table 1. *Minutes of data extracted per sleep stage.*

Measure	WAKE	NREM2	NREM3	REM
Mean	7.9	15.9	18.9	9.8
Standard Deviation	0.0	10.5	18.9	8.0
Minimum (non-zero)	7.9	6.3	4.0	3.6
Maximum	7.9	44.1	67.3	21.6
N	29/34	25/34	11/34	7/34

REM = rapid eye movement sleep stage, NREM2/3 = non-REM2/3 sleep stages.

2.2.2 Functional data

Wake Data Set

A total of 36 participants had recorded wake RSN data. Of these, 29 had 7.9 minutes of data, with the remainder having only 5.4 minutes. To maximize the quality of the group ICA (*i.e.,* by maximizing the number of volumes used in the single subject data) the wake resting state analysis used the 7.9 minute datasets from the aforementioned 29 participants, for a total of 230 minutes of data.

Sleep Data Set

Overall, participants managed to obtain the full spectrum of sleep stages (NREM1, NREM2, NREM3 and REM sleep). On an individual basis however, the majority of participants maintained sleep in only a few of the stages for a duration long enough to be considered sufficient for ICA analysis. Given the difficulty in obtaining REM sleep in non-sleep deprived individuals in the MRI scanner environment (*e.g.,* due to noise and subject comfort), only 4 subjects managed to transition through all three sleep-stages of interest (NREM2, NREM3, REM) for a duration considered sufficient for the ICA analysis. In all cases, sleep scoring identified a pattern in which participants transitioned between sleep stages of variable duration; from less than 20 seconds (the shortest sleep scoring period) to 69.3 minutes (see Table 1 for the distribution of sleep data used in the final set of analyses). As expected, sleep stage NREM1 was mostly insufficient in duration for analysis purposes. Thus, considering the brief and transitional nature of this stage, it was not included in the analyses.

As the group-ICA analysis used in this study requires single-subject inputs of equal-length, participant fMRI data for a given sleep stage was segmented into equal length "blocks". Block length was determined by the length of the shortest available single subject dataset for a given sleep stage (so long as this length exceeded a bare-minimum 3 minutes). For example, if 10 participants had NREM3 data, and the participant with the least amount of data had 3 minutes worth, then the available data for the remaining participants was segmented into 3-minute blocks.

Twenty-eight subjects were able to sustain a sufficient amount of NREM2 sleep for the ICA analysis, with the shortest duration for a given participant being 4 minutes. In many cases, a single participant had more than one continuous bout of NREM2, such that the full group generated a total of 599 minutes of NREM2 data. Given the abundance of NREM2 data, the datasets for 3 participants were not included in order to maximize the length of an NREM2 block. Overall, 63 blocks of 6.3-minute duration acquired from 25 participants were used, for a total of 396.9 minutes.

In the case of NREM3, 11 participants had data above the minimum 3-minute cutoff, for a total of 236.4 minutes of available NREM3 data, with all of these participants having at least 4 minutes of data. Overall, 52 4-minute blocks were used in the ICA analysis of NREM3 data, for a total of 205.9 minutes of data.

Very few EEG-fMRI studies report analysis of REM sleep, and thus knowledge of REM sleep from fMRI studies is limited. Here, 7 participants had REM data above the 3-minute cutoff. Overall, 87.7 minutes of 3-minute plus duration data was available from all subjects. From this, 19 3.6-minute blocks were extracted for the REM ICA analysis, for a total of 68.4 minutes of data.

2.2.3 Experimental procedure

Each participant underwent a screening/orientation session one week prior to the experimental sleep session. The scanning session took place between 21h00 and 24h00, during which time simultaneous EEG-fMRI was recorded while participants slept in the scanner. Unlike the majority of similar past studies, subjects were not sleep deprived. The scanning session consisted of an 8-minute structural scan, followed by an eyes-closed wake resting state scan. Participants were then informed that they were free to fall asleep in the scanner. This period lasted up to 2.2 hours. To be included in the analysis of the sleep data, participants were required to sleep for a period of at least 5 minutes of uninterrupted NREM sleep during the sleep session, however in the final analysis no block of less than 3.6 minute duration was used. Following the sleep session, participants were allowed to sleep in the nearby sleep laboratory for the remainder of the night.

2.2.4 Polysomnographic recording and processing

EEG was recorded using a 64-channel magnetic resonance (MR)-compatible EEG cap (Braincap MR, Easycap, Herrsching, Germany) using two MR-compatible 32-channel amplifiers (Brainamp MR plus, Brain Products GmbH, Gilching, Germany). EEG caps included scalp electrodes referenced to FCz. Two bipolar electrocardiogram (ECG) recordings were taken from V2-V5 and V3-V6 using an MR-compatible 16-channel bipolar amplifier (Brainamp ExG MR, Brain Products GmbH, Gilching, Germany). Using high-chloride abrasive electrode paste (Abralyt 2000 HiCL; Easycap, Herrsching, Germany), electrode-skin impedance was reduced to < 5 KOhm. In order to reduce movement-related EEG artifacts, participants' heads were immobilized in the MRI head-coil using foam cushions. EEG was digitized at 5000 samples per second with a 500-nV resolution. Data were analog filtered by a band-limited low pass filter at 500 Hz and a high pass filter with a 10-sec time constant corresponding to a high pass frequency of 0.0159 Hz. Data was transferred via fiber optic cable to a personal computer where Brain Vision Recorder Software, Version 1.x (Brain Vision, Gilching, Germany) was synchronized to the scanner clock. EEG scanner artifacts were removed in two separate steps: 1) MRI gradient artifacts were removed using an adaptive average template subtraction method (Allen, Josephs, & Turner, 2000) implemented in Brain Products Analyzer, and down-sampled to 250Hz; 2) the r-peaks in the ECG were semi-automatically detected, visually verified, and template subtraction (Allen, Polizzi, Krakow, Fish, & Lemieux, 1998) was used to remove ballistocardiographic artifacts time-locked to the R-peak of the QRS complex of the cardiac rhythm. Finally, EEG was low-pass filtered (60 Hz) and re-referenced to averaged mastoids. Sleep stages were scored in accordance with standard criteria (Iber et al., 2007) using the “VisEd Marks” toolbox (https://github.com/jade466 sjardins/vised_marks) for eeglab (Delorme & Makeig, 2004).

2.2.5 MRI imaging acquisition and analysis

2.2.5.1 Recording Parameters

Brain images were acquired using a 3.0T TIM TRIO magnetic resonance imaging system (Siemens, Erlangen, Germany) and a 64-channel head coil. A structural T1-weighted MRI image was acquired for all participants using a 3D MPRAGE sequence (TR = 2300 ms, TE = 2.98 ms, TI = 900 ms, FA = 9°, 176 slices, FoV = 256 x 256 mm^2, matrix size = 256 x 256 x 176, voxel size = 1 x 1 x 1 mm^3). Multislice T2*-weighted fMRI images were acquired during the sleep session with a gradient echo-planar sequence using axial slice orientation (TR = 2160 ms, TE = 30 ms, FA = 90°, 40 transverse slices, 3 mm slice thickness, 10% inter-slice gap, FoV = 220 x 220 mm^2, matrix size = 64 x 64 x 40, voxel size = 3.44 x 3.44 x 3 mm^3). In order to obtain EEG with time-stable artifacts, which aligned to the timing of the EEG recordings, the MR scan repetition time was set to 2160 ms, such that it matched a common multiple of the EEG sample time (0.2 ms), the product of the scanner clock precision (0.1 μs) and the number of slices (40) used (Multert & Lemieux, 2009).

2.2.5.2 Functional data classification and block parcellation

All sleep session functional volumes were scored according to standard sleep-stage scoring criteria (Iber et al., 2007) by an expert, registered polysomnographic technologist. To be included in the fMRI analysis, the EEG had to be visibly movement artifact-free. Volumes were classified as wake, NREM1, NREM2, NREM3 or REM. Notably, wake data used in the analysis was taken from the wake resting state session only, despite segments of wake being present in the sleep session data. Following scoring, each segment of sleep-stage volumes was parcellated into equal-size blocks, whose length was specific to each given sleep-stage.

2.2.5.3 Preprocessing

Blocks were individually preprocessed using the Oxford Centre for Functional Magnetic Resonance Imaging of the Brain Software Library (FMRIB, Oxford U.K.; FSL version 5.09; Smith et al., 2004). Specifically, functional volumes within each block were realigned using FSL's MCFLIRT tool (Jenkinson, Bannister, Brady, & Smith, 2002)

which performs rigid body transformations. Non-brain voxels were also extracted using FSL's BET tool (Smith, 2002). Volumes were then spatially smoothed using a Gaussian kernel of 5mm full-width at half-maximum (FWHM) and highpass temporal filter (Gaussian-weighted least-squares straight line fitting, FWHM = 2000 s). Functional volumes were then registered to the MNI152 standard space (McConnell Brain Imaging Centre, Montreal Neurological Institute) using 12 degree-of-freedom affine registration. Finally, each block was individually cleaned of non-neuronal artifacts (e.g., cardiac pulsation, motion-related, white matter) using the FIX plug-in for the FSL package (Griffanti et al., 2014; Salimi-Khorshidi et al., 2014) an automatic noise detection and removal algorithm. Prior to using FIX, FSL's MELODIC tool (Beckmann & Smith, 2004) was used to generate a set of ICs for each block. MELODIC prewhitens and variance normalizes all timeseries prior to applying probabilistic ICA (PICA), which outputs a set of spatial maps converted into Z statistic maps based on estimated standard error of residual noise. MELODIC's default dimensionality estimation function automatically estimates the number of ICs by performing a Bayesian analysis. FIX assessed each of these ICs as noise or signal, after generating more than 180 distinct spatial and temporal features of each IC and feeding these into a multi-level classifier. Temporal features associated with non-neuronal ICs include sudden changes in time series' amplitude, frequency-domain power at high frequencies and correlation of the time series with white matter (WM) or cerebrospinal fluid (CSF) extracted time series. Spatial features include having a large number of small clusters and high overlap with brain boundaries or with WM/ventricles/CSF areas. FIX classification performance has been evaluated to have an average true negative rate (noise correctly classified as such) of 98.9% (Salimi-Khorshidi et al., 2014). ICs classified as noise were then subtracted from the ICA mixing matrix and a new set of "clean" functional volumes was generated.

2.2.5.4 Group-level analysis

Group spatial-ICA (with a model order of 30 components) was performed with MELODIC on all available blocks for a given sleep stage in order to maximize the available data for deriving group-level maps. The resulting 30 ICs (per sleep stage) were then individually compared with 10 canonical spatial templates derived from a separate

wake RSN study (see Figure 1A; Smith et al., 2009) using spatial correlation (FSL utility; fslcc). In order to be consistent with current approaches, a liberal spatial correlation threshold of $r = 0.2$ was selected (for comparison, Tong et al. (2015) and Reineberg et al. (2015) used similar cutoffs of $r > 0.25$ and $r > 0.21$, respectively) to help classify ICs as either resembling the canonical set or being a potentially new RSN for further inspection (See Figure 6 in the Supplemental Material for the distribution of available correlation values in this study). However both above- and below-threshold ICs were also (visually) examined carefully for spatial differentiation from the canonical set. It is important to emphasize here that the use of a specific spatial correlation threshold (statistically-based, or otherwise), will always be arbitrary, in the case of classifying ICs as RSNs. This is because RSN classification must always take into account other IC features, such as frequency-power. That said, a threshold of around $r > 0.2$ seems to work as a useful heuristic for early IC screening. Clearly identifiable noise-related below-threshold components were then screened by hand, in accordance with the general guidelines in Griffanti et al. (2017) and Kelly et al. (2010b). Note that it is impossible to completely separate noise from networks in fMRI data, at either the single-subject or group level, therefore noise ICs would be expected at the group level despite cleaning at the single-subject level (more specifically, timecourse patterns associated with noise can be too infrequent for ICA to detect at the single-subject level, yet, importantly, they can repeat sufficiently across multiple subjects, so that they manifest as statistically independent and can therefore be reliably detected at the group level). Briefly, in the screening procedure, IC spatial features were examined for overlap with non-grey matter areas such as those comprising WM or CSF IC and frequency-power spectra were examined for power distribution across all frequencies, or power concentration in high frequencies. The intention was to follow up this screening with a more sophisticated fingerprint analysis tool (De Martino et al., 2007), as well as a functional connectivity analysis between this component and the canonical RSNs, however the lack of remaining components following this screening procedure rendered such steps unnecessary.

Finally, we conducted a follow-up analysis in which we repeated the group-level ICA analysis described above, using a dataset consisting of all of the sleep stages combined together (note: in this analysis, the blocks were cut to the same length across sleep stages;

i.e., to 129 volumes). This was done in an attempt to determine whether the ICA might extract new spatial patterns that would otherwise be missed in an analysis of individual sleep stage data.

2.3 Results

Non-noise group-level above-threshold independent components (ICs) largely matched the RSNs from the external dataset (Smith et al., 2009), with low correlation components comprising constituent regions of a given canonical RSN rather than being located in a different spatial region entirely (see Figure 1 for sample images).

Sample below-threshold ICs are shown in Figure 2, along with their frequency-power spectra. All below-threshold ICs had time course properties which allowed them to be positively identified as non-neuronal artifacts, in accordance with standard identification procedures (Griffanti et al., 2017; Kelly et al., 2010a). For example, the first IC in Figure 2A overlaps significantly with WM regions and the second IC overlaps with CSF-containing regions and also has power distributed across all frequencies (*i.e.,* it is not restricted to low frequencies as is typical of RSNs). As such, contrary to our predictions, none could be said to represent spatially-unique RSNs differentiable from canonical RSNs in any sleep stage of interest.

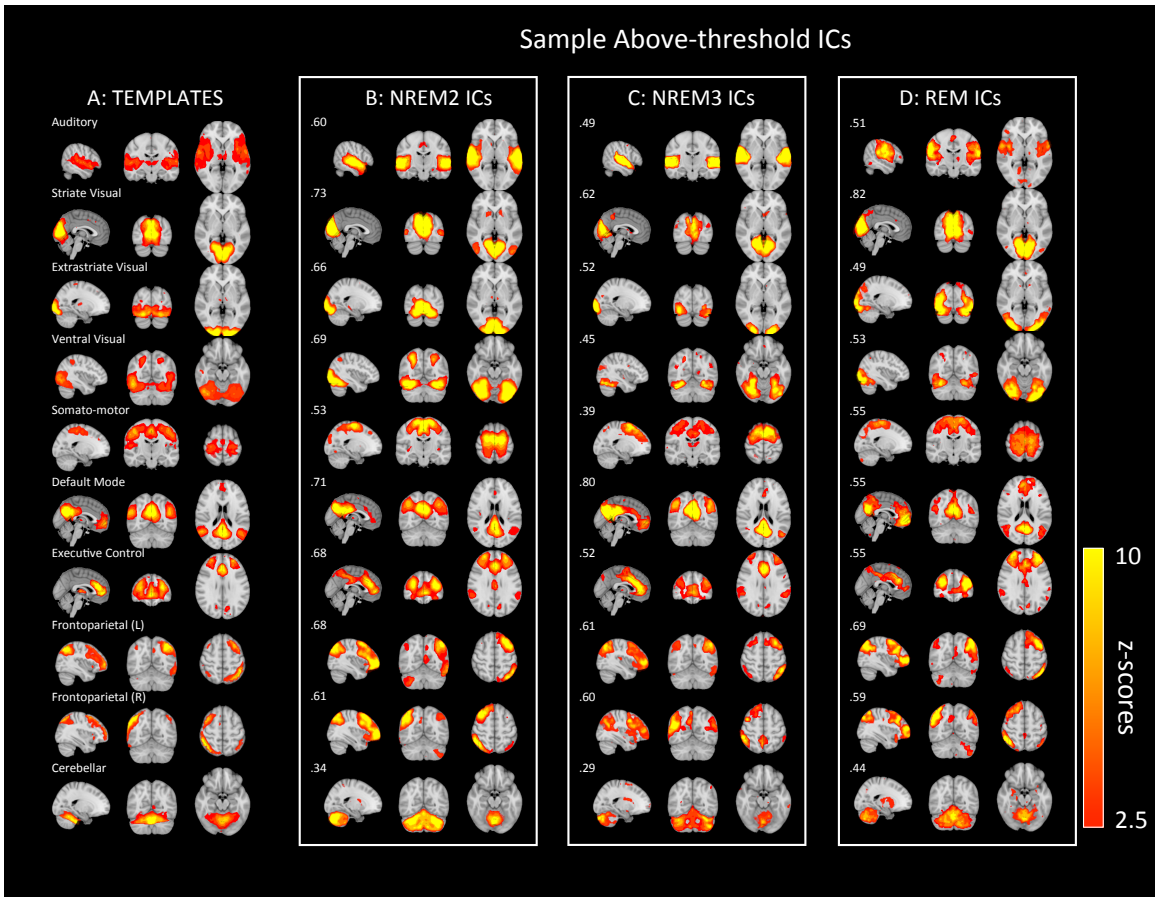

Figure 1. External templates used for spatial comparison and group-level above-threshold independent components (ICs) for each sleep stage.

(A) The 10 external templates used in the spatial correlation, with representative sagittal, coronal and axial slices. (B, C, D) Group-level above-threshold ICs with the highest spatial correlations to each of the 10 external templates, for each sleep stage. Color bars indicate Z statistics based on the estimated standard error of residual noise. Spatial correlation values with respective templates are presented in the upper left corner for each IC. NREM2/3 = non-REM sleep stage 2/3, REM = rapid eye movement sleep stage.

The follow-up analysis (in which the group ICA was performed on a dataset comprised of all the sleep-stage data combined together) yielded similar results; i.e., above-threshold ICs largely matched the RSNs from the external dataset and below-threshold ICs were positively identified as non-neuronal artifacts (see Figure 3 for sample images).

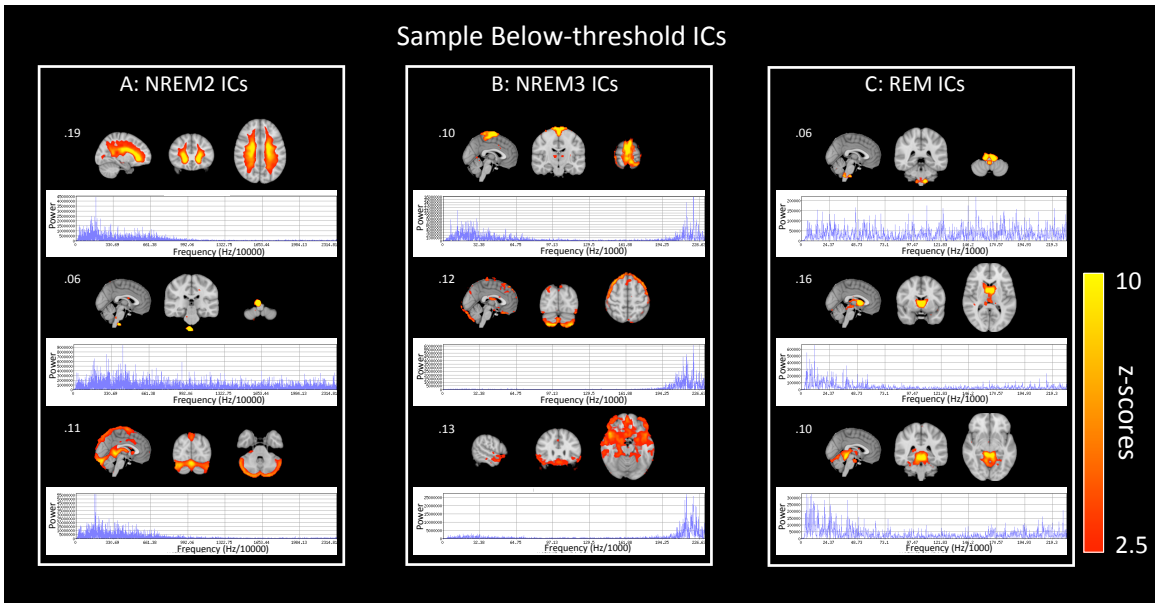

Figure 2. Sample below-threshold independent components (ICs) in each sleep stage.

(A, B, C) A selection of below-threshold group-level ICs, for each sleep stage (representative, sagittal, coronal an axial slices shown). Color bars indicate Z statistics based on the estimated standard error of residual noise. Frequency-power spectra are shown immediately below each IC. Highest template-correlation value is indicated in top left corner for each IC. NREM 2/3 = non-REM sleep stage 2/3, REM = rapid eye movement sleep stage.

Finally, for reference, color-coded correlation values for all 30 group-level ICs for all stages (including the combined-stages dataset) are presented in the Supplemental Material section, below (see Figures 4 and 5), with their best-matched external templates indicated.

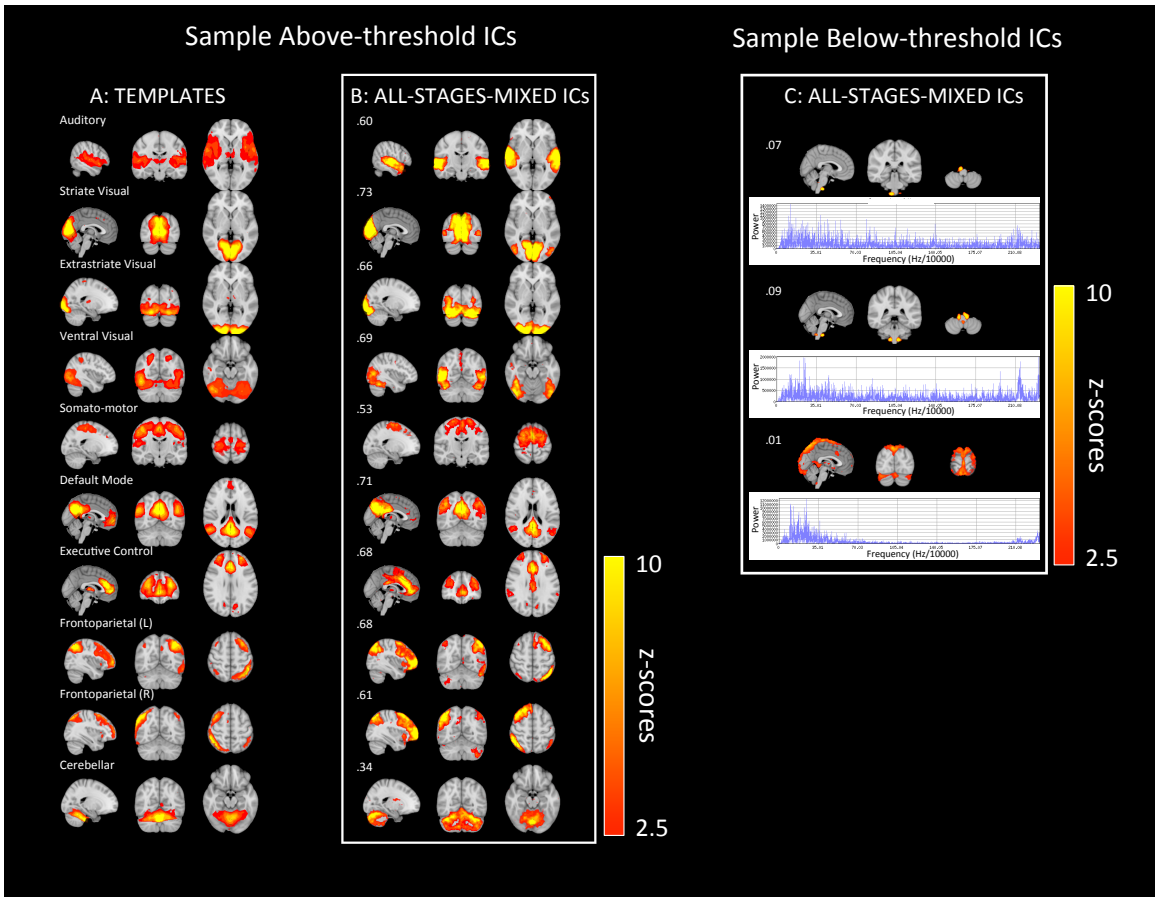

Figure 3. External templates used for spatial comparison and group-level above-threshold independent components (ICs), with sample below-threshold ICs for a dataset comprised of all sleep stages combined.

(A) The 10 external templates used in the spatial correlation, with representative sagittal, coronal and axial slices. (B) Group-level above-threshold ICs with the highest spatial correlations to each of the 10 external templates, for a dataset comprised of all sleep stage data combined together. Color bars indicate Z statistics based on the estimated standard error of residual noise. Spatial correlation values with respective templates are presented in the upper left corner for each IC. (C) A selection of below-threshold group-level ICs (representative, sagittal, coronal an axial slices shown). Color bars indicate Z statistics based on the estimated standard error of residual noise. Frequency-power spectra are shown immediately below each IC. Highest template-correlation value is indicated in top left corner for each IC.

2.4 Discussion

This is the first study to use combined EEG and fMRI to examine all sleep stages with the explicit purpose of identifying non-canonical sleep-specific RSNs. It was

hypothesized that some new RSNs would be discovered and that these could be related to aspects of mentation specific to sleep, much as waking cognitive functions are related to the canonical RSNs. Surprisingly, no new sleep-specific RSNs were found in any sleep stage, despite a directed search using a uniquely rich dataset, as all below-threshold ICs were carefully inspected and positively identified as non-neuronal artifacts. These results strongly suggest that there are no sleep-specific RSNs. Rather, the canonical RSNs that seemingly support waking mentation also support (or at the very least, co-occur with) sleep-specific functions and thus, the repertoire of canonical RSNs present in wake comprises the full set across sleep-wake states. Moreover, the results of previous RSN FC studies which made use of RSN nodes defined by wakefulness studies can now be confirmed to stand on more solid ground, and appear to have not inadvertently overlooked sleep-specific RSNs. Importantly, these findings suggest that unique functions of sleep (*e.g.,* offline memory consolidation), cognitive processes (*e.g.,* dreaming), electrophysiological features and forms of communication (*e.g.,* spindles, k-complexes, slow waves) which characterize sleep stages (*e.g.,* NREM1, 2, 3, REM), surprisingly, do not manifest or require unique sleep-specific RSNs.

There are a number of methodological limitations that could explain this result. In particular, the quality of a search for a new RSN can only be measured against two definitions; what constitutes an RSN and what might constitute an RSN unique from what is currently defined as an RSN. Given that the functional role of RSNs is presently speculative, such definitions must be delimited by a collection of spatial and temporal properties, the most important of which are those that would rule out a potential RSN from being a known source of non-neuronal blood oxygen level dependent (BOLD) artifacts. If this study has failed to recognize the existence of a "sleep-RSN", then this failure likely rests on the assumptions made about the spatial and temporal properties most commonly used to identify RSNs.

As far as spatial properties are concerned, it is reasonable to question whether the spatial templates in Smith et al., (2009) used to rule out group-level ICs as being new RSNs, were a fair representation of canonical RSNs. These 10 templates were themselves generated from a 20 model-order ICA decomposition, and hence their spatial bounds are

specific to this decomposition. A comparison of ICs from the present study against external templates generated from a different model order would surely yield different results. On the other hand, while the correlation values would have changed, visual inspection of components would indicate that the same networks were being represented, albeit in a reduced or more elaborated form. Nevertheless, Ray et al. (2013) performed an assessment of ICA dimensionalities ranging in size from 20 to 200 and found that a dimensionality of around 20 is appropriate for examining RSNs at the scale of the 10 canonical RSNs. This same rationale applies to the use of a 30 model-order decomposition for the data in the present study.

An additional challenge involves the use of an automatic ICA de-noising algorithm to clean the individual blocks. This algorithm makes use of spatial and temporal property weightings that are biased towards what current RSN experts deem to be a non-neuronal artifact in wake resting state data. It is entirely possible that RSNs in sleep exhibit different temporal and spatial properties from their waking counterparts, for example power at oscillatory high-frequency that would cause them to be rejected as noise by an expert (or automated software tuned to the judgement of an expert). Further, without knowing the true functional role and neurological mechanisms of RSNs, there will always be some uncertainty in defining either RSNs or non-neuronal artifacts outside of their normal milieu (*i.e.,* waking conditions).

Such concerns can be mitigated when considering the general robustness of the essential spatial configuration and temporal properties of RSNs under compromised or pathological conditions. There is therefore some measure of confidence that an RSN will have recognizable properties under healthy physiological conditions alternate to wake.

A more contentious issue might be the resting state lengths used in the analysis. The NREM3 and REM analyses made use of 4- and 3.6-minute duration blocks, respectively. Resting state analyses typically utilize 5-7 minutes of data, and it has been suggested that a 12-16 minute resting state scan time is ideal (Birn et al., 2013). However, given the difficulty in acquiring NREM3 and REM fMRI data, the short block lengths were considered reasonable. For comparison, a similar EEG-fMRI sleep study by Chow et al.

(2013; prior to the current study, this was the largest available EEG-fMRI dataset available for REM) acquired 32.4 minutes of REM data from 4 subjects out of an initial pool of 18, all of whom were sleep deprived for 44 hours prior to the study; the present study acquired 75.2 minutes of REM data from 7 subjects out of an initial pool of 35, none of whom were sleep deprived. The inadequacy of these datasets would appear to be unlikely however given the identification of robust canonical RSNs in both of these stages, however Type II error (*i.e.,* concluding that new RSNs are not present in sleep) is still a possibility.

Further, it should be noted that the ICA results are potentially biased by the extra number of blocks drawn from single-subject data with more volumes available for a given sleep stage. This was considered an acceptable risk, in order to maximize the data available for the sleep ICA analysis. In order to test whether this was possibly problematic, we repeated the analysis using only a single block for each subject with data available for a given stage, and were able to confirm the same pattern of results using this alternative approach.

Finally, it is worth pointing out that the well-established finding that the DMN breaks up into anterior and posterior nodes during slow wave sleep (Horovitz et al., 2009) is not contradicted by the present results which indicate that the DMN can be detected across all sleep stages. This apparent discrepancy likely emerges from the different aims and approaches used in previous studies, which employed SCA. SCA looks at whole-brain correlations with the average timecourse within a "seed" region (*e.g.,* the PCC). By contrast, the present study employed ICA, which finds statistically independent components by maximizing the non-Gaussianity of a dataset. It is therefore consistent for a "complete" DMN (*i.e.,* comprising anterior and posterior components), to be detected as a distinct component using ICA, to coexist with a less cohesive DMN, as identified using SCA methodology. Hence, the present results can be considered to be complementary with previous studies, given the differing approaches; our results show that the DMN is present in all sleep stages, but previous studies show that cohesiveness of the DMN varies as a function of sleep depth. Although beyond the scope of the present study,

future studies should consider other approaches, importantly; a comprehensive analysis of RSN functional connectivity differences across wakefulness and all sleep stages.

In conclusion, although canonical RSNs have been identified in sleep in a number of prior studies, these studies were not explicitly looking for RSNs beyond the waking set, and as a consequence would not have included these networks in their investigation, nor were they comprehensive (with REM often excluded; understandable given the difficulty of acquiring REM fMRI data). Consequently, this is the first study that explicitly tested whether the full inventory of RSNs is known across sleep/wake states and represents a further step in the direction of defining a complete taxonomy of RSNs.

2.5 Supplemental material

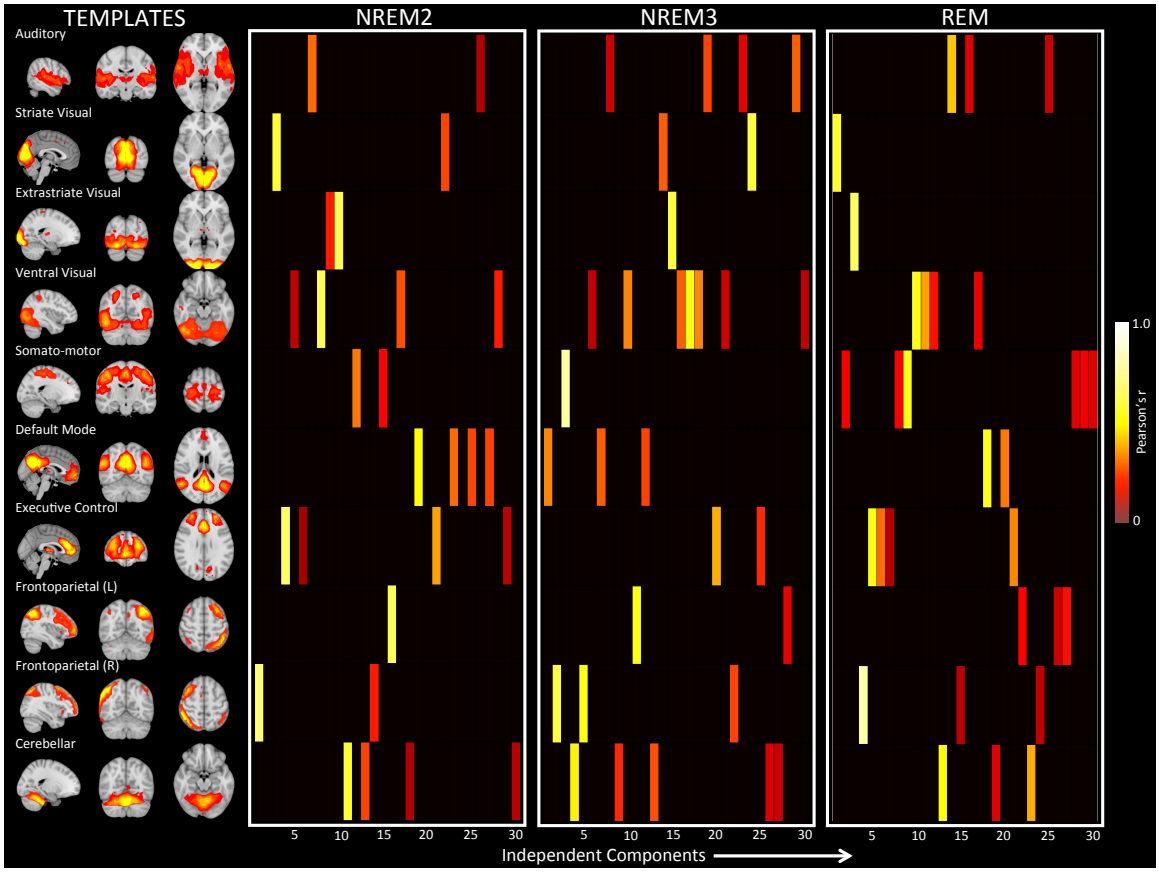

Figure 4. Color-coded correlation values for all group-level independent components (ICs) and their best-matched resting state network (RSN) templates, for rapid eye movement (REM) sleep and non-REM stages 2/3 (NREM2/3).

Ordinate axis presents the ten external RSN templates used in the spatial correlation, with representative sagittal, coronal and axial slices. Abscissa indicates color-coded Pearson's r correlation values for each of the 30 group-level ICs, for each stage, presented in the vertical dimension with their best-matched template.

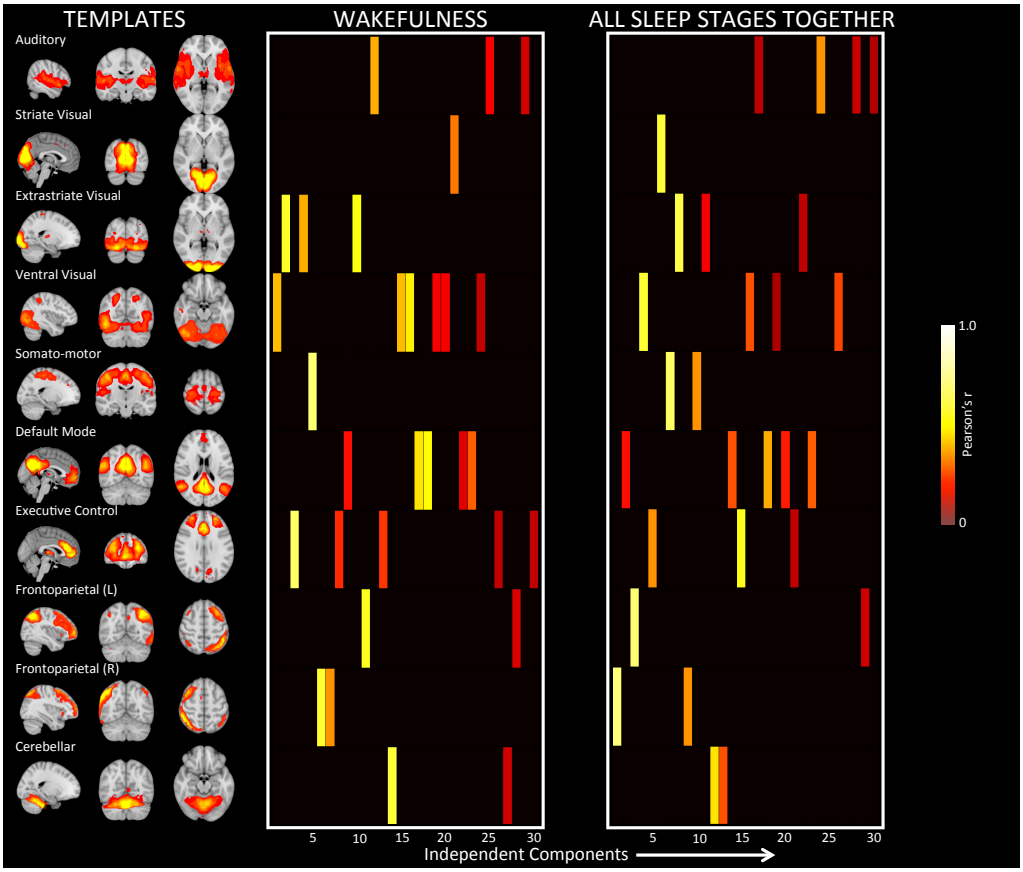

Figure 5. Color-coded correlation values for all group-level independent components (ICs) and their best-matched resting state network (RSN) templates, for wakefulness and the combined sleep stages dataset.

Ordinate axis presents the ten external RSN templates used in the spatial correlation, with representative sagittal, coronal and axial slices. Abscissa indicates color-coded Pearson's r correlation values for each of the 30 group-level ICs for each stage, presented in the vertical dimension with their best-matched template.

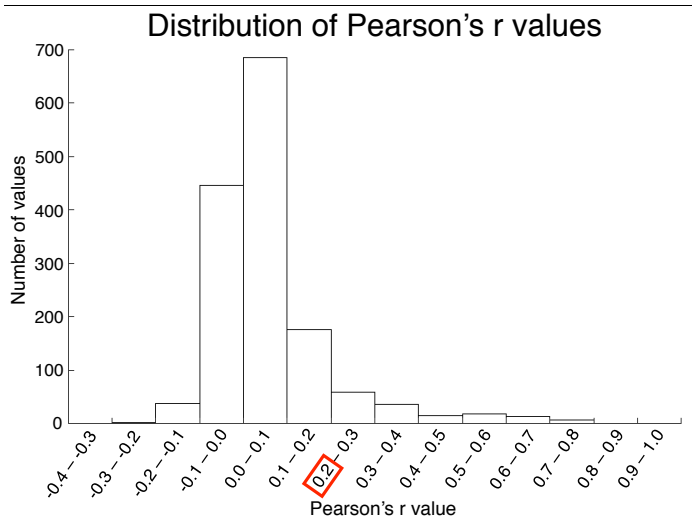

Figure 6. Frequency distribution histogram of the spatial correlations between independent components (ICs) and resting state networks (RSNs).

Frequency distribution histogram based on all available correlation values; 30 ICs X 10 RSN templates X 5 datasets (wakefulness, three sleep stages and the dataset with all sleep stages combined) = 1500 values. The spatial correlation threshold (0.2) is indicated with a red rectangle.

Chapter 3

3 Slow wave sleep is an altered, not a reduced, state of consciousness: resting state network functional connectivity in sleep

3.1 Introduction

Resting state networks (RSNs) are low frequency fluctuations in the functional magnetic resonance imaging (fMRI) blood oxygen level dependent (BOLD) signal that are consistently organized into well-defined spatial networks with a striking similarity to the spatial organization of networks that support discrete cognitive functions (Damoiseaux et al., 2006; Smith et al., 2009). Moreover, it is known that changes in cognitive processing are reflected in changes to functional connectivity (FC) within and between RSNs (Cole, Ito, Bassett, & Schultz, 2016; Hearne, Cocchi, Zalesky, & Mattingley, 2017). Currently, RSN FC has been evaluated for a number of compromised and non-wakefulness states, including sedation (Boveroux et al., 2010; Schrouff et al., 2011), the vegetative state (Boly et al., 2009; Vanhaudenhuyse et al., 2010) and sleep (Horovitz et al., 2009; Larson-Prior et al., 2009, 2011; Tagliazucchi et al., 2013). Collectively, these studies suggest that reduced states of conscious awareness are associated with a reduction in the magnitude of RSN FC, particularly for non-sensory, "higher-order" RSNs such as the default mode network (DMN) (Heine et al., 2012b). As such, RSN FC configurations provide a useful investigative tool for profiling states of conscious awareness. However, RSN FC in sleep is the least well understood, due to the paucity of fMRI data acquired during particular stages of sleep, specifically rapid eye movement (REM) and non-REM stage 3, also known as slow wave sleep (SWS), and the challenges inherent in acquiring electroencephalographic (EEG)-fMRI sleep recordings. These sleep stages are each accompanied by dramatic changes to the neurochemical and electrophysiological milieu of the brain, which can be expected to impact both RSN FC and the accompanying state of awareness. These changes are associated with distinct EEG signatures; indeed, it is primarily EEG features that are used to categorize sleep stages themselves, as well as brain arousal levels and information processing changes across sleep-wake states (Cote,

Epps, & Campbell, 2000a; Dang-Vu, McKinney, Buxton, Solet, & Ellenbogen, 2010; Iber, Ancoli-Israel, Chesson, & Quan, 2007; Klimesch, 2012; MacLean, Arnell, & Cote, 2012; Steriade, 2003). However, it remains to be determined how these broad-level changes are reflected in changes to RSN FC, and, by association, alterations of conscious awareness.

RSN FC is known to change as a function of sleep state (*i.e.,* relative to wakefulness FC configurations), although the literature on this subject is still sparse (Boly et al., 2012; Chow et al., 2013; Larson-Prior et al., 2011). Larson-Prior (2011) showed that there is a reduction of the negative functional correlations between the DMN and both the dorsal attention network (DAN) and the executive control network (ECN) during the transition from wake to sleep. Boly (2012) showed that intra-RSN FC becomes proportionally stronger than inter-RSN FC during non-rapid eye movement (NREM) sleep compared to wake. Horovitz (2009) demonstrated that DMN subregions become dissociated during SWS. Taken together, these studies suggest that there is a reduction in the magnitude of inter-RSN FC and that RSNs become more isolated from each other during NREM sleep, relative to wakefulness. Although NREM inter-RSN FC has been investigated in a handful of studies (especially early NREM/light sleep), no study has comprehensively evaluated inter-RSN FC changes across wake, NREM stage 2 (NREM2), SWS and REM sleep. This was the major aim of the current investigation.

REM and NREM sleep are defined by distinct electrophysiological signatures that have unique neurophysiological substrates, which are well characterized. One of the defining EEG characteristics which dissociates REM from NREM sleep is the extent of cortical synchrony. More specifically, NREM sleep is characterized by the emergence and eventual dominance of delta waves in the neocortex. As measured by EEG, delta waves are ~0.5-2Hz oscillations that are the consequence of widespread synchronized communication, regulated by thalamocortical input in a burst mode (Contreras & Steriade, 1995; Steriade, Timofeev, & Grenier, 2001); a unique mode of cortical-subcortical communication, unlike that seen in wakefulness or REM. NREM sleep is typically (Iber et al., 2007) further subdivided into three stages: 1) NREM1; an intermediate stage between quiet wakefulness and the emergence of clear sleep features,

2) NREM2, which is characteristically defined by EEG signatures such as K-complexes and sleep spindles, and, 3) SWS, when delta/slow waves dominate the EEG. Although these distinct NREM features are thought to serve important functions, such as information processing (Colrain, Webster, & Hirst, 1999), homeostasis (Feinberg & March, 1995) and memory consolidation (Diekelmann & Born, 2010; Fogel & Smith, 2011; Rasch & Born, 2013; Stickgold, 2005), they all involve an expression of highly coordinated and hypersynchronized cortical oscillatory activity (Weigenand, Schellenberger Costa, Ngo, Claussen, & Martinetz, 2014a). This synchrony increases progressively across the NREM stages (*i.e.,* NREM1 < NREM2 < SWS), and is the defining EEG feature used to discriminate between these NREM stages according to standard scoring criteria (Iber et al., 2007).

However, it remains to be determined how this change in global communication as a function of NREM depth is reflected in RSN FC and, by association, how changes in RSN FC are reflected in changes in awareness. The present literature suggests that NREM (and SWS in particular), involves both reduced arousal/awareness of the environment, as well as reduced neural activity, and is therefore best described as a quiescent state. For example, it is known from positron emission spectroscopy (PET) studies that glucose consumption in NREM is half that of wakefulness (Heiss, Pawlik, Herholz, Wagner, & Wienhard, 1985; Kennedy et al., 1982). Further, a 2010 study (Spoormaker et al., 2010) indicated that global FC actually increases in the transition to sleep, but decreases dramatically in slow-wave sleep. However, the polarity of FC changes was not indicated in this study (only the absolute value of FC differences) and cortical regions were not defined by RSN spatial boundaries. As mentioned above, the current literature also suggests that connectivity fragments in NREM sleep (Horovitz et al., 2009; Larson-Prior et al., 2011), which is also consistent with a view of sleep as a state of quiescence. Despite these indications, it is not global FC that necessarily determines awareness. Rather, studies have shown that it is largely the FC of higher-order RSNs (such as the DMN) specifically, that determines conscious awareness (Martuzzi, Ramani, Qiu, Rajeevan, & Constable, 2010; Schrouff et al., 2011; Vanhaudenhuyse et al., 2010). Consequently, although NREM sleep involves reduced conscious arousal, characterized by reduced sensory processing of the environment (Posner, Saper, Schiff, &

Plum, 2008), it is not clear whether it also manifests a qualitatively different state of conscious awareness, with correspondingly unique RSN FC (particularly involving higher-order RSNs), as opposed to merely reduced wake-like FC.

In contrast to NREM, REM sleep is associated with so-called "desynchronized" cortical activity (Brown & McCarley, 2008) that enables the kind of flexible cortico-cortical communication that is no longer driven by burst-mode operations of the thalamocortical circuitry. Rather, cortical input is tonic, as is similarly required for waking cognition. Indeed, REM sleep has also been called "paradoxical sleep" for this very reason. Another feature shared between REM and wakefulness is the activation of the ascending reticular activation system (ARAS), a network of brainstem nuclei which coordinates the cortical release of acetylcholine, a neuromodulator that has the effect of suppressing the highly synchronized oscillatory activity characteristic of NREM, thereby facilitating the desynchronized cortical activity of REM sleep and wake (Lee, 2005; Schwartz & Roth, 2008). Finally, REM dream reports indicate that mentation in REM is perceptually more vivid, animated, is more emotionally charged (Cavallero, Cicogna, Natale, Occhionero, & Zito, 1992; Foulkes, 1962) and is more continuous (*i.e.,* longer dream reports, 41) than that of NREM. This suggests a correlation between desynchronized cortical activity and rich conscious content, similar to rich, wake-like cognition; albeit with important differences such as a bizarre and nonsensical story-like quality to dream content. This distinct state would also be expected to have an important impact on RSN FC that differs from SWS, but perhaps resembles that of the waking brain.

Taken together, these observations suggest systems-level neural network activity that changes as a function of wake, NREM and REM sleep. In this neurophysiological context, it follows that the trend towards cortical synchrony in NREM would have a progressively destabilizing impact on wakefulness cortico-cortical FC and further, that this should be reflected in progressive differentiation of wakefulness and NREM2/SWS inter-RSN FC. Moreover, the desynchronized activity characteristic of REM should facilitate cortico-cortical FC that resembles wakefulness, which should be reflected in similarities between wakefulness and REM inter-RSN FC.

By employing simultaneous EEG-fMRI, this study had two primary aims: The first was to compare inter-RSN FC across all prominent sleep-wake states (*i.e.,* Wake, NREM2, SWS, REM), in order to determine how changes in RSN FC patterns reflect neurochemical, electrophysiological and cognitive differences between NREM and REM. It was hypothesized that inter-RSN FC would trend away from wakefulness-like FC, in a progressive fashion, during NREM stages and subsequently trend back towards wakefulness-like FC in REM sleep.

The second aim was to determine whether NREM FC is merely a reduced version of wakefulness FC, as suggested by the literature, or is in fact an altered FC state altogether. More specifically, reductions in the magnitude of FC during SWS would suggest that it is a weakened version of wakefulness, whereas a reversal of the polarity of connectivity in the opposite direction (*e.g.,* negative to positive, and positive to negative) in SWS would suggest that it represents a qualitatively different state of connectivity (and awareness) from that of wakefulness or REM.

3.2 Methods

3.2.1 Participants

Please see section 2.2.1, above.

3.2.2 Experimental procedure

Please see section 2.2.3, above.

3.2.3 Polysomnographic recording and processing

Please see section 2.2.4, above.

3.2.4 MRI imaging acquisition, processing and analysis

3.2.4.1 Recording parameters

Please see section 2.2.5.1, above.

3.2.4.2 Functional data classification

All sleep session functional volumes were scored according to standard sleep-stage scoring criteria (Iber et al., 2007) by an expert registered polysomnographic technologist. To be included in the fMRI analysis, the EEG had to be visibly movement artifact-free. Volumes were classified as wake, NREM1, NREM2, SWS or REM. Notably, wake data used in the analysis was taken from the wake resting state session only, despite wake segments being present in the sleep session data. This was to avoid including wake periods contaminated with variable levels of drowsiness/sleep inertia from preceding sleep episodes of varying sleep depth. Following sleep scoring, a single epoch was extracted from the total set of functional volumes, for each participant who had data available for a given stage. The length of the epoch extracted per participant was determined by considering the minimum length time series available amongst all the participant data for a given stage. For example, if 25 participants had at least (a bare minimum of) 3 minutes of NREM2 data, with the smallest epoch available for a given participant being 4 minutes, then a single 4-minute NREM2 epoch was extracted from the data available for all participants with NREM2 data. In practice, any participant with less than 4 1/2 minutes of data for a given stage was rejected from the analysis for that stage, as a further consideration of the number of time points required for an accurate functional connectivity analysis.

3.2.4.3 Wake data acquired/extracted for analysis

Of the 34 participants included in the analysis, 29 had 220 MRI volumes worth (approximately 8 minutes) of data, with the remainder having 150 volumes (approximately 5 $^{1}/_{2}$ minutes). One participant had data recorded with slightly different acquisition parameters, so their wake data was excluded, leaving a total of 33 participants, each with150-volume epochs used in the final analysis. For the direct comparison of stages, wake data was truncated (see below).

3.2.4.4 Sleep stage data acquired/extracted for analysis

Overall, participants managed to obtain the full spectrum of sleep stages (NREM1, NREM2, SWS and REM sleep). Given the significant challenges of sustaining sleep in an

MRI scanner environment (due to noise and participant comfort), on an individual basis the majority of participants maintained sleep in only a subset of the sleep stages of interest, for a duration long enough to be considered sufficient for FC analysis. Surprisingly, 4 participants did manage to transition through all three sleep-stages of interest (NREM2, SWS and REM). In all cases, sleep scoring identified a pattern in which participants transitioned between sleep stages of variable duration; from less than 20 seconds (the shortest sleep scoring period) to 69.3 minutes. Notably, sleep stage NREM1 was mostly unavailable, however considering the brief and transitional nature of this stage, it was justifiably eliminated from the analysis at the expense of exploring interesting FC changes that might occur during the sleep onset process; which would likely require an experimental approach tailored to study sleep onset per se.

The majority of participants (28 out of 33) were able to sustain a sufficient amount of NREM2 sleep for the FC analysis. However, it was decided that 24 150-volume epochs be used in the analysis, in order to both match the available wake data and to maximize the robustness of the FC analysis. In the case of SWS, 11 participants had data above the minimum 83-volume (3-minute) cutoff, with 10 having at least one epoch longer than 110 volumes (approximately 4 minutes). However, as 110 volumes was considered unsuitable for a functional connectivity analysis, two datasets were excluded, leaving 9 133-volume (4.8 minute) epochs. Seven participants had REM data above the 83 volume cutoff, with all seven having at least one session longer than 100 volumes (approximately 31/2 minutes). Despite the difficulty in acquiring REM data, 100 volumes was considered unsuitable for a functional connectivity analysis and one dataset was excluded (*n.b.,* resting state analyses typically utilize 5-7 minutes of data; Birn et al., 2013). This left six 129-volume (4.6 minute) epochs for use in the analysis. For the direct comparison of stages, NREM2 and SWS data was truncated (see below).

3.2.4.5 Functional data truncation

In order to have equal length epochs for the inter-stage comparisons (to satisfy the requirements of the analysis approach; see Supplemental Material), data for the stage with more volumes available per subject was truncated to the length of the stage with fewer volumes available. For the wake *vs*. SWS comparison, wake epochs were truncated

to the length of the shorter SWS epochs (*i.e.*, 133 volumes). Similarly, in the comparison of wake vs. REM, wake epochs were truncated to the length of the shorter REM epochs (*i.e.*, 129 volumes). Likewise, NREM2 epochs were reduced to 133 volumes in the NREM2 vs. SWS comparison. Notably, this reduction allowed for two datasets to be re-included in the analysis, resulting in 26 133-volume epochs for the NREM2 vs. SWS comparison. Similarly, 26 129-volume NREM2 epochs were used in the NREM2 vs. REM comparison. Finally, SWS epochs were truncated to 129 volumes for the SWS vs. REM analysis.

3.2.4.6 Preprocessing

Each sleep and wake epoch was individually preprocessed using the Oxford Centre for Functional Magnetic Resonance Imaging of the Brain Software Library (FMRIB, Oxford U.K.; FSL version 5.09; 57). Functional volumes within each epoch were realigned using FSL's MCFLIRT tool (Jenkinson et al., 2002) which performs rigid body transformations. Non-brain voxels were also extracted using FSL's BET tool (Smith, 2002). Volumes were spatially smoothed using a Gaussian kernel of 5mm full-width at half-maximum (FWHM) and high-pass temporal filtered (Gaussian-weighted least-squares straight line fitting, FWHM = 2000s). Functional volumes were then coregistered to the MNI152 standard space (McConnell Brain Imaging Centre, Montreal Neurological Institute) using 12 degree-of-freedom affine registration. Finally, each epoch was individually cleaned of non-neuronal artifacts using the FIX plug-in for the FSL package (Griffanti et al., 2014; Salimi-Khorshidi et al., 2014), an automatic noise detection and removal algorithm. Prior to using FIX, FSL's MELODIC tool (Beckmann & Smith, 2004) was used to generate ICs for each epoch. MELODIC's default dimensionality estimation function automatically estimates the number of ICs by performing a Bayesian analysis. FIX then assessed each of these ICs as noise or signal, after generating more than 180 distinct spatial and temporal features of each IC and feeding these into a multi-level classifier. ICs classified as noise were then subtracted from the ICA mixing matrix and a new set of functional volumes was generated.

3.2.4.7 Functional connectivity analysis

The FC analysis was carried out in a number of stages. First, 20 independent component (IC) templates derived from a separate healthy waking RSN ICA study (Smith et al., 2009) were spatially regressed onto the single-subject 4D epochs available for each sleep stage, using FSL's dual_regression function (Nickerson, Smith, Öngür, & Beckmann, 2017). The spatial regression produced a set of 20 beta values (*i.e.,* one beta value per IC) for each volume of functional data, reflecting how well each of the 20 ICs were represented at each time point. Each IC therefore had a series of beta values across all time points, which was treated as a pseudo time series, for further FC analysis. These pseudo-time series were used as inputs for the FSLNets network modeling toolbox (v0.6.3; http://fsl.fmrib.ox.ac.uk/fsl/fslwiki/FSLNets). The 20 ICs were then reduced to only those 14 that represented RSNs. Although 20 ICs were spatially regressed onto the data, not all of these were considered canonical RSNs. FSL image viewer FSLEyes and the FSLNets' ts_spectra function were used to respectively assess the spatial configuration and power-frequency spectra of each of these 20 ICs. The time courses of six noise-related ICs were regressed out of all other time series and then deleted, leaving 14 RSN time series. Next, full-correlation matrices were generated from these 14 RSN time series, at the single subject level, using FSLNets' nets_netmats function, resulting in 91 unique FC edges for each sleep stage, for each participant (*i.e.,* there are 91 unique pairs amongst 14 RSNs). Full correlation values were converted to z-scores using the Fisher r-to-z transform, with corrections made for degrees of freedom, taking into account autocorrelation.

3.2.4.8 Polynomial fitting to edge functional connectivity data across wakefulness and sleep

In order to test our main hypotheses, we assessed the pattern of FC changes across all sleep stages for a given FC edge. First-, second- and third-order polynomials were fit to stage-coded edge data (whole numbers were assigned according to sleep stage; wake edges were assigned an x-axis value of "1", NREM2 a value of "2", SWS a value of "3" and REM a value of "4"). The quality of fit was assessed by calculating a coefficient of determination (*i.e.,* R-square values) for each polynomial function. To test for the

statistical likelihood of a best fitting function, sample distributions of R-square values for each polynomial fit were generated by resampling the data using permutation hypothesis testing (*i.e.,* by randomly assigning the edge FC data to different sleep stages, calculating new R square values for the polynomial fits and iterating this procedure 10,000 times). P-values were then calculated for the actual fitted polynomials by comparing the R square values to the permuted sample distributions.

Next, each of the 91 edges was assessed as being best described by one of the three polynomial functions, *i.e.,* a first-order non-horizontal line, a second-order quadratic function, or a third-order cubic function (see Figure 1 for a cartoon of possible fits). If only one type of polynomial fit was significant for a given edge, then the pattern of FC change for that edge was categorized as being best described by that fit. Otherwise, the polynomial fit with the lowest p value and highest R square value was used to best describe the pattern of FC change for that edge. If no statistically significant best-fits were identified, then that edge was categorized as being best described by a flat, horizontal line (*i.e.,* no significant changes in edge FC across the sleep stages, in accordance with the null hypothesis; see top left panel of Figure 7).

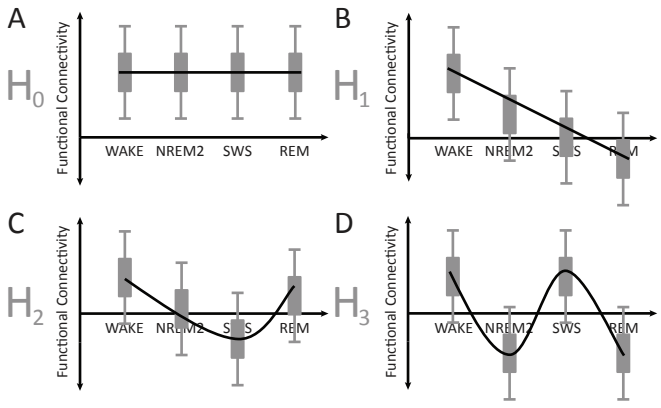

Figure 7. Cartoon of possible polynomial fits for functional connectivity (FC) data across wakefulness and sleep.

(A) null hypothesis (H_0); first-order polynomial, horizontal line fit. (B) alternative hypothesis 1 (H_1); first-order polynomial, non-horizontal line fit. (C) alternative hypothesis 2 (H_2); second-order polynomial, quadratic line fit. (D) alternative hypothesis 3 (H_3); third-order polynomial, cubic line fit. REM=rapid eye movement, NREM2=non-REM stage 2, SWS=slow wave sleep.

Once all the edges were categorized according to best polynomial fit, a one-variable chi-square test was performed to examine the distribution of these categorizations. When quadratic fits were found to be the most prevalent, the distribution of concavity (*i.e.,* convex vs. concave) was tested using a binomial test. Importantly, the categorization of edge data as concave or convex was determined by first reversing data for FC edges that had negative FC in wakefulness. This was done in order to group together only those edges that were changing their magnitudes in the same direction (*i.e.,* reducing or increasing in magnitude, relative to zero), so that changes relative to the FC of wakefulness would become more apparent. Further, edge FC changes best described by convex quadratic fits were tested to determine whether NREM sleep was, on average, accompanied by a reversal or a reduction of wakefulness FC. This was accomplished by performing 1-sample t-tests in the predicted direction on the FC results for each stage. Finally, the same tests were performed on the subset of convex fit edges that reversed their connectivity pattern and were strengthened in the opposite direction.

3.2.4.9 Angular distances between stages

Angular distances were evaluated in order to determine the dissimilarity between each of the sleep stages and wakefulness. This was done by first assembling relevant edge FC values for a given participant in a given stage into a single vector. For example, for NREM2 there were 24 vectors in total, corresponding to the 24 participants with useful NREM2 data. For comparisons of all FC edge data, each of these 24 NREM2 vectors was comprised of 91 values, corresponding to the 91 unique FC edges amongst the 14 RSNs assessed in this study. By contrast, for comparisons of the subset of convex quadratic edge data, each of the 24 NREM2 vectors was comprised of 29 values, corresponding to the 29 FC edges that were best described by convex quadratic fits. Next, angular distances were calculated between mean vectors for each stage (*i.e.,* vectors comprised of edge FC values that have been averaged across participants for a given stage). Angular distances were calculated between pairs of vectors according to the following formula:

$$\text{Angular distance} = \frac{\cos^{-1}\left(\frac{A \cdot B}{\| A \| \| B \|}\right)}{\pi} \qquad (1)$$

where A, B are the vectors of interest, $A \cdot B$ is the vector dot product, and $\| A \| \| B \|$ are the vector lengths.

In order to evaluate the statistical significance of the differences between the vectors belonging to each stage, a non-parametric MANOVA was performed in accordance with (Anderson, 2001; Anderson & Ter Braak, 2003). In this case, Equation (1) was used to evaluate angular distances between vectors defined by single-subject edge FC data for each stage. The test statistic is a multivariate analogue of the F-ratio, as follows:

$$F = \frac{SS_A/(a-1)}{SS_W/(N-a)} \qquad (2)$$

Where the numerator is the between-groups variance and the denominator is the within-groups variance. SS_A is the between-group angular distance sum of squares (SS), calculated as total SS (SS_T) - SS_W, SS_W is the within-group angular distance sum of squares. SS is calculated as the angular distances amongst all single-subject vector pair combinations, divided by the relevant number of vectors, as per (Anderson, 2001; Anderson & Ter Braak, 2003). a=number of groups, N=number of vectors.

A null distribution of this statistic was created by resampling the data (*i.e.,* by randomly assigning the vectors to different sleep stages, calculating new pseudo F-statistics and iterating this procedure 10,000 times). A P-value was then calculated for the actual F value by comparing it to the permuted sample distribution. A significant F value was followed by a posteriori testing, in which t-statistics for specific pairs of sleep-wake stages were calculated as the square root of the F-statistic above, as per (Anderson, 2001), with statistical significance calculated using the same resampling technique.

Finally, this set of procedures was repeated for vectors comprised of FC edge subsets defined by their best-fitted polynomials, as described in the methods above. For example, vectors comprised of convex quadratic edges contained 29 edge FC values.

3.3 Results

3.3.1 Edge functional connectivity polynomial fit results

Of the 91 total FC edges, polynomial fits for 49 edges failed to reject the null hypothesis. This suggests that either FC does not change across sleep-wake states for these edges, or that these results were not robust enough to generate conclusions with respect to the alteration of FC across wakefulness and sleep. This is not surprising however, as it would

not necessarily be expected that all brain region pairings would change the magnitude or direction of their FC from sleep to wake. Importantly, this also suggests that the remaining edges, which we seek to further understand here, are the most responsive to neurophysiological dynamics across sleep/wake states. Of these remaining 42 edges, seven were best described by either linear or cubic fits, with the vast majority, 83% or 35 edges, best described by quadratic fits, in line with our hypothesis. This significant result (Table 2) strongly suggests that whole-brain RSN FC can be best described as deviating away from wakefulness FC during NREM sleep, and returning back towards wakefulness FC in REM sleep.

Table 2. *Tests of the distribution of polynomial fits to resting state network functional connectivity data across wakefulness and sleep*

Chi square test on the distribution of polynomial fit patterns across sleep/wake states

Linear (N)	Quadratic (N)	Cubic (N)	χ^2	p
3	35	4	47.3	< 0.001

Binomial test on concavity of quadratic fits

Convex (N)	Concave (N)	
29	6	$p < 0.001$

Note: Exact p values < .001 are not reported

The quadratic fit edges were then tested for concavity, with 29 found to be convex, and the remaining six being concave. This significant bias towards a convex inflection (Table 2) further suggests that FC in NREM sleep is systematically, and specifically, driven in the opposite direction from wake-like connectivity. For example, where two RSNs are positively correlated with one another in wakefulness, by contrast, in NREM sleep FC is driven in the direction of negative correlation.

The polynomial fits for the significant FC edges are illustrated graphically in Figure 8 (also see Supplemental Material Figures 11 and 12, for FC matrices indicating the direct statistical comparison of edge FC distributions between specific stages). Notably, the convex quadratic fits have been further subdivided into those which reverse their connectivity pattern and are strengthened in the opposite direction (indicated in red) and those which otherwise approach zero correlation (i.e., which could be described as merely reducing their connectivity). By contrast, the remaining polynomial patterns represent a relatively small minority of FC edges.

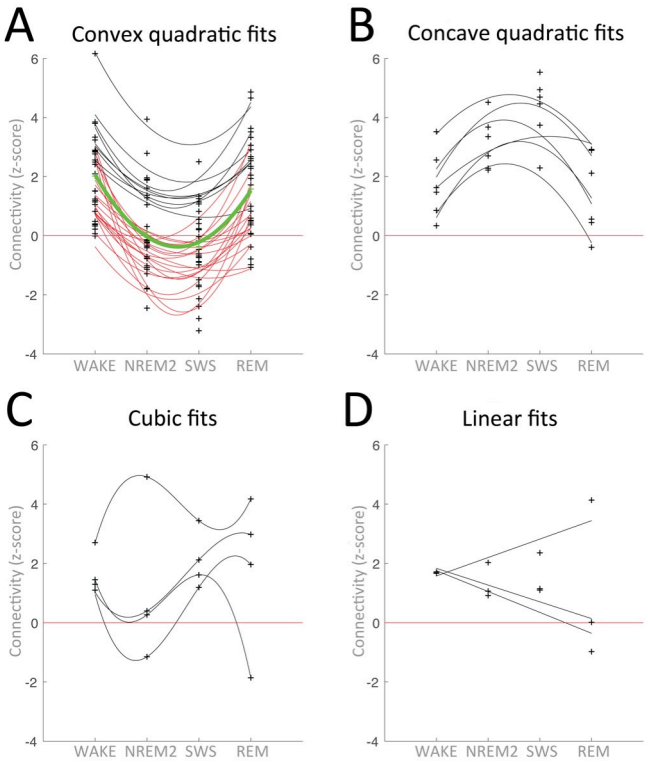

Figure 8. Significant polynomial fits to functional connectivity (FC) data across wakefulness and sleep stages.

(A) FC edges best described by convex quadratic fits (N=29). Plus symbols indicate group-average FC values for a given edge, for a given stage. Polynomials are fit to these group-average values. Units are Fisher r-to-z-transformed full-correlation values, taking into account autocorrelation. Average fitted curve is indicated in green. FC edges that reverse their FC during NREM are indicated as red lines. (B) Concave quadratic fits (N=6). (C) Cubic fits (N=4). (D) Linear fits (N=3). Note: data for FC edges that have

negative FC in wakefulness has been reversed such that inversion of wakefulness FC is more apparent. REM=rapid eye movement, NREM2=non-REM stage 2, SWS=slow wave sleep.

The convex quadratic-fit edges were further tested to determine whether they best described, overall, the NREM stage as a reduction in the magnitude of FC (*i.e.,* only trending in the direction of reversed connectivity) or as an actual reversal of wakefulness FC (*i.e.,* by increasing the magnitude of FC in the opposite direction). If FC in NREM sleep was driven towards the inversion of wakefulness FC, then the expected result[6] would be that FC is significantly different from zero in the negative direction, for the deepest NREM stage, *i.e.,* SWS (with NREM2 being somewhere intermediate between wakefulness and SWS FC). Further, if FC in REM sleep returns towards wakefulness FC, then it would be expected to be significantly different from zero in the positive direction. Remarkably, this is precisely what the results indicate (Table 3; unshaded columns); suggesting that the most common edge FC change across wakefulness and sleep is one in which FC in NREM sleep is inverted and strengthened in the opposite direction relative to wakefulness, and in REM sleep, is restored back to a more wake-like pattern. As would be expected, the results are even stronger for the subset of 20/29 edges whose pattern of changes is indicated by red lines in Figure 8 (see shaded columns in Table 3 for t-test results), as it is clearly these edges that are driving the overall results.

[6] Note: data for FC edges that have negative FC in wakefulness has been reversed such that inversion of wakefulness FC is more apparent.

Table 3. *1-sample t-test to determine if functional connectivity (FC) deviates significantly away from zero connectivity in the predicted direction for convex quadratic-fit edges.*

	WAKE		NREM2		SWS		REM	
	All	Reversal	All	Reversal	All	Reversal	All	Reversal
p	< .001	< .001	.87	< .001	.004	< .001	< .001	< .001
M	2.0	1.4	.1	- .7	- .4	-1.0	1.6	.9
ci	1.9 to ∞	1.2 to ∞	-∞ to .3	-∞ to - .5	-∞ to - .1	-∞ to - .7	1.2 to ∞	.4 to ∞
t	22.6	13.4	1.1	-6.4	-2.7	-6.1	7.2	3.4
d	.73	.52	.04	- .29	- .17	- .45	.55	.31

Note 1: "All" refers to all convex quadratic-fit edges, "Reversal" refers to the subset of convex quadratic-fit edges that reverse their FC pattern and are strengthened in the opposite direction, NREM2=non-rapid eye movement stage 2, SWS=slow wave sleep

Note 2: Exact p values < .001 are not reported

While the polynomial fit results are consistent with the idea that REM is paradoxically similar to wake, they are also surprising in that they appear to challenge the classic view of NREM sleep as merely a quiescent state. Instead, these results suggest for the first time that NREM, and SWS in particular, is a much more active state than previously supposed, such that NREM FC acts in direct opposition to wakefulness FC, rather than being a state characterized by degraded, reduced or disconnected functional communication between brain regions.

3.3.2 Angular distances between stages

Overall, the above pattern of results, combined with the extant literature, strongly suggests that wakefulness and REM sleep could be characterized as FC states that are most similar to one another, and further, that wakefulness and SWS are most dissimilar (with NREM2 being intermediate between the two). However, given that the convex

edges represent a subset of the total number of FC edges (35/91), it is not clear whether it can also be said that overall FC changes reflect this pattern. One method for assessing the dissimilarity of sets of features is angular distance. The complete set of features for a given state (in this case, FC edge data) can be assembled into a vector in multidimensional space (with one dimension per FC edge) and angular distances can be calculated between pairs of such vectors, with larger values indicating greater differentiation. We predicted that, overall (*i.e.,* in the comparison of vectors comprising all 91 FC edges), the angular distances amongst the stages would reflect the suggested pattern described above.

The results (Figure 9, top left) confirm that, overall, RSN FC in SWS sleep is indeed driven the furthest away from wakefulness (*i.e.,* the angular distances between the groups of SWS and wake vectors are greatest), whereas RSN FC in REM sleep recovers back to a state that more closely resembles wakefulness (*i.e.,* the angular distances are smallest), with NREM2 being intermediate. Importantly, the differences between all NREM vectors (*i.e.,* NREM2 and SWS) and those of both wakefulness and REM were also significant and the differences between the vectors of wakefulness and REM were not significant. This indicates that, statistically, REM and wakefulness could not be distinguished from each other on the basis of their overall RSN FC, whereas both NREM2 and SWS can be distinguished from both wakefulness and REM. Based on these results, it is therefore reasonable to describe overall changes in RSN FC in terms of the predicted pattern.

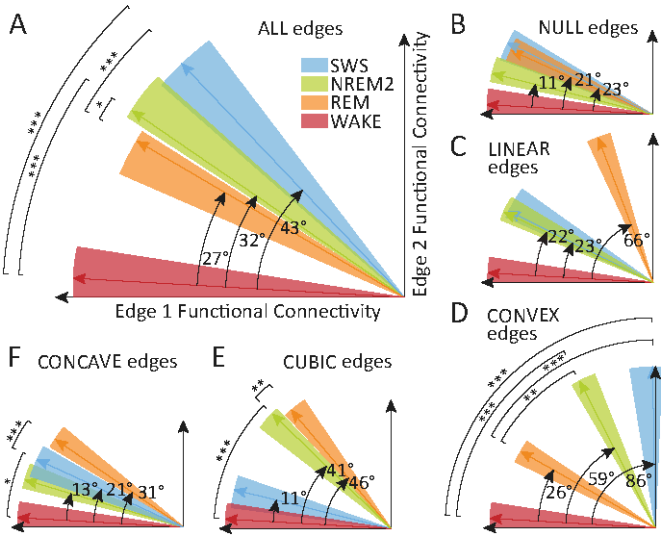

Figure 9. Representative cartoon of the angular distances between vectors representing resting state network (RSN) functional connectivity (FC) in different sleep-wake stages.

(A – F) Vectors exist in multidimensional space, with the number of dimensions dependent on the number of FC edges that are in a given best-polynomial fit category (*e.g.,* each vector exists in 29 dimensional space for the category CONVEX). However, only two dimensions are represented here, for illustrative purposes. Indicated angles are the degree-equivalent of the angular distances between the mean vectors for each stage (indicated as colored arrows), with the mean wakefulness vector always used as the reference point. Angles between sleep stages are not indicated, however the statistical significance of these differences is indicated by asterisks (note that angles between any pair of vectors actually exists in separate dimensional planes and is only represented in the same plane for illustrative purposes). Colored triangles indicate the spread of vectors for each stage, again for illustrative purposes, as they are actually spread across multidimensional space. (A) ALL edges (N=91 dimensions). (B) NULL edges (N=49). (C) LINEAR edges (N=3). (D) CONVEX edges (N=29). (E) CUBIC edges (N=4). (F) CONCAVE edges (N=6). REM=rapid eye movement, NREM2=non-REM stage 2, SWS=slow wave sleep.

Finally, all vectors were separated into component vectors comprising the edges that were best fit by the polynomials tested (as indicated in Figure 8), in order to confirm that the subset of convex edges really are the greatest contributors to the overall pattern. As seen in Figure 9, it is clear that this is the case. Only for the convex edges (lower right panel, Figure 9) is the same pattern indicated, with the same, or greater significance. This suggests that these FC edges are indeed the principal drivers of the overall RSN FC

differences that manifest between wakefulness and each sleep stage. In other words, it appears that it is those FC edges whose dynamics are most consistent with known neurophysiological changes, that are also the most responsible for the overall changes in state (as represented by RSN FC) across wakefulness and sleep.

3.3.3 Distribution of sensory and higher-order nodes

The previous results notwithstanding, there did appear to be a split between individual edges that indicate reversals of wakefulness FC (red lines in Figure 8) and those that indicate a reduction. This warranted a closer look at the RSNs comprised by the individual edges. Figure 10 displays the RSN FC matrix for SWS (also see Supplemental Material Figure 13, for the FC matrices of all examined stages). Importantly, "reversal" edges comprise many "higher-order" RSN nodes, suggesting that SWS involves the increased engagement of RSNs whose activity levels have been associated with the modulation of conscious awareness (Heine et al., 2012b). The following RSNs were classified as higher-order, on account of their involvement in the manipulation of multimodal information: (anterior and posterior) default mode network (aDMN, pDMN), executive control network (ECN), (left and right) fronto-parietal network (lF-P, rF-P), dorsal attention network (DAN). These RSNs were distinguished from the following "sensory" RSNs, which are primarily involved in the manipulation of unimodal sensory information: Auditory (A), somato-motor (SM), striate-, extrastriate- and ventral stream-visual networks (sV, esV, vsV).

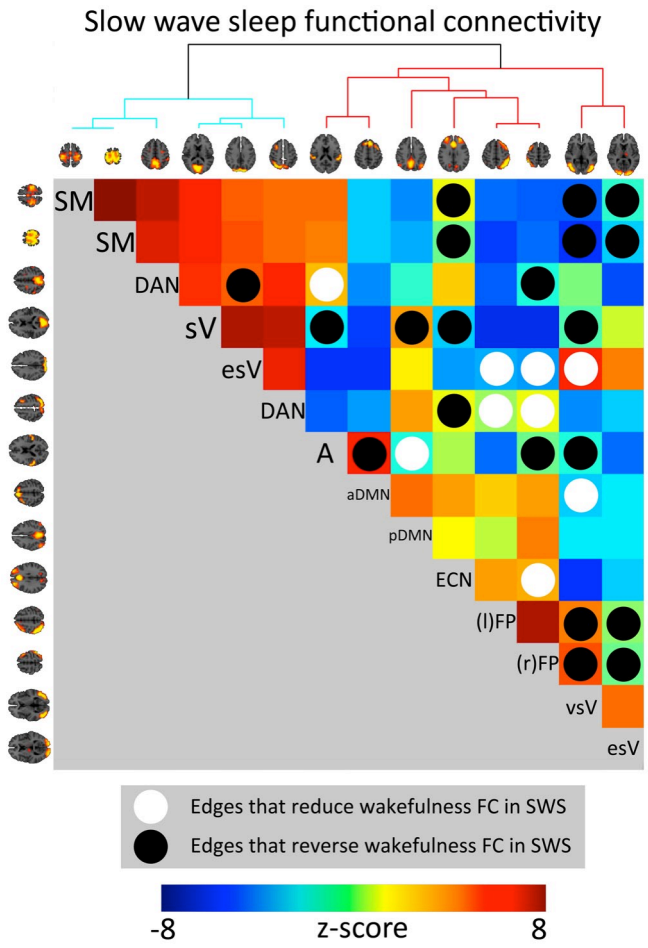

Figure 10. Full-correlation functional connectivity (FC) matrices for 14 resting state networks (RSNs) during slow wave sleep (SWS).

Nodes reordered according to hierarchical clustering (hierarchy visualized above matrix). Colors represent Fisher r-to-z transformed correlations between nodes (taking into account autocorrelation and standard error), with 1-group t-test performed on all participants with data available for a given sleep stage. Black circles indicate FC edges that reverse the polarity of FC during NREM (*i.e.,* negative FC changing to positive FC, or vice versa), relative to wakefulness. White circles indicate FC edges that reduce the magnitude of FC during NREM, relative to wakefulness. SM=somato-motor, sV=striate visual, A=auditory, DAN=dorsal attention network, esV=extra-striate visual, vsV=ventral stream visual, DMN=default mode network, ECN=executive control network, l/rF-P=left/right fronto-parietal.

The nature of RSN nodes involved in both reversal and "reduction" FC edges is further summarized in Table 4. Notably, the majority (13/20) of reversal edges involve higher-order RSNs. There are also more higher-order RSN edges in the reversal category than in

the reduction category. Given the important role that the DMN plays in conscious awareness (Boveroux et al., 2010; Martuzzi, Ramani, Qiu, Rajeevan, & Constable, 2010; Schrouff et al., 2011; Vanhaudenhuyse et al., 2010), Table 5 also summarizes FC changes for the DMN specifically, for all significant-fit polynomial edges, not just convex fits. It is notable that the majority of edges involving DMN nodes increase the magnitude of their FC during SWS (Table 5, box).

Table 4. *Summary of sensory and higher-order resting state network (RSN) nodes involved in reversal/reduction functional connectivity (FC) edges*

	Reduction convex edges (N)	Reversal convex edges (N)
Higher-order - Higher order	3	2
Higher-order - Sensory	5	11
Sensory - Sensory	1	7

Table 5. *FC Edges involving Default Mode Network (DMN) nodes (all significant polynomial fit types)*

RSN nodes involved	Best-fit Polynomial	Change from Wake to SWS FC
extrastriate Visual - aDMN	concave	increasing negative FC (**)
Dorsal attention network - pDMN	cubic	increasing positive FC
Auditory - aDMN	convex	negative to highly positive FC (***)
striate Visual - pDMN	convex	negative to highly positive FC (**)
Auditory - pDMN	convex	decreasing negative FC (***)
ventral stream Visual - aDMN	convex	decreasing negative FC (*)

aDMN=anterior DMN, pDMN=posterior DMN, SWS=slow wave sleep

Note: Indicated significance values (asterisks) reflect differences in the direct comparison of SWS and wakefulness FC values for these edges; these values are not associated with the significance of curve fitting.

3.4 Discussion

There are four notable results from this study, each with important implications for understanding the RSN FC and corresponding levels of awareness of brain states in which neurophysiology varies dramatically. The first, as predicted, was that inter-RSN FC appears to follow the aforementioned neurophysiological trends across wakefulness and sleep (*i.e.,* changing cortical synchrony as a consequence of varying acetylcholine levels) consistently across the majority of FC edges that were found to be best described by significant polynomial fits (*i.e.,* 35/42 were quadratic). Consequently, we have identified, for the first time, a potential correspondence between these two distinctive, dynamic processes, across the complete spectrum of healthy brain states (*i.e.,* wakefulness, NREM and REM). The second is that the direction of this FC change was predictably specific to what the "starting" FC was in wakefulness, for 29/35 of the quadratic fit edges (*i.e.,* the convex edges). For example, if edge FC between two RSNs was highly positively correlated in wakefulness, then this FC would trend increasingly in the direction of negative correlation from NREM2 to SWS and then return towards increasing correlation in REM. Third, we found that the pattern of changes undertaken by the convex edges is so dominant in relation to the patterns undertaken by the remaining edges, that the overall, whole-brain level pattern of changes is actually largely consistent with that of the convex edges. This suggests that those FC edges whose dynamics across wakefulness and sleep are most consistent with known neurophysiological dynamics are also most responsible for the overall changes in state across wakefulness and sleep, at least in terms of RSN FC.

These results support the idea of contrasting functions for NREM and REM, wherein the brain is purposefully driven into a different FC configuration in NREM and is then returned to a wakefulness-like configuration in REM. It is possible that this very specific directional change in RSN FC serves a homeostatic function, such that RSN FC in NREM reduces FC, as it is established during a given day, so that the brain is less biased towards specific RSN connectivity the following day. This could result in cognitive flexibility and thereby facilitate improved adaptability. It is also consistent with the principle of the synaptic homeostasis hypothesis (SHY, 42), which asserts that NREM sleep serves to counterbalance accrued wakefulness long term potentiation (LTP) between specific neurons. This finding is more directly consistent with the so-called REM "wake-up hypothesis" (Klemm, 2011), which proposes that REM serves to counter the effects of NREM, in order to consistently remind the brain how to reactivate wakefulness-like activity, lest it get stuck in the "functionally perturbed" SWS state.

The fourth and most important discovery was that a large majority (*i.e.,* 20/29) of the FC edges that trend towards reduced FC in early NREM (*i.e.,* in the direction of reversed FC), actually reverse their FC polarity in SWS, by increasing in magnitude in the opposite direction. This reversal suggests that at least one of the functions of NREM sleep is to drive cortical FC as far away from wakefulness FC as possible, further consistent with a homeostatic function. Importantly, these edges were found to comprise a substantial number of higher-order RSN nodes. In contrast to sensory RSNs, whose FC has been shown to be largely independent of manipulations of consciousness (Boveroux et al., 2010), higher-order RSNs have been shown to reduce their FC in response to decreases in conscious awareness (Martuzzi et al., 2010; Schrouff et al., 2011; Vanhaudenhuyse et al., 2010). Even more suggestive is the fact that the majority of edges involving the DMN increase their FC between wakefulness and SWS. Many FC studies have indicated an important role for this network in facilitating conscious awareness, with decreased DMN FC shown to parallel reduced consciousness in both the vegetative state (Vanhaudenhuyse et al., 2010) and during sedation (Boveroux et al., 2010; Schrouff et al., 2011). These results notwithstanding, FC between the anterior and posterior nodes of the DMN does decrease during SWS, consistent with the findings of other studies (Horovitz et al., 2009).

These surprising results suggest that it is perhaps incorrect to consider NREM as a quiescent state. Such a conclusion would follow from an observation that edge FC patterns remained the same, yet became reduced during SWS. Instead, the strengthening in the reverse direction, when framed in the context of known connections between increased RSN FC (particularly that of higher-order RSNs such as the DMN) and conscious awareness, suggests that NREM manifests an alternate state of conscious awareness. We refer here to the clinical definition of consciousness, which distinguishes between two subcomponents: conscious arousal (*i.e.,* alertness with respect to the environment) and conscious awareness (*i.e.,* the contents/percepts of consciousness) (Posner, Saper, Schiff, & Plum, 2008). In the case of SWS, there is low arousal, but conscious awareness in the form of endogenously generated mental content, *i.e.,* dreams. Notably, this view is corroborated by NREM dream reports, which can even be distinguished from those of REM based solely on the frequency of descriptive word features (Antrobus, 1983).

It bears emphasizing that this last finding provides compelling evidence that sleep, overall, is not merely a quiescent state; a challenge that could said to have began in the 1950s, with the identification of REM first as a unique sleep state (Aserinsky & Kleitman, 1953) and later as a "paradoxical" sleep state with features more similar to wakefulness than to quiescence (Dement, 1958; Jouvet, Michel, & Courjon, 1959). By combining the established view of REM with the present consideration of NREM as non-quiescent (in terms of RSN FC and perceptual state), these results support the notion that sleep is comprised of a set of alternate states of conscious awareness that the healthy brain naturally manifests.

It is important to note here that the observed reversal of FC is not inconsistent with the findings of other studies that FC is reduced in SWS sleep (Spoormaker et al., 2010; Tagliazucchi & Laufs, 2014), as FC can trend in the direction of reversed FC without increasing in absolute value. Reduced FC also supports the finding that energy consumption is reduced in NREM (Braun et al., 1997a; Dang-Vu et al., 2005),.

Future studies should follow up on the key finding of this study, that RSN FC appears to reverse during SWS. A longitudinal study would be ideal for determining whether the strength of this reversal corresponds to the strength of a given edge on a given day. If so, this would provide further support for the idea that SWS serves a homeostatic function, at the level of RSN FC. It would also be worth investigating edges that don't appear to change as a function of sleep-wake state. In this study, 54% of edges were, statistically, best described by a straight line across wakefulness and sleep, suggesting either that they genuinely do not change, or that our study did not obtain sufficient data to identify a change. It is also important to investigate other functional roles for this FC reversal in SWS; it is already known that NREM plays a key role in memory consolidation and relates to inter-individual differences in human intelligence (Fang, Sergeeva, et al., 2017a; Fogel & Smith, 2011), for example. One means of investigating such functional roles might be to leverage EEG by identifying connections between RSN FC in different sleep stages and EEG-defined frequency band power dynamics, or phasic events such as sleep spindles and K complexes (all with known functional associations).

In conclusion, this study demonstrated for the first time that inter-RSN FC appears to be modulated in accordance with changes in cortical neurophysiology across wakefulness and sleep. It further suggested that NREM sleep progressively modulates RSN FC in a directional fashion, opposite to that of wakefulness, thereby implying a possible wakefulness/SWS homeostatic function, with REM serving to counterbalance the effects of NREM sleep. To our surprise, it also confirmed that this directional change went as far as reversing FC and strengthening it in the opposite direction, for a majority of the edges in the largest category of polynomial fits. A closer examination of these edges revealed substantial involvement of higher-order RSNs. Further, the majority of significant-fit edges involving the DMN were shown to increase their FC. Given the established connection between modulation of conscious awareness and the concomitant modulation of FC involving higher-order RSNs (particularly the DMN), this result supports the supposition that SWS co-occurs with altered, but not necessarily reduced conscious awareness. Thus, NREM sleep (particularly SWS) is better described as an alternate state of awareness, contradicting the historic view that it is a reduced state of consciousness. When this observation is combined with the long-held view of REM as a paradoxical

wakefulness-like state, these results suggest that sleep, overall, cannot be easily described as a quiescent state. Rather, it is best described as a collection of altered states of consciousness that change dynamically in a highly organized and predictable way.

3.5 Supplemental material

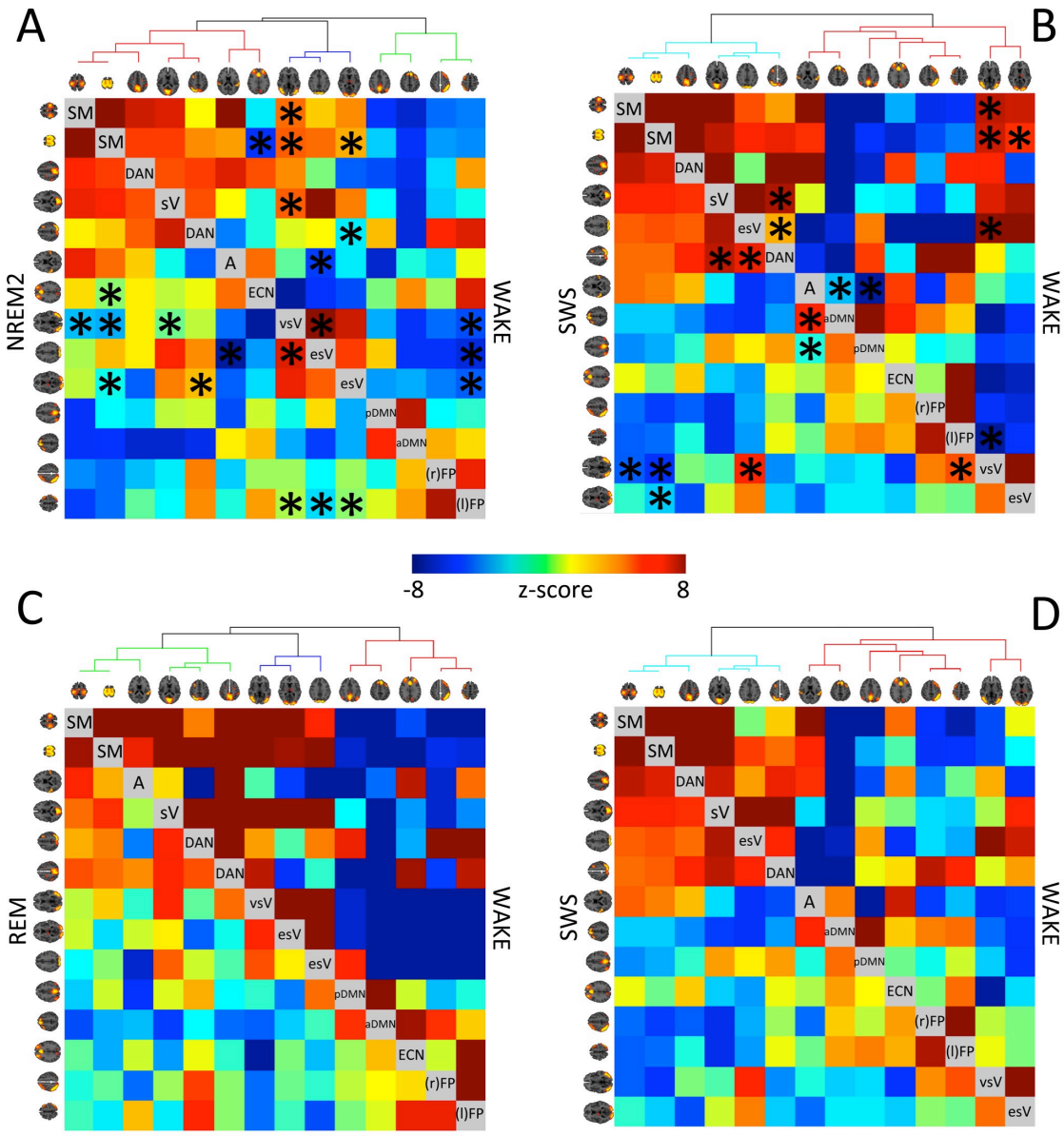

Figure 11. Full-correlation functional connectivity (FC) matrices for 14 resting state networks (RSNs) across wakefulness and sleep.

Nodes reordered according to hierarchical clustering of the below-diagonal sleep stage (hierarchy visualized above each matrix). Colors represent Fisher r-to-z transformed correlations between nodes (taking into account autocorrelation and standard error), with 1-group t-test performed on all subjects with data available for a given sleep stage. Asterisks indicate significant differences ($p < 0.05$ minimum) in edge FC between stages, as determined by univariate 2-sample t-tests. (A) non-rapid eye movement stage 2 (NREM2) matrix below, wake above diagonal. (B) slow wave sleep (SWS) below, wake above diagonal. (C) REM below, wake above diagonal. (D) SWS below, NREM2 above diagonal. SM=somato-motor, sV= striate visual, A=auditory, DAN=dorsal attention network, esV=extra-striate visual, vsV=ventral stream visual, DMN=default mode network, ECN=executive control network, l/rF-P=left/right fronto-parietal.

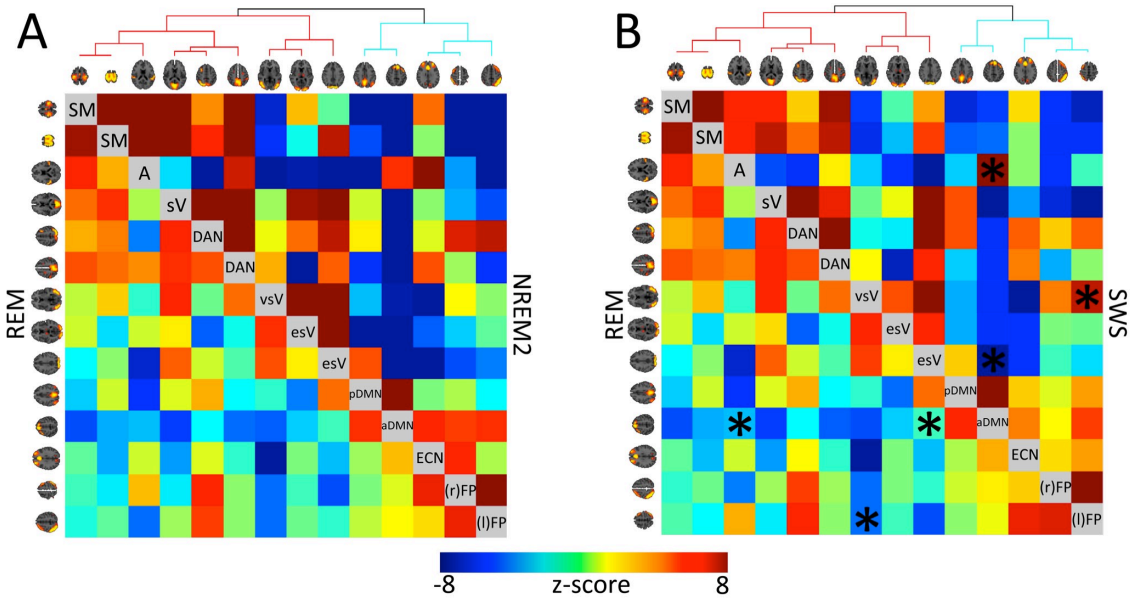

Figure 12. Full-correlation functional connectivity (FC) matrices for 14 resting state networks (RSNs) during sleep.

Nodes reordered according to hierarchical clustering of the below-diagonal sleep stage data (hierarchy visualized above each matrix). Colors represent Fisher r-to-z transformed correlations between nodes (taking into account autocorrelation and standard error), with 1-group t-test performed on all subjects with data available for a given sleep stage. Asterisks indicate significant differences ($p < 0.05$ minimum) in edge FC between stages, as determined by univariate 2-sample t-tests. (A) rapid eye movement (REM) matrix below, non-REM stage 2 (NREM2) above diagonal. (B) REM below, slow wave sleep (SWS) above diagonal. SM=somato-motor, sV=striate visual, A=auditory, DAN=dorsal attention network, esV=extra-striate visual, vsV=ventral stream visual, DMN=default mode network, ECN=executive control network, l/rF-P=left/right fronto-parietal.

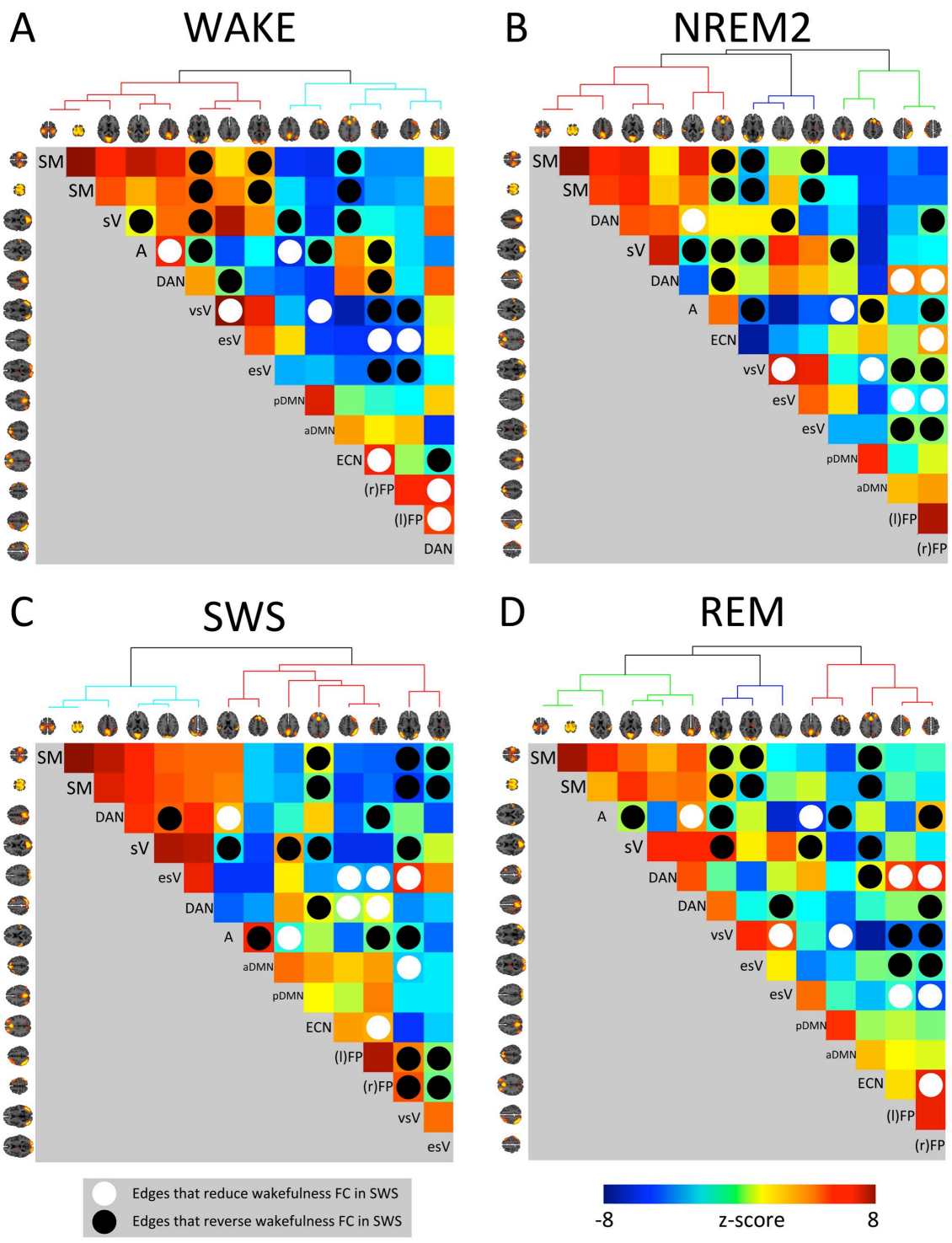

Figure 13. Full-correlation functional connectivity (FC) matrices for 14 resting state networks (RSNs) across wakefulness and sleep.

Nodes reordered according to hierarchical clustering (visualized above each matrix). Colors represent Fisher r-to-z transformed correlations between nodes (taking into account autocorrelation and standard error), with 1-group t-test performed on all participants with data available for a given sleep stage. (A) wakefulness. (B) non-rapid eye movement stage 2 (NREM2). (C) slow wave sleep (SWS). (D) REM. Black circles indicate FC edges that reverse wakefulness FC in NREM. White circles indicate FC edges that reduce wakefulness FC in NREM. SM=somato-motor, sV=striate visual, A=auditory, DAN=dorsal attention network, esV=extra-striate visual, vsV= ventral stream visual, DMN=default mode network, ECN=executive control network, l/rF-P=left/right fronto-parietal

Chapter 4

4 Resting state networks constrain neuronal activity at multiple frequency bands across wakefulness and sleep

4.1 Introduction

Investigations of the potential connection between correlated resting state blood oxygen level dependent (BOLD) activity (manifested as resting state networks, or RSNs) and correlated neuronal activity has continued ever since the idea was first proposed (Biswal, Yetkin, Haughton, & Hyde, 1995). However, the specifics of this connection are still unclear and not fully substantiated (Chen et al., 2017; Leopold & Maier, 2012; Schölvinck, Leopold, Brookes, & Khader, 2013). Given that the BOLD signal is indirectly and inferentially related to neuronal activity (Heeger & Ress, 2002; Logothetis, 2008), efforts to establish this connection have turned to brain activity recording modalities that more directly reflect neuronal activity. In one approach, frequency band limited power (BLP) fluctuations, as recorded using electroencephalography (EEG) or electrocorticography (ECoG), is directly correlated with RSN activity, as recorded using functional magnetic resonance imaging (fMRI). Based on the results of such inter-modality correlations, different frequency bands appear to be recruited in different proportions within each RSN (Mantini, Perrucci, Del Gratta, Romani, & Corbetta, 2007). Thus, each RSN can be said to manifest a unique "fingerprint" of BLP preferences, and, by inference, to manifest different proportions of neuronal populations that express distinct oscillatory frequencies.

However, attempts to settle the specifics of BLP localization within RSNs and/or brain regions have produced mixed and inconclusive results. For example, theta BLP was found to map strongly to the DMN in one ECoG-fMRI study (Hacker, Snyder, Pahwa, Corbetta, & Leuthardt, 2017), but not in another, similar study (Foster, Rangarajan, Shirer, & Parvizi, 2015). The stability of BLP localization within specific RSNs over time and across subjects appears to be unstable, and is marked by high variability of the correlation between RSN activity and BLP fluctuations (Meyer, Janssen, Van Oort, Beckmann, & Barth, 2013). As a consequence of this inconsistent relationship during

wakefulness, it is difficult to substantiate the long-suspected connection between RSNs and neuronal activity.

Significantly however, the relationship between RSNs and BLP across all three healthy functional modes of the brain (namely; wakefulness, rapid eye movement (REM) and non-REM (NREM) sleep), remains to be investigated. It is possible that: (1) correlations between fMRI-derived RSN activity and EEG-derived BLP fluctuations are more stable during sleep, or; (2) *changes* in these correlations across these stages might reveal a stable pattern. By employing simultaneous EEG-fMRI during sleep, the purpose of the present study was to determine how correlations between EEG-derived BLP fluctuations and fMRI-recorded RSN activity change across sleep-wake states (*e.g.*, wakefulness, NREM and REM). We aim to understand the dynamics of this relationship across all three healthy alternate functional modes of the brain, in the hopes of further substantiating the relationship between neuronal activity and RSN activity. More specifically, if there is evidence for a consistent *dynamic* pattern, across sleep-wake states, then the present indications of an inconsistent relationship between neuronal activity and RSNs (when wakefulness is examined *alone*), can be clarified within the larger context of a more stable relationship across all healthy alternate states of the brain.

Importantly, the cortical neurophysiology of REM and NREM are quite distinct, and this can be expected to impact both frequency band dynamics at the global level, as recorded by EEG, as well as RSN activity, as recorded by fMRI. Specifically, NREM is characterized by increasingly synchronized cortical activity (Weigenand, Schellenberger Costa, Ngo, Claussen, & Martinetz, 2014b), as a consequence of lower levels of acetylcholine (ACh), a neuromodulator that is known to disrupt synchronization. By contrast, REM is characterized by desynchronized cortical activity, similar to wakefulness, due to the cortical release of ACh, effected by the reactivation of the ascending reticular activating system during this stage (Brown & McCarley, 2008). We predicted, for each RSN examined, a progressive deviation away from the BLP fingerprint characteristic of wakefulness (*i.e.,* as delineated by correlations between RSN activity timeseries and simultaneously collected EEG-derived BLP timeseries, in several frequency bands of interest), during deepening NREM, which would be maximally

differentiated during slow wave sleep (SWS). Further, we predicted a return to a wake-like BLP fingerprint during REM.

4.2 Methods

4.2.1 Participants

See section 2.2.1, above.

4.2.2 Experimental procedure

See section 2.2.3, above.

4.2.3 Polysomnographic recording and processing

See section 2.2.4, above.

4.2.4 MRI imaging acquisition and analysis

4.2.4.1 Recording parameters

See section 2.2.5.1, above.

4.2.4.2 Functional data classification

All sleep session functional volumes were scored according to standard sleep-stage scoring criteria (Iber et al., 2007) by an expert registered polysomnographic technologist. To be included in the fMRI analysis, the EEG had to be visibly movement artifact-free. Volumes were classified as wake, NREM1, NREM2, SWS or REM. Notably, wake data used in the analysis was taken from the wake resting state session only, despite wake segments being present in the sleep session data. This was to avoid including wake periods contaminated with variable levels of drowsiness/sleep inertia from preceding sleep episodes of varying sleep depth. Following sleep scoring, a single epoch was extracted from the total set of functional volumes, for each participant who had data available for a given stage.

4.2.4.3 Functional data extraction

The length of the epoch extracted per participant was determined by considering the minimum length time series available amongst all the participant data for a given stage. For example, if 25 participants had at least (a bare minimum of) 3 minutes of NREM2 data, with the smallest epoch available for a given participant being 4 minutes, then a single 4-minute NREM2 epoch was extracted from the data available for all participants with NREM2 data. In practice, any participant with less than 4 1/2 minutes of data for a given stage was rejected from the analysis for that stage, as a further consideration of the number of time points required for an accurate functional connectivity analysis.

4.2.4.4 Wake data acquired/extracted for analysis

Of the 34 participants included in the analysis, 29 had 220 MRI volumes (approximately 8 minutes) worth of data, with the remainder having 150 volumes (approximately 5 $^{1}/_{2}$ minutes). One participant had data recorded with slightly different acquisition parameters, so their wake data was excluded, leaving a total of 33 participants, each with 150-volume epochs (wake data was unavailable for 12 of these participants at the time of thesis assembly, however).

4.2.4.5 Sleep stage data acquired/extracted for analysis

Overall, participants managed to obtain the full spectrum of sleep stages (NREM1, NREM2, SWS and REM sleep). Given the significant challenges of sustaining sleep in an MRI scanner environment (due to noise and participant comfort), on an individual basis, the majority of participants maintained sleep in only a subset of the sleep stages of interest, for a duration long enough to be considered sufficient for FC analysis. Remarkably, 4 participants did manage to transition through all three sleep-stages of interest (NREM2, SWS and REM). In all cases, sleep scoring identified a pattern in which participants transitioned between sleep stages of variable duration; from less than 20 seconds (the shortest sleep scoring period) to 69.3 minutes. Notably, sleep stage NREM1 was mostly unavailable, however considering the brief and transitional nature of this stage, it was justifiably eliminated from the analysis at the expense of exploring

interesting correlations that might occur during the sleep onset process; which would likely require an experimental approach tailored to study sleep onset *per se*.

The majority of participants (28 out of 33) were able to sustain a sufficient amount of NREM2 sleep for the correlation analysis. However, it was decided that 24 150-volume epochs be used in the analysis, in order to both match the available wake data and to maximize the robustness of the correlation analysis. In the case of SWS, 11 participants had data above the minimum 83-volume (3-minute) cutoff, with 10 having at least one epoch longer than 110 volumes (approximately 4 minutes). However, as 110 volumes was considered unsuitable for a correlation analysis, two datasets were excluded, leaving 9 133-volume (4.8 minute) epochs. Seven participants had REM data above the 83 volume cutoff, with all seven having at least one session longer than 100 volumes (approximately $3^1/_2$ minutes). Despite the difficulty in acquiring REM data, 100 volumes was considered unsuitable for a correlation analysis and one dataset was excluded (*n.b.*, resting state analyses typically utilize 5-7 minutes of data; Birn et al., 2013). This left six 129-volume (4.6 minute) epochs for use in the analysis.

4.2.4.6 Preprocessing

Each sleep and wake epoch was individually preprocessed using the Oxford Centre for Functional Magnetic Resonance Imaging of the Brain Software Library (FMRIB, Oxford U.K.; FSL version 5.09; 57). Functional volumes within each epoch were realigned using FSL's MCFLIRT tool (Jenkinson et al., 2002) which performs rigid body transformations. Non-brain voxels were also extracted using FSL's BET tool (Smith, 2002). Volumes were spatially smoothed using a Gaussian kernel of 5mm full-width at half-maximum (FWHM) and high-pass temporal filtered (Gaussian-weighted least-squares straight line fitting, FWHM = 2000s). Functional volumes were then coregistered to the MNI152 standard space (McConnell Brain Imaging Centre, Montreal Neurological Institute) using 12 degree-of-freedom affine registration. Finally, each epoch was individually cleaned of non-neuronal artifacts using the FIX plug-in for the FSL package (Griffanti et al., 2014; Salimi-Khorshidi et al., 2014), an automatic noise detection and removal algorithm. Prior to using FIX, FSL's MELODIC tool (Beckmann & Smith, 2004) was used to generate ICs for each epoch. MELODIC's default dimensionality estimation

function automatically estimates the number of ICs by performing a Bayesian analysis. FIX then assessed each of these ICs as noise or signal, after generating more than 180 distinct spatial and temporal features of each IC and feeding these into a multi-level classifier. ICs classified as noise were then subtracted from the ICA mixing matrix and a new set of functional volumes was generated.

4.2.4.7 EEG-fMRI correlation analysis

4.2.4.7.1 Generation of RSN timeseries

10 RSN templates derived from a separate healthy waking RSN ICA study (Smith et al., 2009) were spatially regressed onto the single-subject 4D epochs available for each sleep stage, using FSL's dual_regression function (Nickerson, Smith, Öngür, & Beckmann, 2017). The spatial regression produced a set of 10 beta values (*i.e.,* one beta value per RSN) for each volume of functional data, reflecting how well each of the 10 RSNs were represented at each time point. Each RSN therefore had a series of beta values across all time points, which was treated as a pseudo time series, for use in the correlation with the EEG power spectral data. This procedure was also repeated for 20 independent component (IC) templates from the same external study (Smith et al., 2009), as these templates included separated anterior and posterior DMN components. As not all of these ICs represented RSNs, additional steps were implemented: FSL image viewer FSLEyes and the FSLNets' ts_spectra function were used to respectively assess the spatial configuration and power-frequency spectra of each of these 20 ICs. The time courses of six noise-related ICs were regressed out of all other time series and then deleted, leaving 14 RSN time series, two of which belonged to anterior/posterior DMN RSNs.

4.2.4.7.2 Generation of frequency-band power timeseries

Timeseries were generated for 5 frequency bands of interest; delta (0.3 – 4 Hz), theta (4 – 8 Hz), alpha (8 – 12 Hz), sigma (12 – 16 Hz), beta (16 – 24 Hz). Discrete power values were generated for each frequency band, in 2.16s time bins (corresponding to the fMRI volume length), using a wavelet analysis on the complete EEG timeseries for the Cz electrode. This procedure generated 5 timeseries per subject, one for each frequency band. The relevant EEG power values (corresponding to each fMRI epoch) were then

extracted from each timeseries and convolved with a hemodynamic response function, using SPM's Volterra function.

Finally, each frequency band timeseries was correlated with each RSN timeseries available in each wake and sleep stage, at the single-subject level. The resulting single-subject correlations were plotted on a single scatter plot, across sleep stages, producing a unique plot for each frequency band, for each RSN (*i.e.,* 50 unique plots in total).

4.2.4.7.3 Polynomial fitting to edge FC data across wakefulness and sleep

In order to test our main hypotheses, we assessed the pattern of correlation value changes across all sleep stages for a given frequency band, for a given RSN, by fitting three different polynomial functions, *i.e.,* a first-order non-horizontal line, a second-order quadratic function, or a third-order cubic function (see Figure 14 for a cartoon of possible fits) to stage-coded correlation data. Correlation values were stage coded by assigning a whole number according to sleep stage. Wake correlations were assigned an x-axis value of "1", NREM2 a value of "2", SWS a value of "3" and REM a value of "4". A coefficient of determination (*i.e.,* R-square values) was calculated for each polynomial function. To test for the statistical likelihood of a best fitting function, sample distributions of R-square values for each polynomial fit were generated by resampling the data using permutation hypothesis testing (*i.e.*, by randomly assigning the edge FC data to different sleep stages, calculating new R square values for the polynomial fits and iterating this procedure 1000 times). P-values were then calculated for the actual fitted polynomials by comparing the R square values to the permuted sample distributions. If only one type of polynomial fit was significant for a given frequency band, for a given RSN, then the pattern of correlation value changes was categorized as being best described by that fit. Otherwise, the polynomial fit with the lowest p value and highest R square value was used to best describe the pattern. If no statistically significant best-fits were identified, then the correlation values were categorized as being best described by the polynomial fit with the highest R-square value.

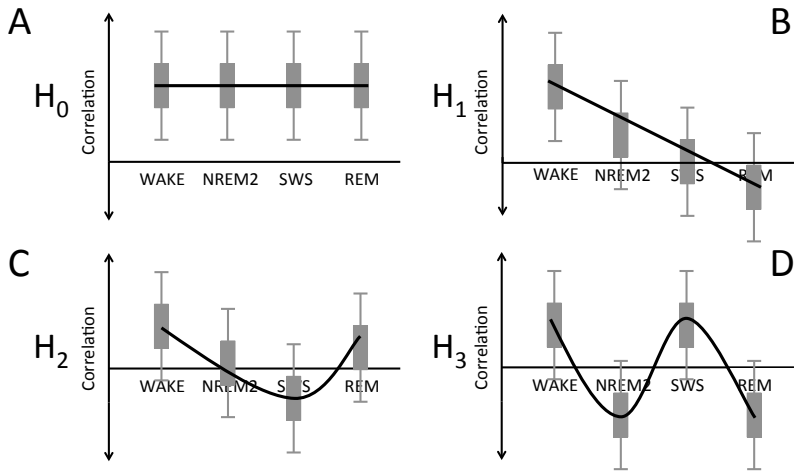

Figure 14. Cartoon of possible polynomial fits for correlation data across wakefulness and sleep.

(A) Null hypothesis (H_0); first-order polynomial, horizontal line fit. (B) Alternative hypothesis 1 (H_1); first-order polynomial, non-horizontal line fit. (C) Alternative hypothesis 2 (H_2); second-order polynomial, quadratic line fit. (D) Alternative hypothesis 3 (H_3); third-order polynomial, cubic line fit. REM=rapid eye movement, NREM2=non-REM stage 2, SWS=slow wave sleep.

4.2.4.8 General linear model analysis

In order to determine the spatial localization of the different frequency-bands, single-subject frequency band timeseries were regressed onto the fMRI data using a general linear model (GLM), for each of wake, NREM2, SWS and REM (performed with SPM). Group level results were generated using first-level beta maps as inputs.

4.3 Results

4.3.1 Correlations between RSN activity and BLP fluctuations

Consistent with our hypotheses, the predicted (quadratic) trend was followed for the majority of frequency bands in more than half (*i.e.,* 5/9) of the cortical RSNs examined; i.e., striate visual (sV), extrastriate visual (esV), executive control network (ECN), left/right fronto-parietal network (l/rF-P) (Figure 15). Notably, the quadratic fits to the correlation data were significantly different (*i.e.* $p < .05$) from a horizontal line for the majority (*i.e.,* 15/25) of frequency bands in these RSNs. Frequency bands in the

remaining RSNs (i.e., ventral stream visual (ventV), default mode network (DMN), cerebellum, somatomotor (SM), auditory) largely followed independent trends. However these trends were largely found not to be significantly different (*i.e.,* $p > .05$) from a horizontal line for the majority (*i.e.,* 21/25) of the frequency bands in these RSNs (see colored asterisks in Figure 15, for significant fits). Fingerprints for these RSNs remained largely consistent across wakefulness and sleep (*i.e.,* auditory, cerebellum, integrated DMN), or followed a consistent decrease across stages (*i.e.,* SM). The follow-up analysis of the anterior and posterior subregions of the DMN, demonstrated that the anterior DMN (aDMN) largely follows the predicted trend, *i.e.,* significant quadratic fits for all frequency bands of interest), By contrast, the posterior DMN (pDMN) did not appear to follow the predicted trend, nor were the polynomial fits to the data significantly different from a horizontal line (Figure 16). These results suggest that frequency BLP in individual RSNs is largely responsive to the dynamics of cortical neural synchrony across wakefulness and sleep. They further suggest that it may be more meaningful to consider the DMN as two separate RSNs; namely, aDMN and pDMN.

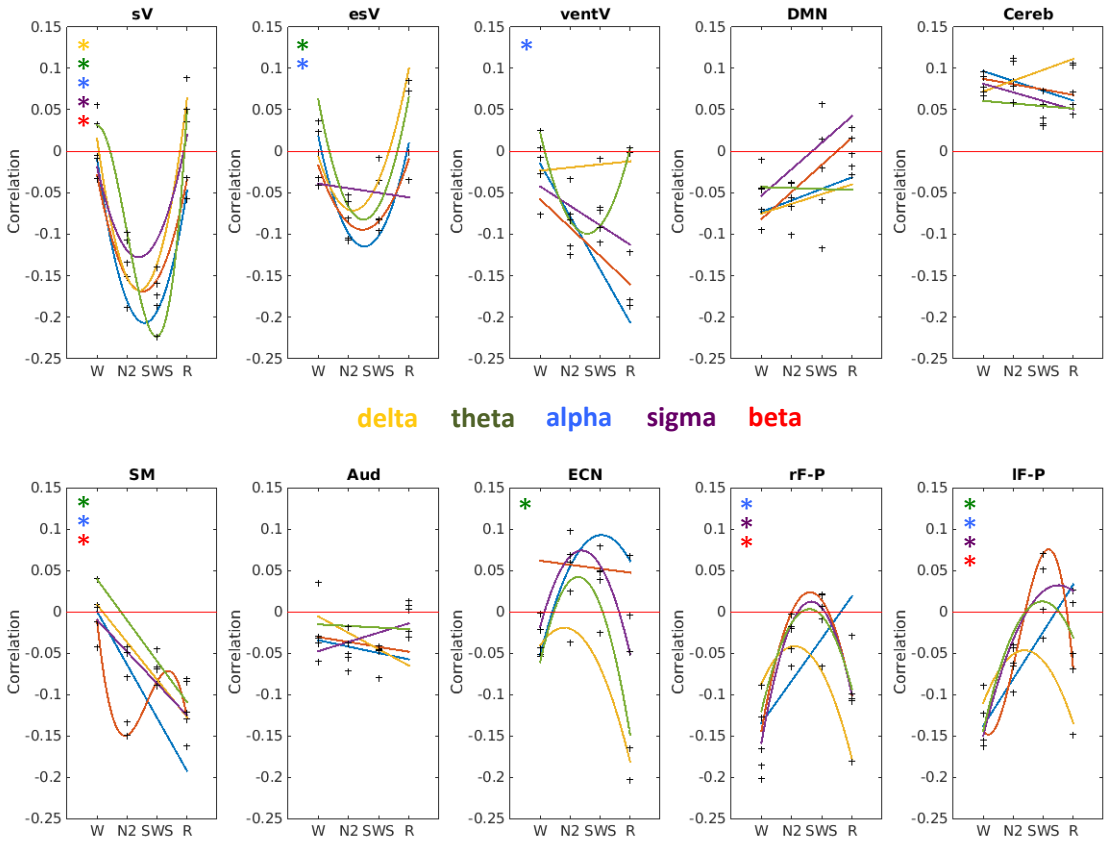

Figure 15. Best-fit polynomials to resting state network (RSN) activity correlations with band limited power fluctuations across wakefulness and sleep, for 5 EEG-derived frequency bands of interest.

Significant fits are indicated with colored asterisks. Mean correlation values across participants are indicated with plus symbols. W=wakefulness, REM=rapid eye movement, N2=non-REM stage 2, SWS=slow wave sleep. sV=striate visual, esV=extrastriate visual, ventV=ventral stream visual, DMN=default mode network, Cereb=cerebellum, SM=somatomotor, Aud=auditory, ECN=executive control network, r/lF-P=right/left frontoparietal network

It is notable that frequency band correlations for the higher-order RSNs (*i.e.,* DMN, ECN, l/rF-P) largely begin as negative correlations during wakefulness and trend towards positive correlations, in a progressive fashion, during NREM. For the ECN and for l/rF-P, there is also a return to wake-like correlations in REM, following the predicted pattern. By contrast, frequency band correlations for the sensory RSNs largely begin as positive correlations during wakefulness and trend towards increasingly negative correlations

during NREM. For sV and esV, there is also a return to wake-like correlations in REM, following the predicted pattern. These results indicate that the boundaries of the canonical RSNs may play a role in defining the specific inflection of the pattern. This could suggest, in turn, that canonical RSN boundaries meaningfully constrain the dynamics of neuronal activity across wake-sleep state changes.

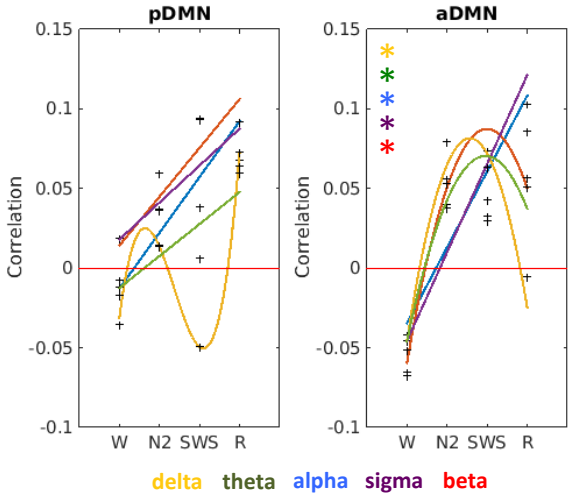

Figure 16. Best-fit polynomials to anterior and posterior default mode network (a/pDMN) activity correlations with band limited power fluctuations across wakefulness and sleep, for 5 EEG-derived frequency bands of interest.

Significant fits are indicated with colored asterisks. Mean correlation values across participants are indicated with plus symbols. W=wakefulness, REM=rapid eye movement, N2=non-REM stage 2, SWS=slow wave sleep.

4.3.2 GLM results

Overall, significant frequency band activity was mostly localized to subcortical regions, such as the thalamus and cerebellum, rather than to (cortical) RSNs, across sleep stages (Figures 17 and 18). Delta, alpha, and beta BLP was localized to the cerebellum in NREM2 ($p_{FWE} < .001$, .018, and .011, respectively, at the cluster-level). Alpha BLP was also localized to the cerebellum in SWS ($p_{FWE} < .033$, at the cluster-level). These results coincide with the results of MEG studies that indicate an important role for alpha in mediating cortico-cerebellar activity in support of cognition (Ben-Soussan, Glicksohn, &

Berkovich-Ohana, 2015; Kujala et al., 2007), albeit during wakefulness, not sleep. Further, slow waves and delta have been linked to the cerebellum in an EEG-fMRI study (Dang-Vu et al., 2008).

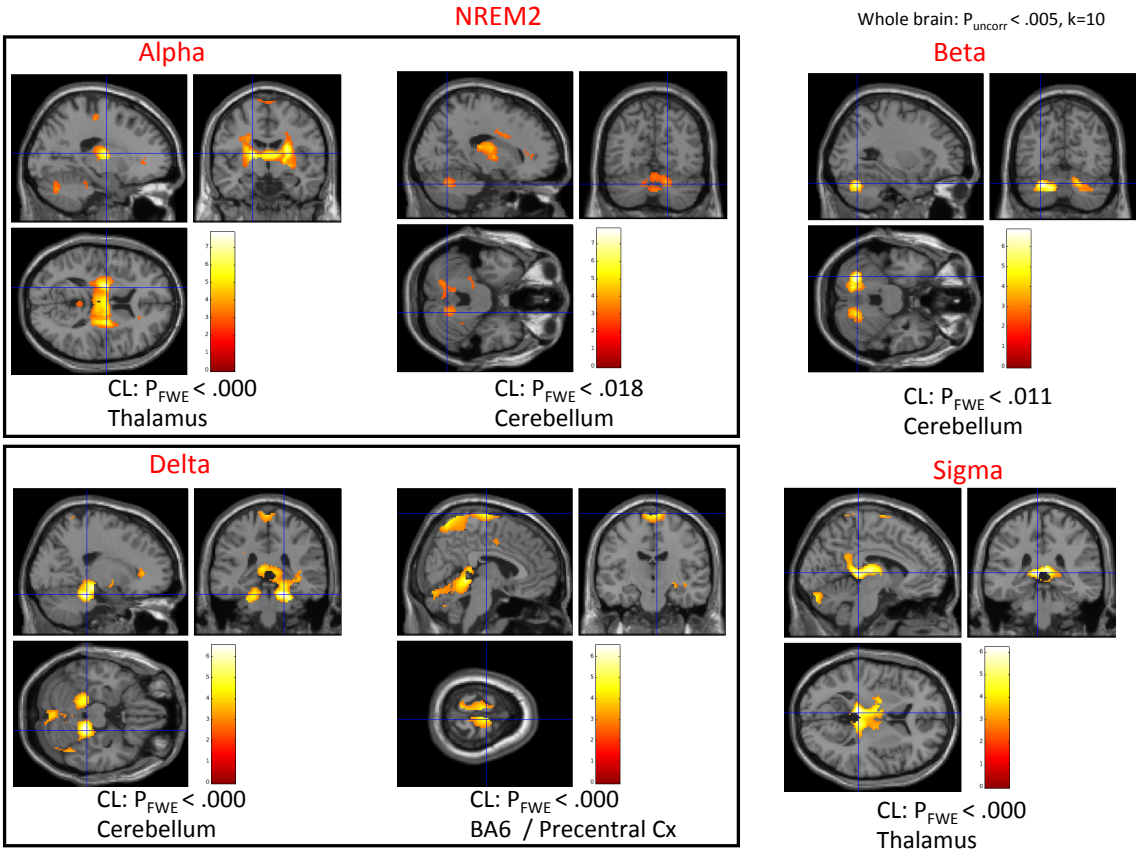

Figure 17. Whole-brain group-level general linear model results, non-REM stage 2 (NREM2).

Only voxels for band-limited-power-related activity that survives family-wise error correction at the cluster level (CL) are shown.

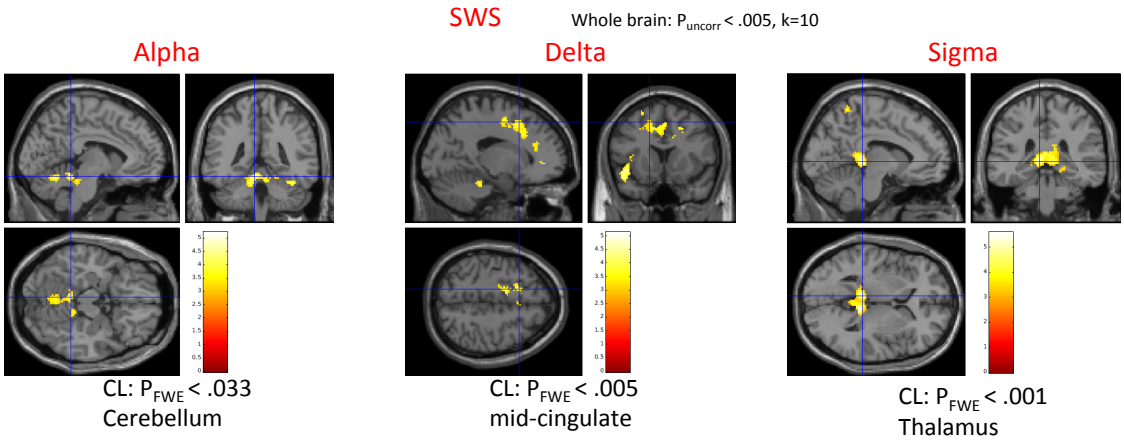

Figure 18. Whole-brain group-level general linear model results, slow wave sleep (SWS).

Only voxels for band-limited-power-related activity that survives family-wise error correction at the cluster level (CL) are shown.

Consistent with the cortical origins of slow rhythms (Steriade, 2001), delta BLP was found to be localized to cortical regions; *i.e.,* to precentral cortex in NREM2 ($p_{FWE} < .001$, at the cluster-level) and to mid-cingulate cortex during SWS ($p_{FWE} < .005$, at the cluster-level). Furthermore, sigma BLP was significantly associated with the thalamus, during both NREM2 and SWS ($p_{FWE} < .001$, at the cluster-level, for both stages). Given that sigma is in the frequency range (*i.e.,* 12 – 16 Hz) of sleep spindles, this finding is consistent with the known thalamic origins of the spindle pacemaker (Contreras, Destexhe, Sejnowski, & Steriade, 1996). None of the REM GLM results were significant at the cluster-level, however, given the limited data available for this stage (N=6), this is not unexpected (Figure 19) given the noisy scanner environment and the fact that REM appears predominantly in later sleep cycles. Thus, given the paucity of available data in the extant literature, we report the uncorrected results here. All results are at $p_{uncorr} < .001$, at the voxel-level, except for alpha-band localization to the post central gyrus ($p_{uncorr} < .003$, at the voxel-level). Notably, each frequency band was localized to at least one cortical location. Theta BLP, in particular, was localized to a number of regions of the temporal cortex, including fusiform and lingual gyrus. The cortical localization of both theta and alpha is reassuring, given that the EEG signatures used to identify REM sleep (Iber, Ancoli-Israel, Chesson, & Quan, 2007) include these frequency bands specifically.

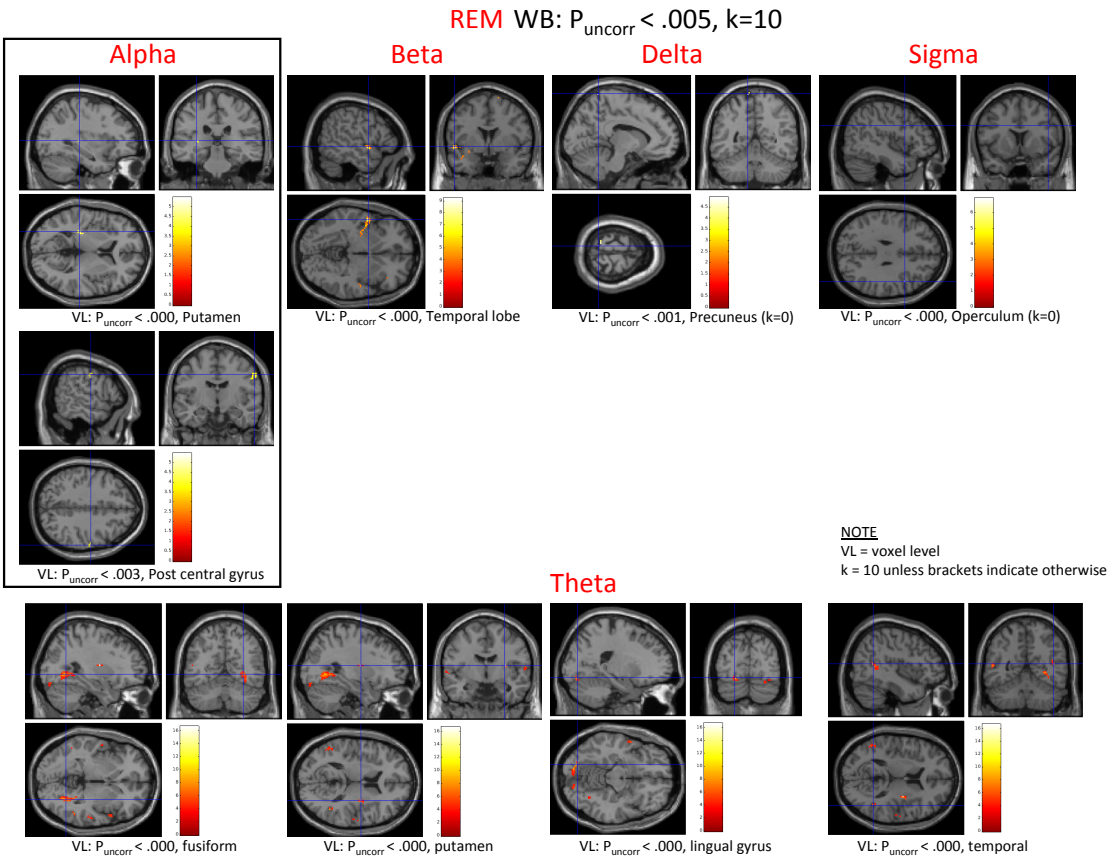

Figure 19. Whole-brain group-level general linear model results, rapid eye movement (REM) sleep.

4.4 Discussion

As predicted, the hypothesized dynamic trend across sleep-wake states was largely followed for the majority (5/9) of cortical RSNs, including two sensory RSNs (*i.e.,* striate and extrastriate visual) and the majority of higher-order RSNs (*i.e.,* executive control network, left/right frontoparietal networks), with the exception of the DMN (where the DMN was considered as a whole). This result suggests that the neurophysiological dynamics across NREM and REM have a predictable global impact on the expression of frequency band power within the majority of individual RSNs. It is remarkable that this finding is also consistent with a recent, preliminary study of RSN functional connectivity (FC) conducted by our group, in which we noted that the majority of functional connections also follow this trend (Houldin, Fang, Ray, Stojanoski, et al., 2019) Together, these two studies suggest that the dynamics of both RSN FC and BLP (as

constrained to RSNs) are dependent upon the global changes in cortical synchrony manifested by NREM and REM. While this finding makes intuitive sense, it is nevertheless reassuring to identify such consistency between otherwise distinctive processes, each of which is defined by unique recording modalities. It is worth noting that these results demonstrate, for the first time, the dynamics of EEG-derived BLP, as it relates specifically to BOLD activity within RSNs, across all sleep-wake states.

It is important to consider the four RSNs that do not appear to follow the predicted trend. Of these, the polynomial fits for three (*i.e.,* DMN, cerebellum, auditory network) are not significantly different from a horizontal line, *i.e.,* group-level BLP fluctuations do not appear to be modulated by known cortical synchrony dynamics across wakefulness and sleep. Among these, the cerebellum is non-cortical and therefore shouldn't be expected to follow neurophysiological trends specific to the cortex. The stability of the cerebellar BLP fluctuations across wakefulness and sleep is reflected in the group-level GLM results, in which the cerebellum is observed persistently (*i.e.,* NREM2 alpha, beta and delta, SWS alpha). By contrast, as far as the GLM results for the cortical RSNs are concerned, it appears that BOLD activity for the majority of cortical regions is not consistently synchronized with any given frequency-band, across subjects. This could be because cortical RSNs are required to flexibly recruit frequency power in accordance with changing cognitive loads. By contrast, the cerebellum may be loaded more consistently over time (across all frequency bands), and, importantly, across all healthy functional brain states in wakefulness and sleep.

It is worth mentioning that the appearance of a significant cluster of voxels in a GLM analysis requires relatively consistent, sustained correlated activity of (BOLD activity in) that cluster with a regressor of interest (in this case, the BLP timeseries convolved with an HRF) across subjects. By comparison, the correlation analysis used in this study could yield relatively low correlations between BLP and RSN activity; so long as different stages yield different correlations however, a significant dynamic pattern across stages could still be found. As discovered by (Meyer, Janssen, Van Oort, Beckmann, & Barth, 2013), there is high variability of BLP representation within specific RSNs, over time and across subjects (at least during wakeful, eyes-closed, rest). This suggests that neuronal

activity in a given RSN is highly dynamic (*i.e.,* not consistent), likely in accordance with the requirements of dynamically changing cognitive activity (which would require changing contributions from the neural populations constrained to individual RSNs, over time). It would therefore be expected that group level GLM results would be less likely to indicate sustained BLP activity in specific cortical regions.

As for the cortical RSNs that do not appear to change across stages, *i.e.,* the DMN and the auditory network, it is important to note that DMN FC is known to be reduced between its anterior and posterior nodes during SWS. This should correspond to differential frequency preferences for these nodes and possibly to different dynamics, during NREM. In order to address this possibility, a separate analysis was conducted, allowing for the anterior/posterior components of the DMN to be examined separately (Figure 16). As expected, this produced a more differentiated mix of patterns for the frequency bands of interest. Importantly, these differences were significant for all frequencies, for the anterior DMN, three of which followed the hypothesized pattern across wakefulness and sleep.

Alpha-band activity was the most common frequency band to demonstrate a significant polynomial fit amongst all RSNs (*i.e.,* 6/10, or 7/11, where the DMN is subdivided). This is consistent with a magnetoencephalography (MEG) study (Hipp, Hawellek, Corbetta, Siegel, & Engel, 2012) that sought to identify the cortical correlation structure of spontaneous oscillatory activity and found that global correlation of spontaneous activity peaks in the alpha-beta frequency range. It could be the case that the methods used in the present study are best able to capture dynamics in the alpha band simply because the alpha signal is strongest across the whole brain.

Most interestingly, irrespective of whether some RSNs follow the predicted trend and some do not, what appears to be the consistent pattern across RSNs is that RSN timeseries-EEG frequency band correlation dynamics within each RSN largely parallel each other. This finding is surprising, given that each sleep-wake state has its own unique electrophysiological signature in terms of relative EEG power spectra (Iber, Ancoli-Israel, Chesson, & Quan, 2007; Steriade, 2003). One possible interpretation of this result

is that, in general, frequency band dynamics within a given RSN genuinely increase or decrease in strength together across stages. This finding corresponds nicely with what we know of both the nature of RSNs, as well as band-limited spontaneous oscillations. First, it supports the idea that RSNs act to constrain neuronal activity, generally (Deco & Corbetta, 2011), even if the profile of this activity changes over time and across healthy alternate brain states. Indeed, the defining characteristic of RSNs is that they are identified (using techniques such as ICA or SCA) as regions with highly correlated activity. Second, it supports the idea of cross frequency phase-amplitude coupling (Bragin et al., 1995a); *i.e.,* that the phase of slower frequencies modulates the power of faster frequencies. If frequency banded activity is changing in the same direction within an RSN, this could be because the activity of slower frequencies is influencing that of faster frequencies, possibly via phase-amplitude coupling.

What is particularly interesting about these results is the fact that the banded-frequency dynamics of spatially proximate RSNs are constrained in different ways. For example, the extrastriate visual RSN is proximate to (posterior) left and right frontoparietal networks, however they have opposite dynamics, emphasizing the spatial authority of each respective RSN. An alternative interpretation of this result is that it is not the frequency band dynamics that are changing together, but instead it is only the correlations between the RSN and EEG timeseries that are changing together. For example, in the case of the ECN, it could be that correlations across frequency bands collectively rise together during NREM because there is a graded decrease in the within-subject variability of frequency banded activity during NREM (as captured by EEG, relative to RSN timeseries variability, as captured by the BOLD signal), and so the BOLD signal begins to more closely match the EEG signals, across NREM. However, this would not necessarily mean that there was increased activity in these bands during NREM.

Overall, an RSN is perhaps best described as a collection of neurons in which all activity is constrained within certain temporal limits. The boundaries of a given RSN end (in a graded fashion), when a given local population of neurons is no longer phase-locked to the collective set of neurons of that RSN. Given the fact that the RSN FC of pathological brains is differentiable from that of the healthy population, (*e.g.,* epilepsy (Centeno &

Carmichael, 2014), Alzheimer's disease (Wang et al., 2006) and schizophrenia (Yu et al., 2012)), it seems that the consequence of an RSN's failure to impose temporal authority is cognitive dysfunction. In the present study, it cannot be determined which frequency band is setting the temporal constraints, however. It may be the case that frequency band dynamics are coordinated outside the boundaries of the canonical RSNs, with different frequency bands having different hubs. For example, the medial temporal lobes appear to be a hub for the theta frequency range (Hipp, Hawellek, Corbetta, Siegel, & Engel, 2012). Despite this possibility, it is intriguing that the slowest band (*i.e.,* delta) matches the predominant trends, in 9/10 RSNs, indicating that faster frequencies are phase-locked to delta activity.

In conclusion, this study confirmed that the majority of RSN frequency-band fingerprint dynamics are responsive to the changing neurophysiological environment across wakefulness, NREM and REM, in a predictable manner. It was further discovered that all RSNs, including those that did not follow the hypothesized trend, appear to constrain within-RSN frequency band dynamics in a consistent manner, supporting the idea that an RSN is a cortical region that imposes consistent temporal constraints upon its neural population, across all healthy alternate functional modes of the brain.

Chapter 5

5 General discussion

The primary aim of this thesis was to employ simultaneous EEG-fMRI during sleep to help illuminate the properties and functions of both sleep and RSNs. In this chapter, the main findings will be summarized along with discussion of the insights gained from this approach. There are three main sections, corresponding to each of the three studies described in Chapters 2 – 4. Within each main section is a subsection discussing the separate implications of the study for the nature and function of RSNs, and of sleep. Finally, a Summary and Conclusions section closes out this chapter.

There were four primary findings, overall, each with significant implications that will be expanded upon, below. In the first study, reported in Chapter 2, all canonical RSNs were positively identified in sleep, and against expectations, all ICs which could not be identified as canonical RSNs, across all sleep stages, were positively identified as noise. This finding suggested that the wakefulness canonical RSNs comprise the complete set across all healthy alternate functional modes of the brain, and that there are likely no sleep-specific networks to putatively support unique sleep brain states and their respective functions. In the second study, reported in Chapter 3, RSN FC dynamics were largely found to reflect the pattern that would be predicted from known cortical neuronal synchrony dynamics across wakefulness and sleep (*i.e.,* a progressive deviation away from wakefulness states during NREM, and a return during REM). This was taken as a convincing indication that RSNs reflect neuronal activity, thereby providing further supportive evidence on this longstanding issue. Within this dynamic pattern, a further, unexpected pattern indicated that NREM FC generally moves in the direction *opposite* to wakefulness FC (*e.g.,* positive correlations specifically becoming negative, and *vice versa*). This finding is consistent with a homeostatic role for NREM sleep, thus potentially providing support for neuro-cognitive theories of sleep function.

Finally, in the third study, reported in Chapter 4, BLP representation in individual RSNs was also found to reflect the aforementioned pattern of cortical synchrony dynamics

across wake/sleep. Notably, the pattern was largely consistent across the examined frequency bands of interest. This provided further evidence that RSNs reflect neuronal activity. Importantly, the specific pattern of these dynamics (*i.e.,* the inflection of the pattern) was different, depending on the canonical RSN examined. This supports the assertion that the canonical RSN boundaries might represent the limits of *meaningfully* coupled neuronal activity, across frequency bands, since BLP largely changes in the same direction, within the canonical RSN borders. Overall, these three studies help to clarify the nature and functions of both RSNs and sleep, individually, and in terms of their interactions with each other.

5.1 First study: Toward a complete taxonomy of RSNs

The primary aim of the first study was to identify spatially unique sleep-specific RSNs. The data-driven ICA methodology was used in order to overcome any *a priori* bias towards the canonical RSNs found in wakefulness. The positive findings (*i.e.,* that all canonical wake RSNs were identified in all sleep stages, and that the remaining ICs were identified as non-neuronal sources of noise) indicated that there are likely no sleep-specific RSNs. This, in turn, suggests that the wakefulness canonical RSNs most likely comprise the complete set across all healthy alternate functional modes of the brain. It further suggests that prior studies which made use of wakefulness RSNs during sleep (without explicitly testing assumptions) were warranted in doing so. These novel findings have implications for the nature of both RSNs and sleep, which are each discussed in turn, below.

5.1.1 What the first study reveals about the nature and function of RSNs

The results of this study have two important implications with respect to the nature of RSNs. Namely; (1) we have a better understanding of the full set of RSNs across all healthy alternate function modes of the brain, and; (2) given that RSNs spatially correspond to areas known to be related to wakefulness functions, and that the spatial correspondence between RSNs and sleep functions is less clear, it is possible that RSNs

may serve wakefulness-related functions only. These two implications are expanded upon, below.

As discussed in Chapter 2, the first, more obvious implication is that we can be more confident that the complete repertoire of RSNs is known. This has not been explicitly investigated to date. As pointed out in Chapter 1, a resting state study that spans wakefulness, NREM and REM constitutes the complete search space for identifying the full repertoire of RSNs. This is because these states comprise the full set of healthy, alternate functional modes of the brain. By contrast to pathological states, TBI or sedation, these states are the only ones in which putative functions associated with RSNs could have evolved. The results of this study also suggest that prior resting state sleep studies were warranted in making use of wakefulness RSNs, despite not testing the implicit assumption that only the wakefulness RSNs apply to sleep. From a broader perspective however, it is perhaps not unreasonable to claim that the catalogue of RSNs (Biswal, Yetkin, Haughton, & Hyde, 1995) is closer to being fully inventoried.

The second implication follows directly from the first, as identifying the specific RSN inventories in each of wakefulness and sleep can help us to infer the functional role of RSNs. Conversely, an incorrect accounting of RSNs could have lead to misleading conclusions with regards to their function. In exploring the functional implications of the negative result of the first study, it is worthwhile to first discuss the alternate implications of a positive result. Specifically, discovering a spatially distinct RSN in one or more sleep stages might, by itself, have suggested that RSNs play an active role in supporting sleep functions. For clarification, this would have been a suggestion only, in the same sense that the sudden manifestation of sleep spindles in NREM2 suggests, by itself, that spindles might support sleep-specific functions. It nevertheless remains possible that spindles have no such role, and that they are instead epiphenomenal with respect to sleep function (of course, in the case of spindles, there is plenty of evidence beyond their mere manifestation that they do, in fact, serve a functional role; Cote, Epps, & Campbell, 2000b; Fang, Sergeeva, et al., 2017b; Fogel & Smith, 2011).

However, since the results of this study suggested that the wakefulness RSNs represent the complete set, the above argument cannot be used to link RSNs to unique sleep function *per se*. In order to determine what these results *do* suggest with respect to RSN function across wakefulness and sleep, it is worth examining the initial evidence that suggested RSNs might be involved in serving wakefulness-related functions. As discussed in the Introduction, there are two lines of evidence. The first is that RSN FC changes in response to changes in cognitive activity (Naci et al., 2018; Reineberg, Andrews-Hanna, Depue, Friedman, & Banich, 2015; Reineberg, Gustavson, Benca, Banich, & Friedman, 2018). The second is that there is a remarkable spatial correspondence between the canonical RSNs and regions known to be involved in supporting wakefulness-related cognition (Smith et al., 2009). Do these two lines of evidence apply to RSNs and sleep?

Clearly, the first line of evidence applies, given the results of the second study, described in Chapter 3, as well as that of prior studies (Boly et al., 2012; Chow et al., 2013; Horovitz et al., 2009; Larson-Prior et al., 2011). As for the second type of evidence, there is little clear indication, based on the present literature, that RSNs have a noticeable spatial correspondence with regions known to be involved with sleep functions. As described in Chapter 1, sleep spindle activity has been localized to both the thalamus and the cortex (Contreras, Destexhe, Sejnowski, & Steriade, 1996). Although RSNs are certainly cortical, localization of spindle activity does not appear to implicate *specific* RSNs. For example, an EEG-fMRI study that attempted to localize spindles and K-complexes implicated areas such as the PCC and right hippocampus as spindle-related areas (Caporro et al., 2012). Despite the association of these regions with posterior DMN, the same study also implicated areas that are *not* associated with the DMN, such as the putamen, precentral gyrus and superior temporal gyrus. Additionally, an fMRI investigation of both hippocampal and spindle activity during NREM (Andrade et al., 2011) found a progressive decrease in hippocampal-DMN FC from wakefulness to SWS, without finding an interaction with spindles. Further, fast and slow spindles were separately localized to anterior cingulate/medial PFC regions (*i.e.,* anterior DMN), amongst a host of other cortical areas (*i.e.,* too many to suggest a specific association with anterior DMN). Similarly, K-complexes have been localized to posterior midline

cortex, as well as striate cortex and precentral gyrus (Caporro et al., 2012). This suggests potential relationships with cortical regions associated with multiple RSNs (*e.g.,* striate visual and somato-motor RSNs), without implicating any individual RSN specifically.

Nevertheless, potential associations between RSNs and spatial localizations of sleep-specific features should be investigated in a future, more directed analysis. On this note, it is also worth mentioning the results of a recent, preliminary study conducted by our group. Namely, evidence was provided that differing DMN FC during spindle events is associated with inter-individual differences in reasoning ability (Fang, Ray, Owen, & Fogel, 2019b). However, the functional nature of this relationship remains to be resolved. It is not clear whether spindles are responsible for triggering DMN FC, or vice versa. Moreover, it is not clear whether DMN activity in this context reflects a passive role. For example, this DMN activity may reflect homeostatic/restorative action (*e.g.,* in the manner of SHY; Tononi & Cirelli, 2003), or it may reflect the passive replay of waking events (*e.g.,* similar to the hypothesis that SPW-Rs prompt the replay of waking events in the cortex, during sleep; Watson & Buzsáki, 2015).

Overall then, it seems that the connection between RSNs and waking function is supported by two lines of evidence (*i.e.,* spatial correspondence and RSN FC dynamics). By contrast, RSNs are connected to sleep functions by only one line of evidence (*i.e.,* RSN FC dynamics). Further, as discussed in the study reported in Chapter 3, RSN FC dynamics across sleep are a positive indicator of the link between RSNs and neuronal activity *generally* (*i.e.,* since the pattern of RSN FC dynamics largely matches the pattern of cortical neuronal synchrony dynamics). Consequently, it is possible that RSN FC dynamics may *only* reflect a link to neuronal activity, more generally, without implicating a more specific relationship between RSNs and sleep-related functions. In conclusion, the link between RSNs and sleep functions requires further substantiation. There is presently more substantial evidence in favor of a conclusion that RSNs serve wake-specific functions, exclusively.

5.1.2 What the first study reveals about the function of sleep

On the surface, it would seem that the first study is only relevant to understanding the nature of RSNs. However, it is also directly relevant to the nature of sleep, because it can help to generate insight into the ordering of sleep and RSNs within a functional hierarchy. One of the open questions raised in the Introduction (section 1.1.4), was whether RSNs serve as a mechanism for supporting sleep functions, or whether, instead, one of the further functions of sleep might be to manipulate RSNs in some way. As discussed above, the lack of a sleep-specific RSN, in combination with weak evidence linking the canonical RSNs to sleep functions, suggests that RSNs might exist to support wake-specific functions only. As a direct consequence of this perspective, the role of sleep, as it relates to RSNs, could be considered as follows (this consideration is speculative of course, and further studies would be required to test these assertions directly):

(a) during wakefulness, the canonical RSNs serve as an active substrate for cognition, facilitating necessary interactions with the environment; (b) during sleep, the brain is largely cut off from the environment, therefore systems that exist to facilitate exteroceptive interactions (such as RSNs) can be safely manipulated, without having to worry about negative effects on the intended functions of such systems; (c) consequently, the true mechanisms of sleep, which presumably do *not* include RSNs, can emerge and act *upon* RSNs, with RSNs playing a passive role.

Moreover, given this suggested relationship between RSNs and sleep functions, it is worth mentioning further implications for the perceptual effects facilitated by RSNs during sleep (*i.e.,* dreams). Specifically, the suggested relationship supports (though certainly does not prove) the proposition that dreams might better be considered as passive epiphenomena. By contrast, a finding that suggested an active role for RSNs during sleep, could have further suggested a similarly active role for the perceptions manifested by RSNs. For example, there is evidence, from other studies, in support of the idea that dreams are a means of replaying wakefulness events during sleep, thereby facilitating memory consolidation (*e.g.,* see review in Wamsley, 2014).

5.2 Second study: SWS is an altered, not a reduced state of awareness

The second study, as reported in Chapter 3, represents the first whole-brain assessment of RSN FC dynamics across wakefulness and all sleep stages (notably including REM sleep). The primary aim of this study was to identify a correlation between RSN FC dynamics and known cortical neuronal synchrony dynamics across wakefulness and sleep. The edge FC results of this study yielded three important patterns, namely: (1) a quadratic fit pattern for the majority (*i.e.,* 35/42) of significant FC edges, matching the neuronal dynamic pattern, as hypothesized; (2) a convex pattern for the majority (*i.e.,* 29/35) of quadratic fit edges, and; (3) an increase in magnitude in the opposite direction (*i.e.,* relative to wakefulness FC), across NREM sleep, for the majority (*i.e.,* 20/29) of convex quadratic fit edges. The primary implication of the first discovered pattern is an increased confidence that RSNs reflect neuronal activity, thus adding to the body of evidence that the two are related, and helping to counter arguments that RSNs might reflect non-neuronal BOLD artifact. The second and third patterns are both consistent with neuro-cognitive theories of sleep function, which supports the idea that sleep might serve a homeostatic role (in particular, a synaptic rescaling function). Finally, the third pattern suggests that SWS is perhaps better described as an altered, rather than a reduced state of consciousness. The discovered patterns have interesting implications for the nature of both RSNs and sleep, which are each discussed in turn, below.

5.2.1 What the second study reveals about the nature of RSNs

<u>The connection between RSNs and neuronal activity</u>

One of the principal means of linking RSNs to neuronal activity is demonstrating that RSN activity is modulated by state changes that are known to modulate neuronal activity. Such demonstrations are particularly important given the inherently inferential quality of both the BOLD signal as well as the data-driven ICA methodology used to identify RSNs. Fortunately, cortical neuronal activity dynamics during sleep are relatively well established, thus offering a template pattern against which RSN dynamics can be compared. As detailed in Chapter 1, suppression of ARAS activity during NREM results

in the downregulation of cortical ACh levels. This, in turn, results in progressively increasing synchronization of cortical neuronal activity across NREM1, NREM2 and SWS. Finally, the reactivation of the ARAS during REM results in wakefulness-like cortical desynchronized neuronal activity. If RSNs truly represent neuronal activity, then RSN FC dynamics should respond to these changes in a predictable way. Data for the majority (*i.e.,* 35/42, or 83%) of significant RSN FC edges were best fit by quadratic functions, across wakefulness, NREM and REM (*i.e.,* FC moved progressively away from wakefulness FC during NREM, and returned during REM, consistent with the aforementioned cortical neuronal synchrony dynamics). This result can therefore be taken as further evidence that RSNs represent neuronal activity in some way.

Beyond this predicted pattern, however, the second study indicated that RSN FC during NREM sleep appears to directly *oppose* wakefulness FC (*e.g.,* positive correlations moved in the direction of negative correlation). Of the 35 quadratic FC edges, 29 were convex, indicating that FC moved in the *opposite direction* from wakefulness FC during NREM, while returning during REM. Even more significantly, 20 of these edges (*i.e.,* 69%) increased in magnitude in the opposite direction during NREM. These results are consistent with a homeostatic function for NREM sleep, in line with theories of a homeostatic function for sleep at the synaptic level (Tononi & Cirelli, 2014; Watson & Buzsáki, 2015). Thus, this connection to the synaptic level, although superficial, helps to reinforce the idea that RSNs are, in some way, linked to neuronal phenomena.

The significance of the canonical RSN spatial boundaries

One of the issues raised in the Introduction is the seemingly arbitrary quality of RSN spatial boundaries. In a sense, these boundaries are one of the most defining characteristics of RSNs (in that they help to distinguish individual RSNs from each other, if not from non-neuronal ICs), yet they are also the only property that is user-defined. It was pointed out that an ICA decomposition of around 20-30, which yields the canonical RSNs, facilitates useful interpretations for RSN activity. As indicated in (Smith et al., 2009), these spatial boundaries correspond to areas known to be relevant to specific kinds of cognitive processing. Beyond this correspondence, however, the precise functional

relevance of these boundaries is not clear, and remains an unresolved problem to solve. One of the exciting implications of the second study is that the three patterns outlined above (*i.e.,* the quadratic, convex quadratic, and increasing SWS magnitude patterns) might be used as criteria for gauging the relevance of the canonical RSN boundaries. Specifically, these patterns were discovered to apply to RSNs defined by a 20-model-order ICA decomposition. Consequently, it can be said that the boundaries defined by this decomposition are decidedly less arbitrary than previously suspected, because they yield added information.

However it remains to be demonstrated whether this added information might *also* be available under different ICA decompositions or even under different non-ICA-based brain parcellations. Only by demonstrating that this information is in some way exclusive to the canonical RSN boundaries can it be said that canonical RSN boundaries "add" this information. One highly-fragmented non-ICA parcellation was in fact applied to the sleep fMRI data, with the intention of beginning to address this issue, although the results were not included in Chapter 2 in order not to distract from the primary aims of that study. In this alternate analysis, a cortical parcellation consisting of 333 regions was used (Gordon et al., 2016). This particular parcellation was selected because it represents a highly fragmented version of resting state FC data.

The results (Table 6, in Appendix B) were promising. Of the significant FC edges, 33% were quadratic, with the majority of edges being either cubic (42%) or linear (25%). For comparison, 83% of the significant fits were quadratic in the original study. Further, 74% of the quadratic edges were convex in the alternate analysis, matching the homeostatic pattern, as compared with 83% in the original study. Thus, these preliminary results suggest that the canonical RSNs are *more informative* than a significantly more fragmented parcellation, in the sense that they better reflect patterns that are known to be associated with (or hypothesized to occur for) neuronal activity during sleep.

Importantly, there was still a non-negligible number of quadratic fits in the alternate analysis. Were *none* of the fits quadratic, this would have indicated that the BOLD data itself was suspect, because if BOLD data is truly linked to neuronal activity, then any

parcellation of BOLD data should yield some amount of FC edges whose dynamics match that of neuronal activity. Thus this result is important insofar as it supports the connection between BOLD data and neuronal activity, while still highlighting the meaningful quality of the spatial boundaries of whole canonical RSNs. Furthermore, the results of this alternate analysis suggest new criteria for the assignment of meaning to specific RSN parcellations, generally. Namely, pattern matching with (1) neuronal synchrony dynamics across sleep (*i.e.,* quadratic functions best fit to FC dynamics), and (2) the discovered pattern that was consistent with a homeostatic function (*i.e.,* convex quadratic functions). As will be discussed below, these criteria can also be applied to the third study.

Dividing the DMN

Finally, as was mentioned above, the only RSN that was not tracked holistically in the second study was the DMN. Instead, as is sometimes done in the extant literature (Xu, Yuan, & Lei, 2016), it was split into anterior and posterior nodes. There were a number of reasons for assuming that this would be a reasonable way of analyzing this particular RSN. First, there is evidence from prior studies that the DMN separates into anterior and posterior nodes during SWS (Horovitz et al., 2009), and further, that this separation begins as early as NREM2 (Larson-Prior et al., 2011). Second, diffusion tensor imaging (DTI) studies indicate important structural connectivity differences between the anterior and posterior DMN nodes. Namely, only the posterior node (*i.e.,* the PCC) connects to the medial temporal lobe (MTL), with no white matter tracts connecting the anterior (dmPFC) node to the MTL (Greicius, Supekar, Menon, & Dougherty, 2009). Given the importance of the MTL to memory-related functions (Squire, Zola-Morgan, & Stuart, 1991), this could suggest a natural functional dissociation between anterior/posterior DMN, as a consequence of these structural connectivity differences. Importantly, the fact that the aforementioned findings apply to a split DMN suggests that it may be more *informative* to consider the DMN as two separate RSNs, consistent with the results of a number of different studies (Damoiseaux et al., 2008; Lei, Zhao, & Chen, 2013). This idea will be expanded upon in section 5.3.1.

5.2.2 What the second study reveals about the nature and function of sleep

Further validation of sleep stage differences

The results of the second study have a number of important implications with respect to the nature and function of sleep. At the broadest level, this was the first study to assess all sleep stage and wakefulness differences from the perspective of whole-brain RSN FC. In particular, angular distance was used to assess differences in whole-brain FC configurations of wakefulness and sleep stages. The angular distance results are particularly reassuring, because they validate findings derived from many other measurements. For example, as detailed in Chapter 1, there is extensive evidence from measures of EEG (*e.g.,* SWA signatures), neurochemistry (*e.g.,* cortical ACh levels), the activity of brainstem nuclei (*e.g.,* those comprising the ARAS), and the behaviour of thalamocortical circuitry, which collectively indicate that: (1) NREM is a radically different state from both REM and wakefulness, and, (2) brain activity during REM shares many similarities to wakefulness. The results of the second study indicated that the angular distances between NREM stage vectors (*i.e.,* NREM2 and SWS) and those of *both* REM and wakefulness were significant. Thus, this is the first study to corroborate the idea that NREM is not the same state as either wakefulness or REM, from the standpoint of the whole-brain RSN FC configurations for these stages.

Similarly exciting was the fact that from this same standpoint, REM and wakefulness were *not* significantly distinguished states. It goes without saying of course (see Chapter 1), that from the perspective of behaviour (*e.g.,* arousal level) and, for example, PFC CBF (which is reduced in REM), there is plenty of evidence that REM and wakefulness are *not* the same state. Nevertheless, it is thought provoking to discover that *from the perspective of whole-brain RSN FC*, these states are difficult to distinguish. Assuming that there is a correspondence between RSN FC and cognition/perception (see section 1.2.3), this result further suggests that the perceptual state facilitated by REM FC configurations might be similar to wakefulness. Indeed, this suggestion is backed up by REM dream reports, which indicate a vivid quality comparable to that of wakefulness (Hobson, Pace-Schott, & Stickgold, 2000b).

Moreover, the categorization of FC edges into different polynomial fits further revealed that the FC edges most responsible for driving these state differences were the very same edges that best reflect cortical neuronal synchrony dynamics across these stages. Given that these cortical dynamics are, in turn, known to be driven by well-established sleep mechanisms (*i.e.,* Process S, involving neuronal circuitry that controls ARAS activation), it is not unreasonable to suggest that: (1) sleep mechanisms may actually *drive* whole-brain RSN FC changes, and, (2) doing so may in fact be one of the critical *functions* of sleep.

These findings help to reinforce our understanding of the functional hierarchy between sleep and RSNs, because it links a known sleep mechanism (*i.e.,* ARAS deactivation prompting an increase in cortical synchrony) to a known RSN property (*i.e.,* RSN FC). In contrast to the results of the first study, this study is better placed to suggest that sleep mechanisms might actively target RSN properties.

A neuro-cognitive function for sleep

As discussed in section 1.1, much of the evidence collected in relation to putative sleep functions indicates that the primary function of sleep is to serve some necessary brain-related purpose, in particular, a neuro-cognitive function (Frank, 2006). Hypothesized neuro-cognitive functions emphasized either (or both) a memory-consolidation function (facilitated by LTP at the neuronal level), or a global synaptic downscaling function (involving the homeostatic recalibration of connectivity weights, to facilitate neuronal plasticity at the whole-brain level). One open question is whether an evaluation of RSN dynamics might provide evidence to support such roles.

The most interesting finding of the second study was not the pattern followed by the majority (*i.e.,* 35/42) of significant FC edges (*i.e.,* the quadratic pattern, which was hypothesized based on known cortical synchrony dynamics), but the particular *inflection* of this pattern. The fact that the majority (*i.e.,* 29/35) of quadratic fits were discovered to have convex inflections was exciting because it appears to suggest that NREM sleep serves to move whole-brain FC configurations in a direction opposite to wakefulness. Moreover, the majority of convex quadratic fits (*i.e.,* 20/29) not only moved in the

opposite direction, by reducing their FC, but remarkably, further *strengthened* their FC in the opposite direction. It was this last result that was particularly surprising, *as it could not have been predicted from the literature*. Technically, known reduced FC (Spoormaker et al., 2010), and reduced glucose consumption (Heiss, Pawlik, Herholz, Wagner, & Wienhard, 1985) during NREM is consistent with convex quadratic fits to the edge FC data. However, these previously established findings give little indication that FC might actually strengthen in the opposite direction. Thus, these findings are particularly exciting, because they actually provide new corroborating evidence for a homeostatic neuro-cognitive role for sleep (in particular, for NREM sleep).

SWS as a state of altered conscious awareness

This last finding is also interesting because it has potential implications beyond the functional role of sleep. Specifically, it could suggest that conscious awareness is not necessarily reduced during SWS. Although this implication is admittedly speculative, it is worth further discussion here, because it challenges a commonly accepted dogma regarding the fundamental nature of SWS, namely that it is a state of dramatically reduced consciousness. This historic belief would be supported if RSN FC were only *reduced in magnitude*. Instead, FC for a majority of the significant edges continues past zero, *reverses polarity and is strengthened in this direction*. Further, a greater number of higher-order RSNs are involved in these reversals, rather than reductions of FC (*i.e.,* 13 vs. 8). Even more notably, four out of six of the significant FC edges that involve the DMN (across all edges, not just the subset of convex quadratic edges) *increase* their FC during SWS. As mentioned in Section 1.2.3 of the Introduction, it is worth elaborating here on RSN FC modulations due to sedation and TBI, because they provide context for higher-order RSN and DMN-specific FC changes associated with consciousness.

Clinical definitions of consciousness distinguish between two subcomponents: conscious *arousal* (*i.e.,* alertness with respect to the environment) and conscious *awareness* (*i.e.,* the contents/percepts of consciousness; Posner, Saper, Schiff, & Plum, 2008). Sedation involves both reduced arousal and awareness, whereas states following TBI (*e.g.,* the vegetative state, or VS, and the minimally conscious state, or MCS) involve normal

levels of arousal but low awareness (Fernández-Espejo & Owen, 2013; Laureys, 2005). Importantly, this difference suggests that a comparison of the findings of sedation and TBI studies can help dissociate markers of conscious awareness from those of conscious arousal.

Sedation studies reveal that the negative correlations between task-positive/-negative networks, as typified by healthy wakefulness, are diminished during sedation, in proportion to administered sedative levels (Boveroux et al., 2010). Further, within-RSN FC in higher-order networks (DMN and F-P) was reduced, and thalamocortical FC involving these networks was found to be negative. By contrast, both within-RSN and thalamocortical FC involving sensory networks were comparable to their connectivity patterns in the unsedated state. Overall, this suggests that changes in *both* conscious arousal and awareness are associated with reductions in the FC profiles of the higher-order RSNs only. TBI studies can help further distinguish which higher-order RSN is important for conscious awareness in particular, however. A study that directly compared locked-in syndrome patients with VS patients found that DMN integrity alone was sufficient to differentiate the aware locked-in syndrome patients, although the F-P network also appears to play an important role in such distinctions (Roquet et al., 2016).

As an important caveat to these findings, a separate study found that within-DMN FC was preserved in a VS patient, though not in a brain-dead patient (Boly et al., 2009). Further, negative correlations were identified between DMN and the task positive network, consistent with healthy subjects. However, the VS patient did not meet criteria indicating covert conscious awareness, such as successfully completing mental imagery paradigms (*e.g.,* Owen et al., 2006). The results of this study suggest that relatively uncompromised DMN FC and preserved negative correlations between task-positive and –negative networks may be a necessary, though not sufficient condition for conscious awareness. Finally, a study investigating the processing of exogenous information (*i.e.,* an auditory story) during both sedation and TBI discovered the common factor to be reduced FC between F-P and auditory networks (Naci et al., 2018).

Collectively, these findings point to the need for future studies, in order to clarify the RSN FC differences in the manifestation of conscious arousal versus conscious awareness. Conscious arousal could be facilitated by the integrity of higher-order RSNs alone. Conscious awareness may be more dependent on DMN integrity as a necessary condition, with sufficient conditions perhaps being further mediated by negative FC between DMN and F-P, in addition to positive FC between F-P and sensory RSNs. An alternative perspective that could potentially resolve these discrepancies is that consciousness is better defined in terms of *dynamic* FC, rather than any specific static FC configuration. In particular, healthy consciousness during wakefulness appears to be marked by the capacity to flexibly and consistently deviate away from any fixed FC pattern, in particular, connectivity patterns defined by anatomical connections (Demertzi et al., 2019).

Nevertheless, the surprising findings of the second study (*i.e.,* the reversal of RSN FC polarity and subsequent *increase in magnitude* in the opposite direction, for edges involving higher-order RSNs, in particular the DMN, during SWS) suggest that prior characterizations of SWS as a state of reduced consciousness might need re-evaluation. Above and beyond the magnitude increase, the *reversal* itself warrants further discussion with respect to conscious awareness. It seems to suggest that SWS perception might, in some way, be *qualitatively different from wakefulness perception*. But how might this alternate state of consciousness manifest? In attempting to substantiate this idea, it is worth examining and contrasting dream reports from both REM and NREM sleep. Dream reports from all stages are arguably strange to begin with, but SWS dream reports are not strange in the same *way* that REM dream reports are strange. In REM, dreams share the similarly vivid quality of wakefulness perception, albeit with particularly bizarre content, which the dreamer has difficulty recognizing as such (Hobson, Pace-Schott, & Stickgold, 2000b). Such a state is consistent with what might be expected from a brain that is connected in a similar way to wakefulness (*i.e.,* similar whole-brain RSN FC), yet, for example, has reduced CBF in the dorsolateral PFC (*i.e.,* a brain region associated with self-reflective awareness; Braun et al., 1997b).

By contrast to the *content* differences of REM, accompanied by a failure to recognize the bizarreness of this content, NREM dream reports suggest possible *structural* failures of perception. The extended narrative sequences that are also associated with REM (Foulkes & Schmidt, 1983), are replaced with dramatically fragmented perceptual sequences during NREM. The median length of REM dream sequences have been found to be over six times longer than their NREM counterparts (Hobson et al., 2000b). Thus, it is possible that a reduced capacity to successfully generate an extended narrative sequence is the direct consequence of RSN FC configurations that have reversed their functional connectivity.

5.3 Third study: Resting state networks constrain neuronal activity at multiple frequency bands across wakefulness and sleep

The third study, reported in Chapter 4, fully exploited the simultaneous EEG-fMRI data by more directly investigating the relationship between RSN activity and an EEG measure of frequency-banded neuronal oscillatory activity. The primary aim of this study was to determine whether correlations between EEG-derived frequency band power and fMRI-derived RSN activity reflect the pattern of cortical neuronal synchrony dynamics across wakefulness and sleep. There were two main discoveries: (1) the majority of RSN frequency-band fingerprints matched the aforementioned pattern, as predicted. This extended the findings of the second study, by more directly indicating a connection between RSNs and neuronal activity; (2) BLP dynamics across wakefulness and sleep were largely consistent within each individual RSN, even in those RSNs in which the dynamics did not match the hypothesized pattern. This second finding suggested that the boundaries delimited by the canonical RSNs might represent the limits of some as-yet-undetermined mechanism for coupling neuronal activity across different frequency bands.

5.3.1 What the third study reveals about the nature of RSNs

The significance of the canonical RSN boundaries

Overall, the results of the third study help to corroborate the contention that RSNs have an important connection to neuronal activity. It was discovered that within-RSN

frequency band representation largely increases and decreases in a seemingly coordinated manner across frequencies, throughout wakefulness and sleep stages. Notably, the specific pattern of frequency band dynamics (*e.g.,* whether frequency band representation increased across NREM and decreased during REM, or vice versa) was largely consistent within an RSN, but could flip in a *spatially adjacent* RSN (*e.g.,* r/l F-P vs. esV). This remarkable consistency has critical implications for the nature of RSNs. Namely, it suggests that the canonical RSN boundaries are meaningful in the sense that they may represent the limits of coordinated neuronal activity, across all frequency bands. Outside the bounds of a given canonical RSN, neuronal populations coordinate their activity, across frequency bands, according to a different phase, for example (*e.g.,* according to phases dictated by the separately-coordinated neuronal populations of neighboring RSNs). Thus, the defining feature of RSNs from the perspective of BOLD resting state (*i.e.,* a region of correlated BOLD activity), may well be their defining feature from the perspective of neuronal oscillatory activity across all frequency bands. As suggested in Chapter 4, PAC is most likely the mechanism by which neuronal activity is coordinated across frequency bands. Further, the fact that delta frequency band dynamics match the dominant pattern in nearly all RSNs is suggestive; it is consistent with the possibility that SWA may coordinate neuronal activity for all faster frequency bands. This exciting possibility will be discussed further in section 5.2.3, below. Overall, these findings provide further support for the often contentious debate regarding the neuronal origins of both the BOLD signal and RSNs (Tong, Hocke, Fan, Janes, & Frederick, 2015; van den Heuvel & Hulshoff Pol, 2010).

As suggested in the previous subsections, it is important to test the relevance of the canonical RSN boundaries by attempting other parcellations delineated by different ICA decompositions, or by non-ICA based parcellations. Although not included in the results section of Chapter 4, a 14-RSN parcellation was analyzed in addition to the 10-RSN parcellation. This parcellation subtly breaks up some of the canonical RSNs. Despite being very similar, the slightly higher-fragmentation analysis yielded fewer frequencies that significantly matched the predicted pattern. According to the new criteria for ascribing meaning to brain parcellations, described in the previous section, this result can

therefore be taken as further evidence that the (holistic) canonical RSNs are actually *meaningful* for systems-level brain communication.

Dividing the DMN

As explained in Chapter 4, there is one notable exception to the above results. Namely, the "whole" canonical DMN did not express the predicted pattern. Moreover, *no* significant pattern of change was identified across wakefulness and sleep. Only when the DMN was subdivided into anterior and posterior components did the predicted pattern emerge to some extent. This finding has potentially significant functional implications. Just as a lack of meaning was the motivation for consolidating N3 and N4 into NREM3/SWS, the added information facilitated by splitting the DMN could suggest that it may be more *meaningful* to consider the DMN as two separate RSNs; *i.e.,* "anterior DMN" and "posterior DMN" (which may function in dissociable ways). As discussed in section 5.2.1, this consideration of the DMN is backed up by the results of a number of different studies (Damoiseaux et al., 2008; Horovitz et al., 2009; Lei, Zhao, & Chen, 2013; Xu, Yuan, & Lei, 2016).

5.3.2 What the third study reveals about the nature of sleep

Although the primary aim of the third study was to use frequency band dynamics during sleep to help elucidate the neuronal nature of RSNs, the results of this study could also help to fill in some important gaps in relation to sleep mechanisms. More specifically, while the second study provided evidence that was consistent with a homeostatic function for sleep, it did not have explanatory power with respect to the neuronal mechanisms by which this function might be achieved. Nor could it, given that it only made use of BOLD data, with its aforementioned inferential limitations. By contrast, the third study provides evidence in support of the possibility that SWA might be the mechanism by which sleep coordinates global RSN FC.

Strictly speaking, if the patterns of changing frequency representation in a given RSN, across stages, were truly independent events, then there would be a .012 probability that

four out of the five examined frequencies followed the same pattern[7]. Given that this occurred in 8/11 RSNs, the total probability is 9.4×10^{-14} [8]. This result suggests that the representations of different frequencies in RSNs are likely *not* independent events and that RSN-bound frequency banded activity might be *coordinated* in some way. Although the results of the third study do not have the power to confirm what this mechanism might be (*i.e.,* by virtue of being a correlational study), the combination of these results with outside evidence, as detailed below, is at least suggestive.

One of the most characteristic features of sleep is SWA. As described in Chapter 1, these oscillations emerge spontaneously in the cortex, with the downregulation of ACh that follows the inhibition of the ARAS during NREM sleep. Remarkably, patterns of delta frequency[9] changes across wakefulness and sleep matched the dominant pattern amongst all other frequency band changes, in nine out of the 11 RSNs examined (*i.e.,* where the DMN is considered as two separate RSNs). For example, in the striate visual RSN and both F-P RSNs, the dominant patterns were best fit by a convex quadratic function and a concave quadratic function, respectively. In each case, the dominant pattern was matched by the delta band frequency dynamics. This finding certainly does not prove that the slow oscillation is responsible for coordinating the activity of faster rhythms, however it is at least consistent with such a possibility. These findings become particularly exciting, however, when they are combined with previous evidence that: (1) slow rhythms have the inherent capacity to coordinate the activity of large neural populations, covering large distances; (2) slow rhythms can coordinate the activity of faster rhythms via PAC (Bragin et al., 1995b; Lakatos et al., 2005), and; (3) the slow oscillation, specifically, has been

---

[7] *i.e.,* there are 7 possible pattern fits: 1st-order polynomial; horizontal, upward slope, downward slope; 2nd-order polynomial: concave, convex; 3rd-order: initial upwards inflection, initial downwards inflection. The probability that four of five frequencies should follow the same pattern is calculated by making use of the Probability Mass Function of the Multinomial Distribution, multiplied by the Permutation formula, as follows: $5!/(4!1!0!0!0!0!0!)(1/7)^4(1/7)^1(1/7)^0(1/7)^0(1/7)^0(1/7)^0(1/7)^0 \times 7!/(7-2)!$

[8] This was calculated using the Binomial Formula, as follows: $11!/((11-8)!8!) \times .012^8(1-.012)^{(11-8)}$

[9] Although the third study identifies the slowest examined frequency as "delta", and delta is not technically categorized the same as the slow oscillation, the frequency range for "delta" used in this particular analysis was actually 0.3 – 4 Hz, so it comprises both delta and the slow oscillation. It is therefore not unreasonable to generate claims about the slow oscillation.

found to coordinate both spindles and delta activity, *i.e.,* faster rhythmic activity (Steriade, 2006). This collection of findings leaves the overall impression that the slow oscillation may be coordinating the activity of all faster rhythms, across wakefulness and sleep, within the boundaries defined by the canonical RSNs.

An important caveat to this suggestion is that SWA is characteristic of NREM sleep, not wakefulness and REM, so it is not clear why it might be influencing the other frequencies during these other stages. It is worth emphasizing however, that slow frequencies such as delta do not simply disappear during wakefulness (Goncalves et al., 2008; Mantini, Perrucci, Del Gratta, Romani, & Corbetta, 2007; Meyer, Janssen, Van Oort, Beckmann, & Barth, 2013). Thus, they might still retain the capacity to influence faster frequencies, despite being less representative of neuronal activity, overall, during this stage (with REM being less well understood). Nevertheless, it is still very possible that there is some other emergent coordination amongst the different frequency bands, which does not implicate the slow oscillation as the instigating mechanism, at least during stages outside of NREM.

5.4 Summary and conclusions

In summary, this thesis employed simultaneous EEG-fMRI during sleep to help illuminate the properties and functions of both sleep and RSNs. With respect to RSNs, it was discovered that the previously established repertoire of wakefulness canonical RSNs likely comprises the complete set across all three alternate functional modes of the brain (*i.e.,* wakefulness, NREM and REM). When this discovery is combined with previously weak evidence of a connection between RSNs and sleep-related functions, it supports (though certainly not decisively) the contention that the function of RSNs may be to facilitate wakefulness-related cognition only. Thus, the presence of RSNs during sleep may be as passive objects of active sleep-related mechanisms, though further research is needed to understand the precise nature of the functional relationships between RSNs and sleep. It was further discovered that RSN FC dynamics largely reflect neuronal synchrony dynamics across wakefulness and sleep, thereby helping to substantiate the connection between RSNs and neuronal activity. This connection was further substantiated by the discovery that frequency banded activity, as measured by EEG,

largely appears to be coordinated across wakefulness and sleep, within RSN boundaries. Importantly, this last finding suggested that RSN boundaries may represent the limits of coordinated neuronal activity across all frequency bands, an appraisal that is consistent with how RSNs are conceptualized based on BOLD data (*i.e.,* as regions of correlated BOLD activity). Finally, the meaningful quality of the canonical RSN boundaries was advocated by preliminary evidence that the aforementioned discoveries were *best demonstrated* by canonical RSN parcellations, as opposed to more highly fragmented parcellations. There was one exception to this principle, however; the second and third studies suggested that it might be more meaningful to consider the DMN as two separate RSNs (namely, an "anterior DMN" and a "posterior DMN"), supporting the findings of other studies.

With respect to sleep, evidence was provided that the modulation of whole-brain RSN FC might be one of its most important functions. RSN FC dynamics were discovered to be largely consistent with the dynamics of phenomena under the direct control of sleep mechanisms (*i.e.,* cortical neuronal synchrony). Since RSN FC dynamics during NREM were also discovered to change in opposition to wakefulness FC configurations, this suggested support for the idea that sleep might serve a homeostatic function, at the level of RSN FC. Importantly, this finding is consistent with previously hypothesized neuro-cognitive theories of sleep function, at the synaptic level (*i.e.,* SHY). Further, the fact that the majority of significant edges reverse, rather than reduce their FC profiles during SWS, suggested that this state might be better characterized as an altered, rather than a reduced state of cognitive activity. Notably, this reversal included a significant number of higher-order RSN nodes, such as the DMN, which has been implicated in studies involving the modulation of conscious awareness. This latter finding is suggestive that SWS might also be better characterized as a state of altered consciousness, though such a contention is only speculative at this stage and requires further substantiation. Finally, it was discovered that delta frequency band dynamics across wakefulness and sleep are consistent with the dominant patterns of the remaining frequency bands in nearly all of the canonical RSNs. This finding is consistent with the possibility that sleep might coordinate RSN frequency banded activity via its well-documented association with the slow oscillation.

Overall, based on the results of the three studies in this thesis, the newly emergent picture of the relationship between canonical RSN and sleep functions might be depicted as follows: (a) during NREM, the ARAS is switched off, in order to increase cortical neuronal synchrony; this increased neuronal synchrony largely manifests as the slow oscillation; (b) the slow oscillation coordinates the activity of faster rhythms, via PAC, however this coordination is constrained to the limits of the canonical RSN boundaries; (c) neuronal activity relationships *between* the canonical RSNs is *not* constrained, therefore the collective interactions of large neural populations (captured, from the BOLD signal, as between-RSN FC) is free to move in independent directions; (d) during NREM, whole-brain between-RSN FC moves, progressively, in a direction opposite to wakefulness configurations, thus reducing wakefulness FC patterns amongst the canonical RSNs; (e) during REM, the ARAS is reactivated, and cortical activity is free to return to desynchronized interactions; whole-brain between-RSN FC returns in the direction of wakefulness FC, reducing the possibility of the system getting stuck in dysfunctional NREM RSN FC configurations; (f) following multiple ultradian cycles, involving the alternation of NREM and REM RSN FC configurations, the system is brought closer to a neutral configuration, in a homeostatic fashion, thereby improving plasticity for the following day.

Future directions

This thesis introduces the idea of using both the pattern of neuronal synchrony dynamics across wakefulness and sleep (characterized by a quadratic fitting function), and a further "homeostatic pattern" (characterized by a convex quadratic function) as criteria for ascribing meaning to cortical resting state brain parcellations. Based on preliminary results (described in section 5.1.2 and 5.1.3), it was suggested that the canonical RSNs might comprise the most meaningful boundaries according to these criteria. However, a more comprehensive study is warranted, in which a wide range of ICA decompositions and cortical parcellations are subjected to the same analysis. The parcellation identified as most meaningful by such a study would be valuable with respect to resolving a longstanding issue in neuroscience; namely, the nature of the functional organization of

the brain. Such analyses could also implement graph-theoretical measures using RSNs generated from different decomposition numbers, as nodes.

As discussed in section 5.1.1, evidence of a link between RSNs and sleep functions is weak, at best. It was suggested that a follow-up study be conducted to determine whether more evidence might be available. One possibility would be a set of separate SCAs performed during each sleep stage of interest. Individual RSNs and BOLD localizations of spindles, k-complexes and other sleep features (*e.g.,* SWA) could be used as seed regions, with the objective of determining correlations amongst these different features.

References

Achermann, P., Dijk, D. J., Brunner, D. P., & Borbély, A. A. (1993). A model of human sleep homeostasis based on EEG slow-wave activity: quantitative comparison of data and simulations. *Brain Research Bulletin*, *31*(1–2), 97–113. Retrieved from http://www.ncbi.nlm.nih.gov/pubmed/8453498

Allen, P. J., Josephs, O., & Turner, R. (2000). A Method for Removing Imaging Artifact from Continuous EEG Recorded during Functional MRI. *NeuroImage*, *12*(2), 230–239. https://doi.org/10.1006/nimg.2000.0599

Allen, P. J., Polizzi, G., Krakow, K., Fish, D. R., & Lemieux, L. (1998). Identification of EEG Events in the MR Scanner: The Problem of Pulse Artifact and a Method for Its Subtraction. *NeuroImage*, *8*(3), 229–239. https://doi.org/10.1006/nimg.1998.0361

Anderson, M. J. (2001). A new method for non-parametric multivariate analysis of variance. *Austral Ecology*, *26*(1), 32–46. https://doi.org/10.1046/j.1442-9993.2001.01070.x

Anderson, M. J., & Ter Braak, C. J. F. (2003). Permutation tests for multi-factorial analysis of variance. *Journal of Statistical Computation and Simulation*, *73*(2), 85–113. https://doi.org/10.1080/00949650215733

Andrade, K. C., Spoormaker, V. I., Dresler, M., Wehrle, R., Holsboer, F., Sämann, P. G., & Czisch, M. (2011). Sleep spindles and hippocampal functional connectivity in human NREM sleep. *The Journal of Neuroscience*, *31*(28), 10331–10339. https://doi.org/10.1523/JNEUROSCI.5660-10.2011

Antrobus, J. (1983). REM and NREM Sleep Reports: Comparison of Word Frequencies by Cognitive Classes. *Psychophysiology*, *20*(5), 562–568. https://doi.org/10.1111/j.1469-8986.1983.tb03015.x

Arslan, S., Ktena, S. I., Makropoulos, A., Robinson, E. C., Rueckert, D., & Parisot, S. (2018). Human brain mapping: A systematic comparison of parcellation methods for the human cerebral cortex. *NeuroImage*, *170*, 5–30. https://doi.org/10.1016/j.neuroimage.2017.04.014

Aserinsky, E., & Kleitman, N. (1953). Regularly occurring periods of eye motility, and concomitant phenomena, during sleep. *Science*, *118*(3062), 273–274. https://doi.org/10.1126/science.118.3062.273

Bear, M. F., & Malenka, R. C. (1994). Synaptic plasticity: LTP and LTD. *Current Opinion in Neurobiology*, *4*(3), 389–99. Retrieved from http://www.ncbi.nlm.nih.gov/pubmed/7919934

Beck, A. T., Epstein, N., Brown, G., & Steer, R. A. (1988). An inventory for measuring clinical anxiety: psychometric properties. *Journal of Consulting and Clinical Psychology*, *56*(6), 893–7. Retrieved from http://www.ncbi.nlm.nih.gov/pubmed/3204199

Beck, A. T., Steer, R., & Brown, G. (1993). Beck Depression Inventory-II (BDI-II). ...

for Beck Depression Inventory-II.

Beckmann, C. F., & Smith, S. M. (2004). Probabilistic Independent Component Analysis for Functional Magnetic Resonance Imaging. *IEEE Transactions on Medical Imaging*, *23*(2), 137–152. https://doi.org/10.1109/TMI.2003.822821

Bell, A. J., & Sejnowski, T. J. (1995). An information-maximization approach to blind separation and blind deconvolution. *Neural Computation*, *7*(6), 1129–59. Retrieved from http://www.ncbi.nlm.nih.gov/pubmed/7584893

Ben-Soussan, T. D., Glicksohn, J., & Berkovich-Ohana, A. (2015). From Cerebellar Activation and Connectivity to Cognition: A Review of the Quadrato Motor Training. *BioMed Research International*, *2015*, 1–11. https://doi.org/10.1155/2015/954901

Benington, J. H., & Craig Heller, H. (1995). Restoration of brain energy metabolism as the function of sleep. *Progress in Neurobiology*, *45*(4), 347–360. https://doi.org/10.1016/0301-0082(94)00057-O

Birn, R. M., Molloy, E. K., Patriat, R., Parker, T., Meier, T. B., Kirk, G. R., … Prabhakaran, V. (2013). The effect of scan length on the reliability of resting-state fMRI connectivity estimates. *NeuroImage*, *83*, 550–558. https://doi.org/10.1016/j.neuroimage.2013.05.099

Biswal, B., Yetkin, F. Z., Haughton, V. M., & Hyde, J. S. (1995). Functional connectivity in the motor cortex of resting human brain using echo-planar MRI. *Magnetic Resonance in Medicine*, *34*(4), 537–41. Retrieved from http://www.ncbi.nlm.nih.gov/pubmed/8524021

Bluhm, R. L., Miller, J., Lanius, R. A., Osuch, E. A., Boksman, K., Neufeld, R., … Williamson, P. (2007). Spontaneous Low-Frequency Fluctuations in the BOLD Signal in Schizophrenic Patients: Anomalies in the Default Network. *Schizophrenia Bulletin*, *33*(4), 1004–1012. https://doi.org/10.1093/schbul/sbm052

Boly, M., Perlbarg, V., Marrelec, G., Schabus, M., Laureys, S., Doyon, J., … Benali, H. (2012). Hierarchical clustering of brain activity during human nonrapid eye movement sleep. *Proceedings of the National Academy of Sciences of the United States of America*, *109*(15), 5856–61. https://doi.org/10.1073/pnas.1111133109

Boly, M., Tshibanda, L., Vanhaudenhuyse, A., Noirhomme, Q., Schnakers, C., Ledoux, D., … Laureys, S. (2009). Functional connectivity in the default network during resting state is preserved in a vegetative but not in a brain dead patient. *Human Brain Mapping*, *30*(8), 2393–2400. https://doi.org/10.1002/hbm.20672

Borbély, A. A. (1982). A two process model of sleep regulation. *Human Neurobiology*, *1*(3), 195–204. Retrieved from http://www.ncbi.nlm.nih.gov/pubmed/7185792

Born, J., & Wilhelm, I. (2012). System consolidation of memory during sleep. *Psychological Research*, *76*(2), 192–203. https://doi.org/10.1007/s00426-011-0335-6

Boveroux, P., Vanhaudenhuyse, A., Bruno, M.-A., Noirhomme, Q., Lauwick, S., Luxen, A., … Boly, M. (2010). Breakdown of within- and between-network Resting State

Functional Magnetic Resonance Imaging Connectivity during Propofol-induced Loss of Consciousness. *Anesthesiology*, *113*(5), 1038–1053. https://doi.org/10.1097/ALN.0b013e3181f697f5

Bragin, A., Jandó, G., Nádasdy, Z., Hetke, J., Wise, K., & Buzsáki, G. (1995a). Gamma (40-100 Hz) oscillation in the hippocampus of the behaving rat. *The Journal of Neuroscience : The Official Journal of the Society for Neuroscience*, *15*(1 Pt 1), 47–60. https://doi.org/10.1523/JNEUROSCI.15-01-00047.1995

Bragin, A., Jandó, G., Nádasdy, Z., Hetke, J., Wise, K., & Buzsáki, G. (1995b). Gamma (40-100 Hz) oscillation in the hippocampus of the behaving rat. *The Journal of Neuroscience : The Official Journal of the Society for Neuroscience*, *15*(1 Pt 1), 47–60. Retrieved from http://www.ncbi.nlm.nih.gov/pubmed/7823151

Bramham, C. R., Maho, C., & Laroche, S. (1994). Suppression of long-term potentiation induction during alert wakefulness but not during "enhanced" REM sleep after avoidance learning. *Neuroscience*, *59*(3), 501–9. Retrieved from http://www.ncbi.nlm.nih.gov/pubmed/8008204

Braun, A. R., Balkin, T. J., Wesensten, N. J., Gwadry, F., Carson, R. E., Varga, M., … Herscovitch, P. (1998). Dissociated pattern of activity in visual cortices and their projections during human rapid eye movement sleep. *Science (New York, N.Y.)*, *279*(5347), 91–5. Retrieved from http://www.ncbi.nlm.nih.gov/pubmed/9417032

Braun, A. R., Balkin, T. J., Wesenten, N. J., Carson, R. E., Varga, M., Baldwin, P., … Herscovitch, P. (1997a). Regional cerebral blood flow throughout the sleep-wake cycle. An H2(15)O PET study. *Brain : A Journal of Neurology*, *120 (Pt 7*, 1173–1197. https://doi.org/10.1093/brain/120.7.1173

Braun, A. R., Balkin, T. J., Wesenten, N. J., Carson, R. E., Varga, M., Baldwin, P., … Herscovitch, P. (1997b). Regional cerebral blood flow throughout the sleep-wake cycle. An H2(15)O PET study. *Brain : A Journal of Neurology*, *120 (Pt 7)*, 1173–97. Retrieved from http://www.ncbi.nlm.nih.gov/pubmed/9236630

Brown, R. E., & McCarley, R. W. (2008). Neuroanatomical and neurochemical basis of wakefulness and REM sleep systems. In *Neurochemistry of Sleep and Wakefulness* (pp. 23–58). https://doi.org/10.1017/CBO9780511541674.003

Buxton, R. B. (2013). The physics of functional magnetic resonance imaging (fMRI). *Reports on Progress in Physics. Physical Society (Great Britain)*, *76*(9), 96601. https://doi.org/10.1088/0034-4885/76/9/096601

Buzsáki, G., Anastassiou, C. A., & Koch, C. (2012). The origin of extracellular fields and currents — EEG, ECoG, LFP and spikes. *Nature Reviews Neuroscience*, *13*(6), 407–420. https://doi.org/10.1038/nrn3241

Buzsaki, G., & Draguhn, A. (2004). Neuronal Oscillations in Cortical Networks. *Science*, *304*(5679), 1926–1929. https://doi.org/10.1126/science.1099745

Caporro, M., Haneef, Z., Yeh, H. J., Lenartowicz, A., Buttinelli, C., Parvizi, J., & Stern, J. M. (2012). Functional MRI of sleep spindles and K-complexes. *Clinical Neurophysiology : Official Journal of the International Federation of Clinical Neurophysiology*, *123*(2), 303–9. https://doi.org/10.1016/j.clinph.2011.06.018

Cash, S. S., Halgren, E., Dehghani, N., Rossetti, A. O., Thesen, T., Wang, C., … Ulbert, I. (2009). The human K-complex represents an isolated cortical down-state. *Science (New York, N.Y.)*, *324*(5930), 1084–7. https://doi.org/10.1126/science.1169626

Cavallero, C., Cicogna, P., Natale, V., Occhionero, M., & Zito, A. (1992). Slow wave sleep dreaming. *Sleep*, *15*(6), 562–566. https://doi.org/10.1093/sleep/15.6.562

Centeno, M., & Carmichael, D. W. (2014). Network Connectivity in Epilepsy: Resting State fMRI and EEGâ€“fMRI Contributions. *Frontiers in Neurology*, *5*, 93. https://doi.org/10.3389/fneur.2014.00093

Chang, C., Liu, Z., Chen, M. C., Liu, X., & Duyn, J. H. (2013). EEG correlates of time-varying BOLD functional connectivity. *NeuroImage*, *72*, 227–36. https://doi.org/10.1016/j.neuroimage.2013.01.049

Chen, L. M., Yang, P.-F., Wang, F., Mishra, A., Shi, Z., Wu, R., … Gore, J. C. (2017). Biophysical and neural basis of resting state functional connectivity: Evidence from non-human primates. *Magnetic Resonance Imaging*, *39*, 71–81. https://doi.org/10.1016/j.mri.2017.01.020

Chow, H. M., Horovitz, S. G., Carr, W. S., Picchioni, D., Coddington, N., Fukunaga, M., … Braun, A. R. (2013). Rhythmic alternating patterns of brain activity distinguish rapid eye movement sleep from other states of consciousness. *Proceedings of the National Academy of Sciences of the United States of America*, *110*(25), 10300–5. https://doi.org/10.1073/pnas.1217691110

Cole, M. W., Ito, T., Bassett, D. S., & Schultz, D. H. (2016). Activity flow over resting-state networks shapes cognitive task activations. *Nature Neuroscience*, *19*(12), 1718–1726. https://doi.org/10.1038/nn.4406

Cologan, V., Schabus, M., Ledoux, D., Moonen, G., Maquet, P., & Laureys, S. (2010). Sleep in disorders of consciousness. *Sleep Medicine Reviews*, *14*(2), 97–105. https://doi.org/10.1016/j.smrv.2009.04.003

Colrain, I. M., Webster, K. E., & Hirst, G. (1999). The N550 component of the evoked K-complex: A modality non-specific response? *Journal of Sleep Research*, *8*(4), 273–280. https://doi.org/10.1046/j.1365-2869.1999.00163.x

Contreras, D., Destexhe, A., Sejnowski, T. J., & Steriade, M. (1996). Control of spatiotemporal coherence of a thalamic oscillation by corticothalamic feedback. *Science (New York, N.Y.)*, *274*(5288), 771–4. Retrieved from http://www.ncbi.nlm.nih.gov/pubmed/8864114

Contreras, D., & Steriade, M. (1995). Cellular basis of EEG slow rhythms: a study of dynamic corticothalamic relationships. *The Journal of Neuroscience : The Official Journal of the Society for Neuroscience*, *15*(1 Pt 2), 604–622. https://doi.org/10.1523/jneurosci.0279-06.2006

Cooke, S. F., & Bliss, T. V. P. (2006). Plasticity in the human central nervous system. *Brain*, *129*(7), 1659–1673. https://doi.org/10.1093/brain/awl082

Corbetta, M., & Shulman, G. L. (2002). Control of goal-directed and stimulus-driven attention in the brain. *Nature Reviews Neuroscience*, *3*(3), 201–215.

https://doi.org/10.1038/nrn755

Cote, K. A., De Lugt, D. R., Langley, S. D., & Campbell, K. B. (2002). Scalp topography of the auditory evoked K-complex in stage 2 and slow wave sleep. *Journal of Sleep Research*, *8*(4), 263–272. https://doi.org/10.1046/j.1365-2869.1999.00164.x

Cote, K. A., Epps, T. M., & Campbell, K. B. (2000a). The role of the spindle in human information processing of high-intensity stimuli during sleep. *Journal of Sleep Research*, *9*(1), 19–26. https://doi.org/10.1046/j.1365-2869.2000.00188.x

Cote, K. A., Epps, T. M., & Campbell, K. B. (2000b). The role of the spindle in human information processing of high-intensity stimuli during sleep. *Journal of Sleep Research*, *9*(1), 19–26. https://doi.org/10.1046/j.1365-2869.2000.00188.x

Damoiseaux, J. S., Beckmann, C. F., Arigita, E. J. S., Barkhof, F., Scheltens, P., Stam, C. J., … Rombouts, S. A. R. B. (2008). Reduced resting-state brain activity in the "default network" in normal aging. *Cerebral Cortex*, *18*(8), 1856–1864. https://doi.org/10.1093/cercor/bhm207

Damoiseaux, J. S., Rombouts, S. A. R. B., Barkhof, F., Scheltens, P., Stam, C. J., Smith, S. M., & Beckmann, C. F. (2006). Consistent resting-state networks across healthy subjects. *Proceedings of the National Academy of Sciences of the United States of America*, *103*(37), 13848–53. https://doi.org/10.1073/pnas.0601417103

Dang-Vu, T. T., Desseilles, M., Laureys, S., Degueldre, C., Perrin, F., Phillips, C., … Peigneux, P. (2005). Cerebral correlates of delta waves during non-REM sleep revisited. *NeuroImage*, *28*(1), 14–21. https://doi.org/10.1016/j.neuroimage.2005.05.028

Dang-Vu, T. T., McKinney, S. M., Buxton, O. M., Solet, J. M., & Ellenbogen, J. M. (2010). Spontaneous brain rhythms predict sleep stability in the face of noise. *Current Biology : CB*, *20*(15), R626-7. https://doi.org/10.1016/j.cub.2010.06.032

Dang-Vu, T. T., Schabus, M., Desseilles, M., Albouy, G., Boly, M., Darsaud, A., … Maquet, P. (2008). Spontaneous neural activity during human slow wave sleep. *Proceedings of the National Academy of Sciences of the United States of America*, *105*(39), 15160–5. https://doi.org/10.1073/pnas.0801819105

De Luca, M., Beckmann, C. F., De Stefano, N., Matthews, P. M., & Smith, S. M. (2006). fMRI resting state networks define distinct modes of long-distance interactions in the human brain. *NeuroImage*, *29*(4), 1359–1367. https://doi.org/10.1016/J.NEUROIMAGE.2005.08.035

De Martino, F., Gentile, F., Esposito, F., Balsi, M., Di Salle, F., Goebel, R., & Formisano, E. (2007). Classification of fMRI independent components using IC-fingerprints and support vector machine classifiers. *NeuroImage*, *34*(1), 177–194. https://doi.org/10.1016/j.neuroimage.2006.08.041

Deco, G., & Corbetta, M. (2011). The Dynamical Balance of the Brain at Rest. *The Neuroscientist*, *17*(1), 107–123. https://doi.org/10.1177/1073858409354384

Delorme, A., & Makeig, S. (2004). EEGLAB: An open source toolbox for analysis of single-trial EEG dynamics including independent component analysis. *Journal of*

Neuroscience Methods, *134*(1), 9–21. https://doi.org/10.1016/j.jneumeth.2003.10.009

Dement, W. (1958). The occurence of low voltage, fast, electroencephalogram patterns during behavioral sleep in the cat. *Electroencephalography and Clinical Neurophysiology*, *10*(2), 291–296. https://doi.org/10.1016/0013-4694(58)90037-3

Demertzi, A., Tagliazucchi, E., Dehaene, S., Deco, G., Barttfeld, P., Raimondo, F., … Sitt, J. D. (2019). Human consciousness is supported by dynamic complex patterns of brain signal coordination. *Science Advances*, *5*(2), eaat7603. https://doi.org/10.1126/sciadv.aat7603

Diekelmann, S., & Born, J. (2010). The memory function of sleep. *Nature Reviews Neuroscience*. https://doi.org/10.1038/nrn2762

Douglass, A. B., Bornstein, R., Nino-Murcia, G., Keenan, S., Miles, L., Zarcone, V. P., … Dement, W. C. (1994). The Sleep Disorders Questionnaire. I: Creation and multivariate structure of SDQ. *Sleep*, *17*(2), 160–7. Retrieved from http://www.ncbi.nlm.nih.gov/pubmed/8036370

Fang, Z., Ray, L. B., Owen, A. M., & Fogel, S. M. (2017). Neural Correlates of human cognitive abilities during sleep. *Doi.org*, 130500. https://doi.org/10.1101/130500

Fang, Z., Ray, L. B., Owen, A. M., & Fogel, S. M. (2019a). Brain Activation Time-Locked to Sleep Spindles Associated With Human Cognitive Abilities. *Frontiers in Neuroscience*, *13*, 46. https://doi.org/10.3389/fnins.2019.00046

Fang, Z., Ray, L. B., Owen, A. M., & Fogel, S. M. (2019b). Sleep spindle-dependent functional connectivity correlates with cognitive abilities. In *World Sleep 2019 Congress on Sleep Medicine*.

Fang, Z., Sergeeva, V., Ray, L. B., Viczko, J., Owen, A. M., & Fogel, S. M. (2017a). Sleep Spindles and Intellectual Ability: Epiphenomenon or Directly Related? *Journal of Cognitive Neuroscience*, *29*(1), 167–182. https://doi.org/10.1162/jocn_a_01034

Fang, Z., Sergeeva, V., Ray, L. B., Viczko, J., Owen, A. M., & Fogel, S. M. (2017b). Sleep Spindles and Intellectual Ability: Epiphenomenon or Directly Related? *Journal of Cognitive Neuroscience*, *29*(1), 167–182. https://doi.org/10.1162/jocn_a_01034

Feinberg, I., & March, J. D. (1995). Observations on delta homeostasis, the one-stimulus model of NREM-REM alternation and the neurobiologic implications of experimental dream studies. *Behavioural Brain Research*, *69*(1–2), 97–108. https://doi.org/10.1016/0166-4328(95)00010-Q

Fernández-Espejo, D., & Owen, A. M. (2013). *Detecting awareness after severe brain injury*. *Nature Publishing Group*. https://doi.org/10.1038/nrn3608

Finelli, L. A., Borbély, A. A., & Achermann, P. (2001). Functional topography of the human nonREM sleep electroencephalogram. *The European Journal of Neuroscience*, *13*(12), 2282–90. Retrieved from http://www.ncbi.nlm.nih.gov/pubmed/11454032

Florin, E., & Baillet, S. (2015). The brain's resting-state activity is shaped by synchronized cross-frequency coupling of neural oscillations. *NeuroImage*, *111*, 26–35. https://doi.org/10.1016/j.neuroimage.2015.01.054

Fogel, S. M., Albouy, G., King, B. R., Lungu, O., Vien, C., Bore, A., … Doyon, J. (2017). Reactivation or transformation? Motor memory consolidation associated with cerebral activation time-locked to sleep spindles. *PLOS ONE*, *12*(4), e0174755. https://doi.org/10.1371/journal.pone.0174755

Fogel, S. M., & Smith, C. T. (2011). The function of the sleep spindle: A physiological index of intelligence and a mechanism for sleep-dependent memory consolidation. *Neuroscience & Biobehavioral Reviews*, *35*(5), 1154–1165. https://doi.org/10.1016/J.NEUBIOREV.2010.12.003

Forget, D., Morin, C. M., & Bastien, C. H. (2011). The role of the spontaneous and evoked k-complex in good-sleeper controls and in individuals with insomnia. *Sleep*, *34*(9), 1251–60. https://doi.org/10.5665/SLEEP.1250

Foster, B. L., Rangarajan, V., Shirer, W. R., & Parvizi, J. (2015). Intrinsic and task-dependent coupling of neuronal population activity in human parietal cortex. *Neuron*, *86*(2), 578–90. https://doi.org/10.1016/j.neuron.2015.03.018

Foulkes, D. (1962). Dream reports from different stages of sleep. *Journal of Abnormal and Social Psychology*, *65*(1), 14–25. https://doi.org/10.1037/h0040431

Foulkes, D., & Schmidt, M. (1983). Temporal sequence and unit composition in dream reports from different stages of sleep. *Sleep*, *6*(3), 265–80. Retrieved from http://www.ncbi.nlm.nih.gov/pubmed/6622882

Fox, M. D., Snyder, A. Z., Vincent, J. L., Corbetta, M., Van Essen, D. C., & Raichle, M. E. (2005). The human brain is intrinsically organized into dynamic, anticorrelated functional networks. *Proceedings of the National Academy of Sciences of the United States of America*, *102*(27), 9673–8. https://doi.org/10.1073/pnas.0504136102

Frank, M. G. (2006). The mystery of sleep function: current perspectives and future directions. *Reviews in the Neurosciences*, *17*(4), 375–92. Retrieved from http://www.ncbi.nlm.nih.gov/pubmed/17139839

Friston, K. J., Holmes, A. P., Worsley, K. J., Poline, J.-P., Frith, C. D., & Frackowiak, R. S. J. (1994). Statistical parametric maps in functional imaging: A general linear approach. *Human Brain Mapping*, *2*(4), 189–210. https://doi.org/10.1002/hbm.460020402

Gavrilescu, M., Rossell, S., Stuart, G. W., Shea, T. L., Innes-Brown, H., Henshall, K., … Egan, G. F. (2010). Reduced connectivity of the auditory cortex in patients with auditory hallucinations: a resting state functional magnetic resonance imaging study. *Psychological Medicine*, *40*(7), 1149–1158. https://doi.org/10.1017/S0033291709991632

Gonçalves, S. I., de Munck, J. C., Pouwels, P. J. W., Schoonhoven, R., Kuijer, J. P. A., Maurits, N. M., … Lopes da Silva, F. H. (2006). Correlating the alpha rhythm to BOLD using simultaneous EEG/fMRI: Inter-subject variability. *NeuroImage*, *30*(1), 203–213. https://doi.org/10.1016/j.neuroimage.2005.09.062

Goncalves, Só. I., Bijma, F., Pouwels, P. W. J., Jonker, M., Kuijer, J. P. A., Heethaar, R. M., … de Munck, J. C. (2008). A Data and Model-Driven Approach to Explore Inter-Subject Variability of Resting-State Brain Activity Using EEG-fMRI. *IEEE Journal of Selected Topics in Signal Processing*, *2*(6), 944–953. https://doi.org/10.1109/JSTSP.2008.2009082

Gordon, E. M., Laumann, T. O., Adeyemo, B., Huckins, J. F., Kelley, W. M., & Petersen, S. E. (2016). Generation and Evaluation of a Cortical Area Parcellation from Resting-State Correlations. *Cerebral Cortex*, *26*(1), 288–303. https://doi.org/10.1093/cercor/bhu239

Gott, J. A., Liley, D. T. J., & Hobson, J. A. (2017). Towards a Functional Understanding of PGO Waves. *Frontiers in Human Neuroscience*, *11*, 89. https://doi.org/10.3389/fnhum.2017.00089

Greicius, M. D., Supekar, K., Menon, V., & Dougherty, R. F. (2009). Resting-state functional connectivity reflects structural connectivity in the default mode network. *Cerebral Cortex (New York, N.Y. : 1991)*, *19*(1), 72–8. https://doi.org/10.1093/cercor/bhn059

Griffanti, L., Douaud, G., Bijsterbosch, J., Evangelisti, S., Alfaro-Almagro, F., Glasser, M. F., … Smith, S. M. (2017). Hand classification of fMRI ICA noise components. *NeuroImage*, *154*, 188–205. https://doi.org/10.1016/j.neuroimage.2016.12.036

Griffanti, L., Salimi-Khorshidi, G., Beckmann, C. F., Auerbach, E. J., Douaud, G., Sexton, C. E., … Smith, S. M. (2014). ICA-based artefact removal and accelerated fMRI acquisition for improved resting state network imaging. *NeuroImage*, *95*, 232–247. https://doi.org/10.1016/j.neuroimage.2014.03.034

Hacker, C. D., Snyder, A. Z., Pahwa, M., Corbetta, M., & Leuthardt, E. C. (2017). Frequency-specific electrophysiologic correlates of resting state fMRI networks. *NeuroImage*, *149*, 446–457. https://doi.org/10.1016/j.neuroimage.2017.01.054

He, B. J., Snyder, A. Z., Zempel, J. M., Smyth, M. D., & Raichle, M. E. (2008). Electrophysiological correlates of the brain's intrinsic large-scale functional architecture. *Proceedings of the National Academy of Sciences*, *105*(41), 16039–16044. https://doi.org/10.1073/pnas.0807010105

Hearne, L. J., Cocchi, L., Zalesky, A., & Mattingley, J. B. (2017). Reconfiguration of brain network architectures between resting state and complexity-dependent cognitive reasoning. *The Journal of Neuroscience*, 485–17. https://doi.org/10.1523/JNEUROSCI.0485-17.2017

Heeger, D. J., & Ress, D. (2002). What does fMRI tell us about neuronal activity? *Nature Reviews Neuroscience*, *3*(2), 142–151. https://doi.org/10.1038/nrn730

Heine, L., Soddu, A., Gómez, F., Vanhaudenhuyse, A., Tshibanda, L., Thonnard, M., … Demertzi, A. (2012a). Resting State Networks and Consciousness. *Frontiers in Psychology*, *3*, 295. https://doi.org/10.3389/fpsyg.2012.00295

Heine, L., Soddu, A., Gómez, F., Vanhaudenhuyse, A., Tshibanda, L., Thonnard, M., … Demertzi, A. (2012b). Resting state networks and consciousness Alterations of multiple resting state network connectivity in physiological, pharmacological, and

pathological consciousness states. *Frontiers in Psychology*, *3*(AUG). https://doi.org/10.3389/fpsyg.2012.00295

Heiss, W.-D., Pawlik, G., Herholz, K., Wagner, R., & Wienhard, K. (1985). Regional cerebral glucose metabolism in man during wakefulness, sleep, and dreaming. *Brain Research*, *327*(1–2), 362–366. https://doi.org/10.1016/0006-8993(85)91537-9

Hinard, V., Mikhail, C., Pradervand, S., Curie, T., Houtkooper, R. H., Auwerx, J., … Tafti, M. (2012). Key Electrophysiological, Molecular, and Metabolic Signatures of Sleep and Wakefulness Revealed in Primary Cortical Cultures. *Journal of Neuroscience*, *32*(36), 12506–12517. https://doi.org/10.1523/JNEUROSCI.2306-12.2012

Hipp, J. F., Hawellek, D. J., Corbetta, M., Siegel, M., & Engel, A. K. (2012). Large-scale cortical correlation structure of spontaneous oscillatory activity. *Nature Neuroscience*, *15*(6), 884–890. https://doi.org/10.1038/nn.3101

Hobson, J. A., & Pace-Schott, E. F. (2002). The cognitive neuroscience of sleep: neuronal systems, consciousness and learning. *Nature Reviews Neuroscience*, *3*(9), 679–693. https://doi.org/10.1038/nrn915

Hobson, J. A., Pace-Schott, E. F., & Stickgold, R. (2000a). Dreaming and the brain: Toward a cognitive neuroscience of conscious states. *Behavioral and Brain Sciences*, *23*(6), 793–842. https://doi.org/10.1017/S0140525X00003976

Hobson, J. A., Pace-Schott, E. F., & Stickgold, R. (2000b). Dreaming and the brain: toward a cognitive neuroscience of conscious states. *The Behavioral and Brain Sciences*, *23*(6), 793-842-1121. Retrieved from http://www.ncbi.nlm.nih.gov/pubmed/11515143

Horovitz, S. G., Braun, A. R., Carr, W. S., Picchioni, D., Balkin, T. J., Fukunaga, M., & Duyn, J. H. (2009). Decoupling of the brain's default mode network during deep sleep. *Proceedings of the National Academy of Sciences of the United States of America*, *106*(27), 11376–81. https://doi.org/10.1073/pnas.0901435106

Horovitz, S. G., Fukunaga, M., de Zwart, J. A., van Gelderen, P., Fulton, S. C., Balkin, T. J., & Duyn, J. H. (2008). Low frequency BOLD fluctuations during resting wakefulness and light sleep: A simultaneous EEG-fMRI study. *Human Brain Mapping*, *29*(6), 671–682. https://doi.org/10.1002/hbm.20428

Houldin, E., Fang, Z., Ray, L. B., Owen, A. M., & Fogel, S. M. (2019). Toward a complete taxonomy of resting state networks across wakefulness and sleep: an assessment of spatially distinct resting state networks using independent component analysis. *Sleep*, *42*(3). https://doi.org/10.1093/sleep/zsy235

Houldin, E., Fang, Z., Ray, L. B., Stojanoski, B., Owen, A. M., & Fogel, S. M. (2019). Slow wave sleep is an altered, not a reduced, state of consciousness: resting state network functional connectivity in sleep. 23rd Annual Meeting of the Association for Scientific Study of Consciousness.

Huster, R. J., Debener, S., Eichele, T., & Herrmann, C. S. (2012). Methods for simultaneous EEG-fMRI: an introductory review. *The Journal of Neuroscience : The Official Journal of the Society for Neuroscience*, *32*(18), 6053–60.

https://doi.org/10.1523/JNEUROSCI.0447-12.2012

Iber, C., Ancoli-Israel, S., Chesson, A. L., & Quan, S. F. (2007). *The AASM manual for the scoring of sleep and associated events: rules, terminology and technical specifications*. *American Academy of Sleep Medicine, Westchester, IL.* American Academy of Sleep Medicine Westchester, IL.

Jenkinson, M., Bannister, P., Brady, M., & Smith, S. (2002). Improved optimization for the robust and accurate linear registration and motion correction of brain images. *NeuroImage*, *17*(2), 825–841. https://doi.org/10.1016/S1053-8119(02)91132-8

Jones, B. E. (2008). *Modulation of Cortical Activation and Behavioral Arousal by Cholinergic and Orexinergic Systems*. *Annals of the New York Academy of Sciences*, *1129*(1), 26–34. https://doi.org/10.1196/annals.1417.026

Jouvet, M., Michel, F., & Courjon, J. (1959). Sur un stade d'activité électrique cérébrale rapide au cours du sommeil physiologique. *Comptes Rendus Des Séances de l'Académie Des Sciences*, *Tome CLIII*(No. 6), 1024.

Jung, C. M., Melanson, E. L., Frydendall, E. J., Perreault, L., Eckel, R. H., & Wright, K. P. (2011). Energy expenditure during sleep, sleep deprivation and sleep following sleep deprivation in adult humans. *The Journal of Physiology*, *589*(1), 235–244. https://doi.org/10.1113/jphysiol.2010.197517

Karlsson, M. P., & Frank, L. M. (2009). Awake replay of remote experiences in the hippocampus. *Nature Neuroscience*, *12*(7), 913–918. https://doi.org/10.1038/nn.2344

Kattler, Dijk, & Borbély. (1994). Effect of unilateral somatosensory stimulation prior to sleep on the sleep EEG in humans. *Journal of Sleep Research*, *3*(3), 159–164. Retrieved from http://www.ncbi.nlm.nih.gov/pubmed/10607121

Kelly, R. E., Alexopoulos, G. S., Wang, Z., Gunning, F. M., Murphy, C. F., Morimoto, S. S., … Hoptman, M. J. (2010a). Visual inspection of independent components: Defining a procedure for artifact removal from fMRI data. *Journal of Neuroscience Methods*, *189*(2), 233–245. https://doi.org/10.1016/j.jneumeth.2010.03.028

Kelly, R. E., Alexopoulos, G. S., Wang, Z., Gunning, F. M., Murphy, C. F., Morimoto, S. S., … Hoptman, M. J. (2010b). Visual inspection of independent components: Defining a procedure for artifact removal from fMRI data. *Journal of Neuroscience Methods*, *189*(2), 233–245. https://doi.org/10.1016/j.jneumeth.2010.03.028

Kennedy, C., Gillin, J. C., Mendelson, W., Suda, S., Miyaoka, M., Ito, M., … Sokoloff, L. (1982). Local cerebral glucose utilization in non-rapid eye movement sleep. *Nature*, *297*(5864), 325–327. https://doi.org/10.1038/297325a0

Klemm, W. R. (2011). Why Does Rem Sleep Occur? A Wake-Up Hypothesis1. *Frontiers in Systems Neuroscience*, *5*, 73. https://doi.org/10.3389/fnsys.2011.00073

Klimesch, W. (2012). Alpha-band oscillations, attention, and controlled access to stored information. *Trends in Cognitive Sciences*, *16*(12), 606–617. https://doi.org/10.1016/j.tics.2012.10.007

Krueger, J. M., Frank, M. G., Wisor, J. P., & Roy, S. (2016). Sleep function: Toward

elucidating an enigma. *Sleep Medicine Reviews*, *28*, 46–54. https://doi.org/10.1016/j.smrv.2015.08.005

Krueger, J. M., Huang, Y. H., Rector, D. M., & Buysse, D. J. (2013). Sleep: a synchrony of cell activity-driven small network states. *The European Journal of Neuroscience*, *38*(2), 2199–209. https://doi.org/10.1111/ejn.12238

Kujala, J., Pammer, K., Cornelissen, P., Roebroeck, A., Formisano, E., & Salmelin, R. (2007). Phase Coupling in a Cerebro-Cerebellar Network at 8–13 Hz during Reading. *Cerebral Cortex*, *17*(6), 1476–1485. https://doi.org/10.1093/cercor/bhl059

Lakatos, P., Shah, A. S., Knuth, K. H., Ulbert, I., Karmos, G., & Schroeder, C. E. (2005). An Oscillatory Hierarchy Controlling Neuronal Excitability and Stimulus Processing in the Auditory Cortex. *Journal of Neurophysiology*, *94*(3), 1904–1911. https://doi.org/10.1152/jn.00263.2005

Larson-Prior, L. J., Power, J. D., Vincent, J. L., Nolan, T. S., Coalson, R. S., Zempel, J., … Petersen, S. E. (2011). Modulation of the brain's functional network architecture in the transition from wake to sleep. *Progress in Brain Research*, *193*, 277–294. https://doi.org/10.1016/B978-0-444-53839-0.00018-1

Larson-Prior, L. J., Zempel, J. M., Nolan, T. S., Prior, F. W., Snyder, A. Z., & Raichle, M. E. (2009). Cortical network functional connectivity in the descent to sleep. *Proceedings of the National Academy of Sciences*, *106*(11), 4489–4494. https://doi.org/10.1073/pnas.0900924106

Laureys, S. (2005). The neural correlate of (un)awareness: lessons from the vegetative state. *Trends in Cognitive Sciences*, *9*(12), 556–559. https://doi.org/10.1016/J.TICS.2005.10.010

Lee, M. G. (2005). Cholinergic Basal Forebrain Neurons Burst with Theta during Waking and Paradoxical Sleep. *Journal of Neuroscience*, *25*(17), 4365–4369. https://doi.org/10.1523/JNEUROSCI.0178-05.2005

Lei, X., Zhao, Z., & Chen, H. (2013). Extraversion is encoded by scale-free dynamics of default mode network. *NeuroImage*, *74*, 52–57. https://doi.org/10.1016/j.neuroimage.2013.02.020

Leopold, D. A., & Maier, A. (2012). Ongoing physiological processes in the cerebral cortex. *NeuroImage*, *62*(4), 2190–2200. https://doi.org/10.1016/j.neuroimage.2011.10.059

Logothetis, N. K. (2008). What we can do and what we cannot do with fMRI. *Nature*, *453*(7197), 869–878. https://doi.org/10.1038/nature06976

MacLean, M. H., Arnell, K. M., & Cote, K. A. (2012). Resting EEG in alpha and beta bands predicts individual differences in attentional blink magnitude. *Brain and Cognition*, *78*(3), 218–229. https://doi.org/10.1016/j.bandc.2011.12.010

Mantini, D., Perrucci, M. G., Del Gratta, C., Romani, G. L., & Corbetta, M. (2007). Electrophysiological signatures of resting state networks in the human brain. *Proceedings of the National Academy of Sciences*, *104*(32), 13170–13175. https://doi.org/10.1073/pnas.0700668104

Marrosu, F., Portas, C., Mascia, M. S., Casu, M. A., Fà, M., Giagheddu, M., … Gessa, G. L. (1995). Microdialysis measurement of cortical and hippocampal acetylcholine release during sleep-wake cycle in freely moving cats. *Brain Research*, *671*(2), 329–332. https://doi.org/10.1016/0006-8993(94)01399-3

Marshall, L., & Born, J. (2007). The contribution of sleep to hippocampus-dependent memory consolidation. *Trends in Cognitive Sciences*, *11*(10), 442–450. https://doi.org/10.1016/j.tics.2007.09.001

Martuzzi, R., Ramani, R., Qiu, M., Rajeevan, N., & Constable, R. T. (2010). Functional connectivity and alterations in baseline brain state in humans. *NeuroImage*, *49*(1), 823–834. https://doi.org/10.1016/j.neuroimage.2009.07.028

McCarley, R. W., & Hobson, J. A. (1975). Neuronal excitability modulation over the sleep cycle: a structural and mathematical model. *Science (New York, N.Y.)*, *189*(4196), 58–60. Retrieved from http://www.ncbi.nlm.nih.gov/pubmed/1135627

McCarley, R. W., & Massaquoi, S. G. (1986). A limit cycle mathematical model of the REM sleep oscillator system. *The American Journal of Physiology*, *251*(6 Pt 2), R1011-29. https://doi.org/10.1152/ajpregu.1986.251.6.R1011

McKeown, M. J., Makeig, S., Brown, G. G., Jung, T. P., Kindermann, S. S., Bell, A. J., & Sejnowski, T. J. (1998). Analysis of fMRI data by blind separation into independent spatial components. *Human Brain Mapping*, *6*(3), 160–88. Retrieved from http://www.ncbi.nlm.nih.gov/pubmed/9673671

Meyer, M. C., Janssen, R. J., Van Oort, E. S. B., Beckmann, C. F., & Barth, M. (2013). The Quest for EEG Power Band Correlation with ICA Derived fMRI Resting State Networks. *Frontiers in Human Neuroscience*, *7*. https://doi.org/10.3389/fnhum.2013.00315

Moruzzi, G., & Magoun, H. W. (1949). Brain stem reticular formation and activation of the EEG. *Electroencephalography and Clinical Neurophysiology*, *1*(4), 455–73. Retrieved from http://www.ncbi.nlm.nih.gov/pubmed/18421835

Mulders, P. C., van Eijndhoven, P. F., & Beckmann, C. F. (2016). Identifying Large-Scale Neural Networks Using fMRI. *Systems Neuroscience in Depression*, 209–237. https://doi.org/10.1016/B978-0-12-802456-0.00007-8

Multert, C., & Lemieux, L. (2009). EEG-fMRI; Physiological Basis, Technique, and Applications. *Book*, 538. https://doi.org/10.1007/978-3-540-87919-0

Naci, L., Haugg, A., MacDonald, A., Anello, M., Houldin, E., Naqshbandi, S., … Owen, A. M. (2018). Functional diversity of brain networks supports consciousness and verbal intelligence. *Scientific Reports*, *8*(1), 13259. https://doi.org/10.1038/s41598-018-31525-z

Nashiro, K., Sakaki, M., Braskie, M. N., & Mather, M. (2017). Resting-state networks associated with cognitive processing show more age-related decline than those associated with emotional processing. *Neurobiology of Aging*, *54*, 152–162. https://doi.org/10.1016/j.neurobiolaging.2017.03.003

Nelson, J. P., McCarley, R. W., & Hobson, J. A. (1983). REM sleep burst neurons, PGO

waves, and eye movement information. *Journal of Neurophysiology*, *50*(4), 784–97. https://doi.org/10.1152/jn.1983.50.4.784

Nickerson, L. D., Smith, S. M., Öngür, D., & Beckmann, C. F. (2017). Using Dual Regression to Investigate Network Shape and Amplitude in Functional Connectivity Analyses. *Frontiers in Neuroscience*, *11*, 115. https://doi.org/10.3389/fnins.2017.00115

Owen, A. M., Coleman, M. R., Boly, M., Davis, M. H., Laureys, S., & Pickard, J. D. (2006). Detecting awareness in the vegetative state. *Science (New York, N.Y.)*, *313*(5792), 1402. https://doi.org/10.1126/science.1130197

Pasquale, V., Massobrio, P., Bologna, L. L., Chiappalone, M., & Martinoia, S. (2008). Self-organization and neuronal avalanches in networks of dissociated cortical neurons. *Neuroscience*, *153*(4), 1354–1369. https://doi.org/10.1016/j.neuroscience.2008.03.050

Posner, J. B., Saper, C. B., Schiff, N., & Plum, F. (2008). *Plum and Posner's Diagnosis of Stupor and Coma*. Oxford University Press. https://doi.org/10.1093/med/9780195321319.001.0001

Raichle, M. E. (2015). The Brain's Default Mode Network. *Annual Review of Neuroscience*, *38*(1), 433–447. https://doi.org/10.1146/annurev-neuro-071013-014030

Raichle, M. E., MacLeod, A. M., Snyder, A. Z., Powers, W. J., Gusnard, D. A., & Shulman, G. L. (2001a). A default mode of brain function. *Proceedings of the National Academy of Sciences of the United States of America*, *98*(2), 676–82. https://doi.org/10.1073/pnas.98.2.676

Raichle, M. E., MacLeod, A. M., Snyder, A. Z., Powers, W. J., Gusnard, D. A., & Shulman, G. L. (2001b). A default mode of brain function. *Proceedings of the National Academy of Sciences of the United States of America*, *98*(2), 676–82. https://doi.org/10.1073/pnas.98.2.676

Raizen, D. M., Zimmerman, J. E., Maycock, M. H., Ta, U. D., You, Y., Sundaram, M. V., & Pack, A. I. (2008). Lethargus is a Caenorhabditis elegans sleep-like state. *Nature*, *451*(7178), 569–572. https://doi.org/10.1038/nature06535

Rasch, B., & Born, J. (2013). About Sleep's Role in Memory. *Physiological Reviews*, *93*(2), 681–766. https://doi.org/10.1152/physrev.00032.2012

Rattenborg, N. C., Martinez-Gonzalez, D., Roth, T. C., Pravosudov, V. V, & Pravosudov, V. V. (2011). Hippocampal memory consolidation during sleep: a comparison of mammals and birds. *Biological Reviews of the Cambridge Philosophical Society*, *86*(3), 658–91. https://doi.org/10.1111/j.1469-185X.2010.00165.x

Ray, K. L., McKay, D. R., Fox, P. M., Riedel, M. C., Uecker, A. M., Beckmann, C. F., … Laird, A. R. (2013). ICA model order selection of task co-activation networks. *Frontiers in Neuroscience*, *7*, 237. https://doi.org/10.3389/fnins.2013.00237

Rechtschaffen, A., & Kales, A. (1968). *A manual of standardized terminology, techniques and scoring system of sleep stages in human subjects.* Los Angeles:

Brain Information Service/Brain Research Institute.

Rector, D. M., Schei, J. L., Van Dongen, H. P. A., Belenky, G., & Krueger, J. M. (2009). Physiological markers of local sleep. *The European Journal of Neuroscience*, *29*(9), 1771–8. https://doi.org/10.1111/j.1460-9568.2009.06717.x

Reineberg, A. E., Andrews-Hanna, J. R., Depue, B. E., Friedman, N. P., & Banich, M. T. (2015). Resting-state networks predict individual differences in common and specific aspects of executive function. *NeuroImage*, *104*, 69–78. https://doi.org/10.1016/j.neuroimage.2014.09.045

Reineberg, A. E., Gustavson, D. E., Benca, C., Banich, M. T., & Friedman, N. P. (2018). The Relationship Between Resting State Network Connectivity and Individual Differences in Executive Functions. *Frontiers in Psychology*, *9*. https://doi.org/10.3389/FPSYG.2018.01600

Roquet, D., Foucher, J. R., Froehlig, P., Renard, F., Pottecher, J., Besancenot, H., … Kremer, S. (2016). Resting-state networks distinguish locked-in from vegetative state patients. *NeuroImage. Clinical*, *12*, 16–22. https://doi.org/10.1016/j.nicl.2016.06.003

Salimi-Khorshidi, G., Douaud, G., Beckmann, C. F., Glasser, M. F., Griffanti, L., & Smith, S. M. (2014). Automatic denoising of functional MRI data: Combining independent component analysis and hierarchical fusion of classifiers. *NeuroImage*, *90*, 449–468. https://doi.org/10.1016/j.neuroimage.2013.11.046

Saper, C. B., Chou, T. C., & Scammell, T. E. (2001). The sleep switch: hypothalamic control of sleep and wakefulness. *Trends in Neurosciences*, *24*(12), 726–31. Retrieved from http://www.ncbi.nlm.nih.gov/pubmed/11718878

Schölvinck, M. L., Leopold, D. A., Brookes, M. J., & Khader, P. H. (2013). The contribution of electrophysiology to functional connectivity mapping. *NeuroImage*, *80*, 297–306. https://doi.org/10.1016/j.neuroimage.2013.04.010

Schrouff, J., Perlbarg, V., Boly, M., Marrelec, G., Boveroux, P., Vanhaudenhuyse, A., … Benali, H. (2011). Brain functional integration decreases during propofol-induced loss of consciousness. *NeuroImage*, *57*, 198–205. https://doi.org/10.1016/j.neuroimage.2011.04.020

Schwartz, J. R. L., & Roth, T. (2008). Neurophysiology of sleep and wakefulness: basic science and clinical implications. *Current Neuropharmacology*, *6*(4), 367–78. https://doi.org/10.2174/157015908787386050

Shrivastava, D., Jung, S., Saadat, M., Sirohi, R., & Crewson, K. (2014). How to interpret the results of a sleep study. *Journal of Community Hospital Internal Medicine Perspectives*, *4*(5), 24983. https://doi.org/10.3402/jchimp.v4.24983

Shulman, G. L., Corbetta, M., Buckner, R. L., Fiez, J. A., Miezin, F. M., Raichle, M. E., & Petersen, S. E. (1997). Common Blood Flow Changes across Visual Tasks: I. Increases in Subcortical Structures and Cerebellum but Not in Nonvisual Cortex. *Journal of Cognitive Neuroscience*, *9*(5), 624–647. https://doi.org/10.1162/jocn.1997.9.5.624

Slotnick, S. D., Moo, L. R., Kraut, M. A., Lesser, R. P., & Hart, J. (2002). Interactions between thalamic and cortical rhythms during semantic memory recall in human. *Proceedings of the National Academy of Sciences*, *99*(9), 6440–6443. https://doi.org/10.1073/pnas.092514899

Smith, S. M. (2002). Fast robust automated brain extraction. *Human Brain Mapping*, *17*(3), 143–155. https://doi.org/10.1002/hbm.10062

Smith, S. M., Beckmann, C. F., Andersson, J., Auerbach, E. J., Bijsterbosch, J., Douaud, G., … WU-Minn HCP Consortium. (2013). Resting-state fMRI in the Human Connectome Project. *NeuroImage*, *80*, 144–168. https://doi.org/10.1016/j.neuroimage.2013.05.039

Smith, S. M., Fox, P. T., Miller, K. L., Glahn, D. C., Fox, P. M., Mackay, C. E., … Beckmann, C. F. (2009). Correspondence of the brain's functional architecture during activation and rest. *Proceedings of the National Academy of Sciences of the United States of America*, *106*(31), 13040–5. https://doi.org/10.1073/pnas.0905267106

Smith, S. M., Jenkinson, M., Woolrich, M. W., Beckmann, C. F., Behrens, T. E. J., Johansen-Berg, H., … Matthews, P. M. (2004). Advances in functional and structural MR image analysis and implementation as FSL. In *NeuroImage* (Vol. 23). https://doi.org/10.1016/j.neuroimage.2004.07.051

Sorg, C., Riedl, V., Mühlau, M., Calhoun, V. D., Eichele, T., Läer, L., … Wohlschläger, A. M. (2007). Selective changes of resting-state networks in individuals at risk for Alzheimer's disease. *Proceedings of the National Academy of Sciences of the United States of America*, *104*(47), 18760–18765. https://doi.org/10.1073/pnas.0708803104

Spoormaker, V. I., Schröter, M. S., Gleiser, P. M., Andrade, K. C., Dresler, M., Wehrle, R., … Czisch, M. (2010). Development of a Large-Scale Functional Brain Network during Human Non-Rapid Eye Movement Sleep. *Journal of Neuroscience*, *30*(34). Retrieved from http://www.jneurosci.org/content/30/34/11379

Squire, L. R., Zola-Morgan, & Stuart. (1991). *The Medial Temporal Lobe Memory System*. *Science* (Vol. 253). Retrieved from https://s3.amazonaws.com/academia.edu.documents/11808558/medial_temporal_lobe_memory_system.pdf?AWSAccessKeyId=AKIAIWOWYYGZ2Y53UL3A&Expires=1556835352&Signature=VhwX2sRyciECtFvFQqpBYrNf0tY%3D&response-content-disposition=inline%3B filename%3Dmedial_temporal_lobe_memory_system.pdf

Steriade, M. (2001). Active neocortical processes during quiescent sleep. *Archives Italiennes de Biologie*, *139*(1–2), 37–51. Retrieved from http://www.ncbi.nlm.nih.gov/pubmed/11256186

Steriade, M. (2003). The corticothalamic system in sleep. *Frontiers in Bioscience : A Journal and Virtual Library*, *8*, d878-99. Retrieved from http://www.ncbi.nlm.nih.gov/pubmed/12700074

Steriade, M. (2005, June). Sleep, epilepsy and thalamic reticular inhibitory neurons. *Trends in Neurosciences*. https://doi.org/10.1016/j.tins.2005.03.007

Steriade, M. (2006). Grouping of brain rhythms in corticothalamic systems. *Neuroscience*, *137*(4), 1087–1106. https://doi.org/10.1016/j.neuroscience.2005.10.029

Steriade, M., Amzica, F., & Contreras, D. (1996). Synchronization of fast (30-40 Hz) spontaneous cortical rhythms during brain activation. *The Journal of Neuroscience : The Official Journal of the Society for Neuroscience*, *16*(1), 392–417. Retrieved from http://www.ncbi.nlm.nih.gov/pubmed/8613806

Steriade, M., Timofeev, I., & Grenier, F. (2001). Natural waking and sleep states: a view from inside neocortical neurons. *Journal of Neurophysiology*, *85*(5), 1969–1985. https://doi.org/10.1016/j.neuroimage.2009.03.074

Stickgold, R. (2005). Sleep-dependent memory consolidation. *Nature*, *437*(7063), 1272–1278. https://doi.org/10.1038/nature04286

Stickgold, R., & Walker, M. P. (2005). Sleep and memory: the ongoing debate. *Sleep*, *28*(10), 1225–7. Retrieved from http://www.ncbi.nlm.nih.gov/pubmed/16295206

Tagliazucchi, E., & Laufs, H. (2014). Decoding Wakefulness Levels from Typical fMRI Resting-State Data Reveals Reliable Drifts between Wakefulness and Sleep. *Neuron*, *82*(3), 695–708. https://doi.org/10.1016/j.neuron.2014.03.020

Tagliazucchi, E., & van Someren, E. J. W. (2017, June 12). The large-scale functional connectivity correlates of consciousness and arousal during the healthy and pathological human sleep cycle. *NeuroImage*. https://doi.org/10.1016/j.neuroimage.2017.06.026

Tagliazucchi, E., von Wegner, F., Morzelewski, A., Brodbeck, V., Jahnke, K., & Laufs, H. (2013). Breakdown of long-range temporal dependence in default mode and attention networks during deep sleep. *Proceedings of the National Academy of Sciences*, *110*(38), 15419–15424. https://doi.org/10.1073/pnas.1312848110

Tong, Y., Hocke, L. M., Fan, X., Janes, A. C., & Frederick, B. deB. (2015). Can apparent resting state connectivity arise from systemic fluctuations? *Frontiers in Human Neuroscience*, *9*. https://doi.org/10.3389/fnhum.2015.00285

Tononi, G., & Cirelli, C. (2003). Sleep and synaptic homeostasis: a hypothesis. *Brain Research Bulletin*, *62*(2), 143–150. https://doi.org/10.1016/J.BRAINRESBULL.2003.09.004

Tononi, G., & Cirelli, C. (2014). Sleep and the Price of Plasticity: From Synaptic and Cellular Homeostasis to Memory Consolidation and Integration. *Neuron*, *81*(1), 12–34. https://doi.org/10.1016/j.neuron.2013.12.025

Toscani, M., Marzi, T., Righi, S., Viggiano, M. P., & Baldassi, S. (2010). Alpha waves: a neural signature of visual suppression. *Experimental Brain Research*, *207*(3–4), 213–219. https://doi.org/10.1007/s00221-010-2444-7

Toth, L. A. (1995). Sleep, sleep deprivation and infectious disease: Studies in animals. *Advances in Neuroimmunology*, *5*(1), 79–92. https://doi.org/10.1016/0960-5428(94)00045-P

Tzourio-Mazoyer, N., Landeau, B., Papathanassiou, D., Crivello, F., Etard, O., Delcroix,

N., … Joliot, M. (2002). Automated Anatomical Labeling of Activations in SPM Using a Macroscopic Anatomical Parcellation of the MNI MRI Single-Subject Brain. *NeuroImage*, *15*(1), 273–289. https://doi.org/10.1006/nimg.2001.0978

van den Heuvel, M. P., & Hulshoff Pol, H. E. (2010). Exploring the brain network: A review on resting-state fMRI functional connectivity. *European Neuropsychopharmacology*, *20*(8), 519–534. https://doi.org/10.1016/j.euroneuro.2010.03.008

Vanhaudenhuyse, A., Noirhomme, Q., Tshibanda, L. J. F., Bruno, M. A., Boveroux, P., Schnakers, C., … Boly, M. (2010). Default network connectivity reflects the level of consciousness in non-communicative brain-damaged patients. *Brain*, *133*(1), 161–171. https://doi.org/10.1093/brain/awp313

Vemuri, P., Jones, D. T., Jack, C. R., & Jr. (2012). Resting state functional MRI in Alzheimer's Disease. *Alzheimer's Research & Therapy*, *4*(1), 2. https://doi.org/10.1186/alzrt100

Vossel, S., Geng, J. J., & Fink, G. R. (2014). Dorsal and ventral attention systems: distinct neural circuits but collaborative roles. *The Neuroscientist : A Review Journal Bringing Neurobiology, Neurology and Psychiatry*, *20*(2), 150–9. https://doi.org/10.1177/1073858413494269

Vyazovskiy, V. V., Olcese, U., Hanlon, E. C., Nir, Y., Cirelli, C., & Tononi, G. (2011). Local sleep in awake rats. *Nature*, *472*(7344), 443–447. https://doi.org/10.1038/nature10009

Walker, M. P., Brakefield, T., Morgan, A., Hobson, J. A., & Stickgold, R. (2002). Practice with Sleep Makes Perfect. *Neuron*, *35*(1), 205–211. https://doi.org/10.1016/S0896-6273(02)00746-8

Wamsley, E. J. (2014). Dreaming and offline memory consolidation. *Current Neurology and Neuroscience Reports*, *14*(3), 433. https://doi.org/10.1007/s11910-013-0433-5

Wang, K., Jiang, T., Liang, M., Wang, L., Tian, L., Zhang, X., … Liu, Z. (2006). Discriminative analysis of early Alzheimer's disease based on two intrinsically anti-correlated networks with resting-state fMRI. *Medical Image Computing and Computer-Assisted Intervention : MICCAI ... International Conference on Medical Image Computing and Computer-Assisted Intervention*, *9*(Pt 2), 340–347. https://doi.org/10.1007/11866763_42

Watson, B. O., & Buzsáki, G. (2015). Sleep, Memory & Brain Rhythms. *Daedalus*, *144*(1), 67–82. https://doi.org/10.1162/DAED_a_00318

Weigenand, A., Schellenberger Costa, M., Ngo, H.-V. V., Claussen, J. C., & Martinetz, T. (2014a). Characterization of K-complexes and slow wave activity in a neural mass model. *PLoS Computational Biology*, *10*(11), e1003923. https://doi.org/10.1371/journal.pcbi.1003923

Weigenand, A., Schellenberger Costa, M., Ngo, H. V. V., Claussen, J. C., & Martinetz, T. (2014b). Characterization of K-Complexes and Slow Wave Activity in a Neural Mass Model. *PLoS Computational Biology*, *10*(11). https://doi.org/10.1371/journal.pcbi.1003923

Werth, E., Achermann, P., & Borbély, A. A. (1996). Brain topography of the human sleep EEG: antero-posterior shifts of spectral power. *Neuroreport*, *8*(1), 123–7. Retrieved from http://www.ncbi.nlm.nih.gov/pubmed/9051765

Xie, L., Kang, H., Xu, Q., Chen, M. J., Liao, Y., Thiyagarajan, M., … Nedergaard, M. (2013). Sleep Drives Metabolite Clearance from the Adult Brain. *Science*, *342*(6156), 373–377. https://doi.org/10.1126/science.1241224

Xu, X., Yuan, H., & Lei, X. (2016). Activation and Connectivity within the Default Mode Network Contribute Independently to Future-Oriented Thought. *Scientific Reports*, *6*(1), 21001. https://doi.org/10.1038/srep21001

Yu, Q., Allen, E. A., Sui, J., Arbabshirani, M. R., Pearlson, G., & Calhoun, V. D. (2012). Brain connectivity networks in schizophrenia underlying resting state functional magnetic resonance imaging. *Current Topics in Medicinal Chemistry*, *12*(21), 2415–25. Retrieved from http://www.ncbi.nlm.nih.gov/pubmed/23279180

Appendices

Appendix A: Copyright permissions

This Agreement between Mr. Evan Houldin ("You") and Oxford University Press ("Oxford University Press") consists of your license details and the terms and conditions provided by Oxford University Press and Copyright Clearance Center.

License number	4601421123508
License date	Jun 03, 2019
Licensed content publisher	Oxford University Press
Licensed content publication	SLEEP
Licensed content title	Toward a complete taxonomy of resting state networks across wakefulness and sleep: an assessment of spatially distinct resting state networks using independent comp
Licensed content author	Houldin, Evan; Fang, Zhuo; Ray, Laura; Owen, Adrian; Fogel, Stuart
Licensed content date	Nov 26, 2018
Type of use	Thesis/Dissertation
Publisher of your work	Western University
Expected publication date	Jul 2019
Portions	Complete document without abstract
Institution name	Western University
Expected presentation date	Jul 2019

Appendix B: Additional parcellation analysis for the second study

Table 6. *Number of functional connectivity (FC) edges per best-fit polynomial, for two brain parcellation types*

	Number of FC edges, by parcellation type	
Best-fit polynomial	*Smith* (14 RSNs)	*Gordon* (333 ROIs)
Quadratic	35 (83% of sig. edges)	3,841 (33% of sig. edges)
Convex Quadratic	29 (83% of quad. edges)	2,837 (74% of quad. edges)
Cubic	4	4,834
Linear	3	2,927
Total # of *sig.* FC edges	42 (46% of total edges)	11,602 (21% of total edges)
Total # of FC edges	91	55,278

Note: *Smith* refers to brain parcellations taken from (Smith et al., 2009) and used in implementing the second study (Chapter 3). *Gordon* refers to brain parcellations taken from (Gordon et al., 2016).

Curriculum Vitae

Name:	Evan Houldin
Post-secondary Education and Degrees:	**Ph.D.** Western University Neuroscience, Schulich School of Medicine & Dentistry, London, Ontario, Canada, In Progress
	M.Cog.Sc. Carleton University Institute of Cognitive Science, Ottawa, Ontario, Canada, 2014
	B.A.Sc. University of Toronto Department of Mechanical and Industrial Engineering, Toronto, Ontario, Canada, 2002
Honours and Awards:	Graduate Research Scholarship, Western University, 2014-2018
	Graduate Scholarship, Carleton University, 2012
	B.A.Sc. with Honors standing (above 80%), Mechanical Engineering program, University of Toronto, 2002
Related Work Experience	Teaching Assistant The University of Western Ontario, 2014-2018

Publications:

Houldin E, Fang Z, Ray LR, Owen AM, Fogel SM. Toward a Complete Taxonomy of Resting State Networks Across Wakefulness and Sleep: An Assessment of Spatially Distinct Resting State Networks Using Independent Component Analysis. *Sleep,* Volume 42, Issue 3, March 2019, DOI:10.1093/sleep/zsy235

Naci L, Haugg A, MacDonald A, Anello M, **Houldin E**, Naqshbandi S, Ganzalez-Lara LE, Arango M, Harle C, Cusack R, Owen AM. Functional Diversity of Brain Networks Supports Consciousness and Intelligence. *Nature Scientific Reports*: September 2018 - Volume 8 - Issue 1 - pp 1-15 - Article number: 13259, DOI:10.1038/s41598-018-31525-z